Scorodite Stabilization with Aluminum Hydroxy-Gels

Karl Leetmaa

Department of Mining and Materials Engineering
McGill University
Montreal
Canada

October 2008

A thesis submitted to McGill University
in partial fulfillment of the requirements of the degree of
Master of Engineering

Abstract

The disposal of arsenic in the form of scorodite presently attracts a lot of interest. However, even scorodite under certain pH and redox conditions may decompose potentially releasing arsenic to the environment. A novel way of arsenic fixation is to encapsulate/stabilize scorodite particles with mineral coatings/matrices that are not prone to decomposition. In this work, amorphous aluminum hydroxyl-gels were identified and investigated as a potential encapsulating material and a procedure was developed towards this end. The research work presented in this thesis included (1) synthesis of scorodite particles; (2) production and characterization of aluminum gels; (3) ageing of aluminum gel/scorodite blends; and (4) stability evaluation in terms of arsenic release in the pH range 6.5 to 8 at 22˚C. The gels were produced by partial (molar ratio OH/Al = 2.5) quick neutralization of 2M $AlCl_3$ or $Al(SO_4)_{1.5}$ solutions at 22˚C. The gels were determined, following ageing and water washing, to consist of 60 – 70 wt.% $Al(OH)_3$, 5 – 18 wt.% Cl or SO_4 and ~20 wt.% water. ATR-IR and Raman spectra revealed the aluminum sulphate-derived gel to be different than the corresponding aluminum chloride-derived gel in its molecular make-up, most likely having the Keggin type structure. Ageing aluminum sulphate gel and scorodite for at least one day at 22˚C was shown via BSE images and x-ray maps of cross sections to lead to development of an aluminum hydroxide matrix around the scorodite particles. Arsenic release from the aged gel/scorodite blends was found to be drastically reduced with respect to gel-free scorodite. Thus a 0.1 Al/As sulphate gel/scorodite mixture reached an equilibrium arsenic concentration of 0.2 ± 0.1 mg/L As at pH = 7.3, which is 50 times lower than unprotected scorodite under the same conditions.

Résumé

Au sein des procédés d'industrie minière, la neutralisation de l'arsenic sous forme de scorodite est aujourd'hui un sujet d'attrait majeur. Cependant, même la scorodite s'avère parfois instable dans certaines conditions de pH et d'oxydoréduction, pouvant mener au rejet d'arsenic dans l'environnement. L'une des nouvelles méthodes développées en vue de neutraliser l'arsenic consiste à encapsuler/stabiliser les particules de scorodite à l'aide de revêtements/matrices caractérisés par une forte résistance à la décomposition en milieu d'enfouissement. Dans ce travail, des gels amorphes d'hydroxyle d'aluminium ont été identifiés et étudiés comme potentiels matériaux d'encapsulation. Une procédure correspondante d'encapsulation a également été développée en fin de projet. Le travail de recherche présenté ici inclut (1) la synthèse de particules de scorodite ; (2) la production et la caractérisation des gels d'aluminium ; (3) le vieillissement de particules de scorodite au sein de gels d'aluminium; (4) l'évaluation de la stabilité de ce système en terme de rejet d'arsenic pour des pH variant de 6.5 à 8 et à une température de 22ºC. La production des gels a été réalisée par neutralisation rapide et partielle (fraction molaire OH/Al = 2.5), à 22ºC, de solutions de chlorure d'aluminium ($AlCl_3$) et de sulfate d'aluminium ($Al(SO_4)_{1.5}$) chacune d'une concentration de 2 mol/L. La composition des gels, en pourcentage massique, a été déterminée après vieillissement et rinçage à l'eau de ces derniers: 60-70% d'hydroxyde d'aluminium ($Al(OH_3)$), 5% de chlore ou respectivement 18% de sulfates et environ 20% d'eau ont été mesurés. Des analyses réalisées par spectroscopie ATR-IR et Raman ont révélé des différences structurales de gels au niveau moléculaire selon qu'ils étaient dérivés de solutions de chlorure ou bien de sulfate d'aluminium, ces derniers adoptants vraisemblablement une structure de type Keggin. Des images obtenues au MEB en mode d'électrons rétrodiffusés et des cartographies aux rayons X de coupes transversales d'échantillons ont permis de montrer le développement d'une matrice d'hydroxyde d'aluminium autour des particules de scorodite, ceci dans le cas du vieillissement de particules de scorodite au sein de gels dérivés de sulfate d'aluminium, pour une durée minimum d'une journée et à une température de 22ºC. Une diminution considérable du taux de rejet d'arsenic a été observée dans le cas d'expériences de vieillissement pratiquées sur des particules de

scorodite encapsulées au moyen des gels en comparaison avec le cas de particules non encapsulées. Aussi, l'encapsulation de particules de scorodite au sein de gels sulfatés, telle que la fraction molaire Al/As = 0.1, a atteint un état d'équilibre tel qu'une concentration de 0.2 ± 0.1mg/L en arsenic rejeté a été mesurée à un pH de 7.3. Cette concentration à l'équilibre s'est avérée 50 fois inférieure à celle mesurée dans le cas de particules non encapsulées.

Acknowledgements

First and foremost I would like to thank my supervisor, Professor George P. Demopoulos, for giving me an opportunity to conduct research under his supervision, for his invaluable guidance and especially for the enormous amount of time devoted to correcting this thesis.

This work would not have been possible without the support of industrial partners, including; AREVA Resources Inc., Barrick Gold, Cameco, Hatch and Teck Cominco. Their sponsorship is enthusiastically acknowledged. The generous support of the Natural Sciences and Engineering Research Council of Canada (NSERC) is also recognized.

I would also like to thank members of the Hydrometallurgy Group at McGill, who helped me with my time at McGill in the form of discussions, advice and friendship. Thanks go to Sebastian, Kee Eun, Nick, Renaud and Richard. Special thanks go to Cecile for help in translating the abstract. The help of Levente and Vincent is gratefully acknowledged for their in depth advice and for sharing the benefit of their experience. Thanks to Vera for insight into the aluminum system and to Jeff for general advice and help in SEM imaging. Thanks to Mario for conducting vibrational spectroscopy and helping me with interpretation of NMR, ATR-IR and Raman data.

Special thanks to Ranjan Roy for method development, troubleshooting and general advice in solution analysis by ICP-AES. Thanks to Glenna Keating for confirmation of the ICP results by Atomic Absorption analysis. I would also like to acknowledge the invaluable help of Helen Campbell, Monique Riendeau, Petr Fiurasek and Frederick Morin for solids characterization using a variety of techniques.

Thanks go to my family and friends outside of McGill, who have given me general advice and have always been there to encourage me over the last two years. I would also like to recognize my friends in the Department of Materials Engineering who were always willing to stop in the halls for a quick chat and to go out for a few drinks at

the end of a long week. Thanks go to Dave, Max, Nathan, Pat, Phil, Ryan and to the others that are too many to name!

Last, but certainly not least, a very big thank you to Alexandra Kallos for her love, support and advice over the past two years. Without her encouragement and faith in my abilities I do not think it would have been to keep my spirits up when the going got tough.

Table of Contents

List of Figures

List of Tables

Chapter 1: Introduction

Arsenic is a common impurity element in many non-ferrous metallurgical operation feedstocks. The presence of arsenic can adversely affect metal extraction as well as product purity and must therefore be removed and disposed of in a stable form [1]. Arsenic is highly toxic to both plants and animals and disposed solids must be sufficiently stable to prevent release of soluble arsenic to the environment. Current environmental regulations in the USA dictate that arsenic levels, as established by the Environmental Protection Agency's (EPA) Toxicity Characteristic Leaching Procedure (TCLP), should not exceed 100 times the Drinking Water Standards Maximum Contaminant Level (MCL) [2]. As the standard (MCL) was recently reduced to 10 μg/L, this implies that the TCLP leachability should therefore not exceed 1 mg/L arsenic.

A common technique for arsenic removal and fixation from process streams involves co-precipitation with ferric iron via lime neutralization. This results in a sludge with poor settling characteristics, which is sufficiently stable if the molar ratio of Fe(III) to As(V) is 4 or higher [3]. However, this technique is not feasible for arsenic-rich and iron-deficient streams such as smelter flue dusts due to the need for large amounts of excess iron. An alternative method of arsenic disposal is the formation of the crystalline ferric arsenate, scorodite ($FeAsO_4 \bullet 2H_2O$), which has better settling characteristics and lower iron demand (Fe/As = 1 vs. 4 for the co-precipitation system). Despite passing the current Environmental Protection Agency's (EPA) Toxicity Characteristic Leaching Procedure (TCLP), it has recently been shown that scorodite will undergo incongruent dissolution at pH greater than 5 (pH used in the TCLP test) with the release of soluble arsenic and formation of ferrihydrite (FeOOH) [4]. Arsenic release is highly pH dependent and under typical tailings disposal conditions (pH = 7 - 8.5) the long term stability of scorodite may be inadequate. In addition to arsenic release at elevated pH, scorodite can also undergo reductive decomposition with the release of ferrous iron and soluble arsenic species.

An alternative method of arsenic fixation is the encapsulation of scorodite with mineral coatings that are not prone to oxidative or reductive dissolution. Previous

research at McGill University focused on aluminum and calcium phosphate coatings and it was shown that uniform coatings could be produced on scorodite particles. Although there was a significant reduction in arsenic release compared with pure scorodite, the encapsulation materials were not sufficiently robust over the long term [5].

The main objective of the present work is to explore the encapsulation of scorodite particles with a different inert material, namely aluminum hydroxides. The encapsulation process investigated involves blending scorodite with amorphous aluminum hydroxyl-gel and allowing sufficient ageing for the formation of a protective aluminum hydroxide matrix. The specific objectives of this research are:

i. Atmospheric production of crystalline scorodite by means of seeded crystallization and characterization of the resulting solids.

ii. Production of amorphous aluminum gels suitable for this application and determination of the gel nature.

iii. Ageing of gel/scorodite mixtures with characterization of the mixtures and long term stability evaluation.

This thesis is organized into several chapters, which include: Chapter 1 and Chapter 2 are the introduction and literature review of the relevant material, respectively. The literature review covers current arsenic disposal practices in the metallurgical industry along with a review of the formation and stability of scorodite and previous encapsulation work. The formation of aluminum gels is discussed as well as arsenic adsorption by crystalline aluminum hydroxides.

Chapter 3 includes the experimental procedures employed for the synthesis of scorodite, production of aluminum gel, blending and ageing of the two products and subsequent evaluation of their stability. The various chemical reagents and characterization techniques employed are also outlined. Chapter 4 presents results from the experimental work with relevant discussion and Chapter 5 draws global conclusions regarding the findings of the present work.

Chapter 2: Literature Review

2.1 Arsenic Problem

Arsenic is an abundant element in the earth's crust that is present in over 300 different arsenates and related minerals and has an average terrestrial concentration of 5 ppm [6]. Some of the common arsenic minerals associated with base metal ores and concentrates include various arsenides, sulphides and oxide forms, which will inevitably end up in metallurgical streams. This will not only increase production costs at metallurgical operations, but can also interfere with metal extraction and adversely affect product purity [7]. The contained arsenic is thus an impurity element and it is critical that it be removed from process streams and disposed of in environmentally stable forms.

In pyrometallurgical operations such as smelting or converting, the majority of arsenic will be volatilized to a sulphide (As_2S_3) or oxide (As_2O_3) [8] and is recovered by electrostatic precipitators or wet gas scrubbers. These forms of arsenic have a relatively high solubility in water and can therefore not be stockpiled for long periods of time due to the danger of soluble arsenic release to the environment [9].

In hydrometallurgical plants, arsenic is present in a variety of different processes. Arsenic appears in the electrolyte of copper electrorefineries and is commonly removed as copper arsenate by processing bleed streams through liberator cells to keep arsenic concentrations low [10]. In high temperature/pressure oxidation operations such as those used to treat refractory gold ores, or several copper containing ores, arsenic can report as the relatively insoluble crystalline ferric arsenate, scorodite ($FeAsO_4 \bullet 2H_2O$) [11]. Depending on conditions of temperature, Fe/As molar ratio, acidity and retention time, the formation of other phases such as iron(III) arsenate sub-hydrate (IAsH; $FeAsO_4 \bullet 0.68\text{-}0.77H_2O$) and basic iron(III) arsenate sulphate (BIAS; $Fe(AsO_4)_x(SO_4)_y(OH)_z \bullet wH_2O$ where $0.36 \leq x \leq 0.69$, $0.19 \leq y \leq 0.5$, $0.55 \leq z \leq 0.8$ and $0.2 \leq w \leq 0.45$) has also been reported [12]. However, other leaching operations may result in soluble arsenic species.

Arsenic bearing minerals are also present in flotation tailings and may dissolve with the release of soluble arsenic as a result of pH changes from acid mine drainage. Common arsenic-containing minerals in flotation tailings include arsenopyrite, enargite, scorodite, mixed Fe-Ca arsenate hydrates and arsenate containing jarosite [13].

Due to the highly toxic nature of arsenic and increased environmental awareness, the disposal of arsenic is becoming more stringent. The element is toxic to both plants and animals [14] and has numerous adverse health effects in humans including cancer as well as cardiovascular and neurological problems. Currently, certain environmental regulations dictate that arsenic concentration in tailings pore water in Canada should not exceed 1 ppm [15].

2.2 Arsenic Removal and Fixation

In order to properly dispose of the arsenic by-product generated from the metallurgical processing of ores, the element must be fixed into a solid phase. There is a wide range of processing options from producing arsenical compounds such as scorodite ($FeAsO_4 \bullet 2H_2O$) to co-precipitation with iron(III) [1], but the resulting solids must be sufficiently stable to avoid release of soluble arsenic. The stability of arsenic compounds depend on characteristics of the solid particles and disposal site, where arsenic release should not occur under both oxidizing and reducing conditions over a wide pH range.

2.2.1 Co-precipitation of Fe(III) and As(V)

When a ferric (Fe^{3+}) salt solution is rapidly neutralized, an iron oxyhydroxide phase commonly known as ferrihydrite (FeOOH) has been reported to form. Ferrihydrite is excellent at adsorbing a variety of ions, including arsenate (As^{5+}) and arsenite (As^{3+}) species. When arsenic is co-precipitated with iron at pH 4-7 an arsenical ferrihydrite is has been reported to form, which is believed to be ferrihydrite with strongly chemisorbed As(V) [16]. Recent research investigations have indicated that during co-precipitation from Fe(III)-As(V) solutions, an amorphous ferric arsenate forms in addition to arsenical ferrihydrite [17]. The process is affected by numerous factors such as the Fe(III)/As(V)

ratio, type of base (CaO vs. NaOH) and the presence of co-ions like Ni and Al [18, 19]. The product resulting from this rapid neutralization process is a sludge with poor settling characteristics, but is nonetheless stable and hence widely used in hydrometallurgical facilities. Due to the high iron requirements during production, this process is not feasible for arsenic-rich and iron-deficient wastes such as flue dusts and acid plant effluents [1, 3].

2.2.2 Scorodite and Related Compounds

Autoclave processing of arsenic-containing feedstocks tends to produce crystalline arsenate-containing phases the most common of which is scorodite ($FeAsO_4 \bullet 2H_2O$). *Swash and Monhemius* [20] reported that scorodite is produced under hydrothermal conditions from sulphate solutions up to 175˚C, while at higher temperatures, some other crystalline iron(III) arsenate phases formed The latter were labeled Type 1 and Type 2 with their formation being favored at Fe/As > 1.5. Currently, work performed by other researchers of the hydrometallurgy group at McGill University [12] has demonstrated that the so-called Type 1 and Type 2 phases are respectively iron(III) arsenate sub-hydrate (IAsH; $FeAsO_4 \bullet 0.68\text{-}0.77H_2O$) and basic iron(III) arsenate sulphate (BIAS; $Fe(AsO_4)_x(SO_4)_y(OH)_z \bullet wH_2O$ where $0.36 \leq x \leq 0.69$, $0.19 \leq y \leq 0.5$, $0.55 \leq z \leq 0.8$ and $0.2 \leq w \leq 0.45$. Finally, it is interesting to note that scorodite was found to form during chloride pressure leaching of arsenopyritic gold concentrates at 170-190˚C.

2.2.2.1 Production of Scorodite

Already reference was made above that scorodite can be produced hydrothermally in an autoclave at temperatures up to 175˚C in nitrate [21], chloride [22] and sulphate [20] media. Alternatively, scorodite may be produced below the boiling point of water (at 98˚C) via supersaturation-controlled precipitation techniques [23]. This atmospheric precipitation approach to producing well-crystalline scorodite was first demonstrated for chloride [24] media and later for sulphate [25] solutions. The level of supersaturation is controlled below the onset of homogeneous nucleation via proper pH selection and deposition on seed or foreign particles. Alternatively, supersaturation may be controlled

by the rate of oxidation of ferrous iron [26, 27]. Reaction temperatures can vary from 85˚C up to 100˚C, with reaction kinetics increasing dramatically with small increases in temperature [25]. The reaction kinetics generally increase with amount of seed added, since there is a higher available surface area for precipitation. Effective seed candidates include hydrothermally and atmospherically produced scorodite, as well as non-scorodite materials such as hematite and gypsum [25].

It has been shown that the presence of cations such as Co^{2+}, Cu^{2+}, Mn^{2+}, Ni^{2+} and Zn^{2+} will not affect the precipitation or stability of scorodite [28]. There is virtually no incorporation of these elements into the crystal structure, so atmospheric precipitation of scorodite can be conducted at industrial operations without loss of valuable metals.

2.2.2.2 Stability of Scorodite

Scorodite is found as a naturally-occurring mineral formed through the oxidation of arsenic bearing minerals such as arsenopyrite. Due to its widespread occurrence in a variety of climates, it is believed that it is a highly stable mineral and can control the soluble arsenic level in natural water systems [10]. One measure on the release of hazardous elements from solid waste is the U.S. Environmental Protection Agency's (EPA) Toxicity Characteristic Leaching Procedure (TCLP). This involves equilibrating solids with water at pH 5 for 20 hours and subsequently analyzing the solution for toxic element concentrations [29]. Despite passing the permissible 1 mg/L As level required by the test, scorodite has been shown to undergo incongruent dissolution at elevated pH with the formation of ferrihydrite and release of soluble arsenic [4]:

$$FeAsO_4 \bullet 2H_2O_{(s)} \rightarrow FeOOH_{(s)} + H_3AsO_{4(aq)} \qquad \text{Eqn. 2.1}$$

The effect of pH on the solubility of hydrothermally produced scorodite at 22˚C is shown in Table 1, where it is evident that release of soluble arsenic is only 0.35 mg/L at pH 5, but increases to > 95 mg/L at pH 8 [4]. These figures indicate that unacceptable levels of arsenic can potentially be released under tailings disposal conditions (pH ~ 7).

Table 1: Effect of pH on the solubility of autoclave produced scorodite [4].

pH	As Concentration (mg/L)
5	0.35
6	0.61
7	5.89
8	> 95.44
9	> 386.05

Another consideration is that at increased depths in tailings ponds, conditions become anaerobic, and hence reducing. Scorodite may undergo reductive decomposition if the Eh of the system drops below ~100 mV, releasing ferrous iron and soluble arsenic [4]:

$$FeAsO_4 \bullet 2H_2O_{(s)} + 3H^+ + e^- \rightarrow Fe^{+2} + H_3AsO4_{(aq)} + 2H_2O \qquad \text{Eqn. 2.2}$$

$$FeAsO_4 \bullet 2H_2O_{(s)} + 5H^+ + 3e^- \rightarrow Fe^{+2} + H_3AsO_{3(aq)} + 3H_2O \qquad \text{Eqn. 2.3}$$

2.3 Encapsulation of Scorodite

Given the limited stability of scorodite at high pH or under reducing conditions, encapsulation of scorodite particles with inert mineral coatings that are not prone to decomposition under reducing or oxidizing conditions may enhance its stability.

2.3.1 General Encapsulation Techniques

Previous research relating to the coating or encapsulation of particles has looked at preventing the oxidation of pyrite (FeS_2), which is a major contributor to acid rock drainage problems. By creating a mineral coating around pyrite particles, exposure to oxygen and ferric iron is prevented and oxidation is not possible. Several encapsulation procedures were tested and the most effective one in acidic environments involved the formation of an iron-oxide-silica coating. This coating was formed by passing a solution containing H_2O_2, silica and acetate through a leaching column containing sand and pyrite particles [30].

A slightly different approach to producing mineral coatings involved the in situ precipitation of calcium phosphate on sand formations surrounding oil reservoirs. This procedure involved the injection of aqueous calcium chloride and potassium phosphate solutions into sand, resulting in a consolidated yet porous structure. These are important characteristics during oil production since oil extraction is still possible, but problematic sand entrainment is eliminated [31].

Coating technology has also been studied for the application of water softening in the Netherlands. In this application, solution containing calcium (Ca^{+2}) and hydrogen carbonate (HCO_3^-) was passed through a fluidized bed reactor containing sand and a calcium carbonate coating formed on the substrate [32].

2.3.2 Aluminum Phosphate Coatings

Lagno [5] investigated the encapsulation of scorodite with the hydrated aluminum phosphate $AlPO_4 \cdot 1.5H_2O$. Homogeneous and heterogeneous precipitation experiments were first conducted in order to determine the metastable region for hydrated aluminum phosphate at 95˚C, which is shown in Figure 1 [33]. By adjusting pH to control the level of supersaturation and operating in the metastable region, homogeneous nucleation is prevented and only heterogeneous growth on foreign particles occurs.

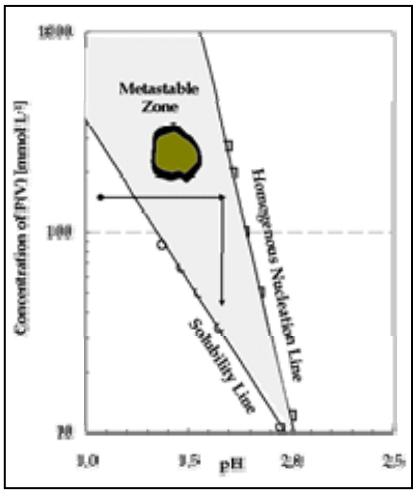

Figure 1: Metastable region for the hydrated aluminum phosphate, $AlPO_4 \cdot 1.5H_2O$, at 95˚C [33].

After synthesis of the aluminum phosphate mineral, emphasis was placed on characterizing the material and determining the mechanism of dissolution [34]. At pH less than 4, hydrated aluminum phosphate dissolves congruently with the release of soluble aluminum and phosphates. When the pH exceeds 4, soluble aluminum first builds up to a critical level in solution and then re-precipitates as the aluminum hydroxide gibbsite. The overall incongruent dissolution reaction is presented in Equation 1.4.

$$AlPO_4 \bullet 1.5H_2O_{(s)} + 1.5H_2O \rightarrow Al(OH)_{3(s)} + H_3PO_{4(aq)} \qquad \text{Eqn. 1.4}$$

Supersaturation control was subsequently used to enable direct deposition of the hydrated aluminum phosphate, $AlPO_4 \bullet 1.5H_2O$, on atmospherically produced scorodite particles. Synthesis was conducted at 95˚C at an initial concentration of 4.5 g/L Al(III) and an Al(III):P(V) molar ratio of one. Sodium hydroxide (NaOH) was used to reach the desired level of supersaturation, at which point 50 g/L scorodite seed was added and the reaction was allowed to proceed for 6 hours. Numerous deposition cycles were used to ensure a coating of effective thickness and a cross section of the coated scorodite particles is shown in Figure 2 (BSE image). It is evident that a fairly thick coating has been produced on the scorodite particle, but the coating does not completely adhere to the substrate material. This can be problematic since the coating may flake off when coated particles are subjected to mechanical impact during materials handling.

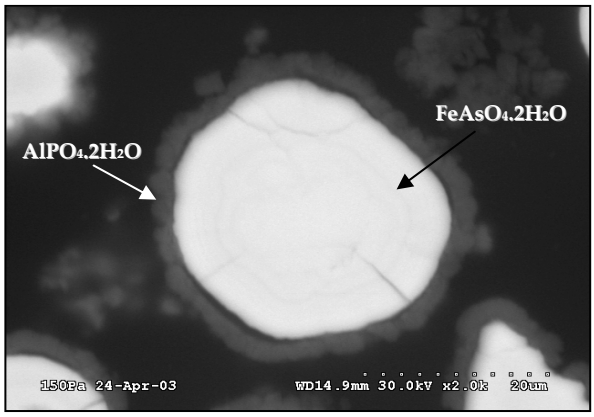

Figure 2: Scanning Electron Microscope image of the cross section of an aluminum phosphate coated scorodite particle [5].

The aluminum phosphate coating was able to partially control arsenic release under oxidizing conditions and long term stability results at pH 8 are included in Figure 3, along with the scorodite control material. Arsenic release from the coated material was an order of magnitude lower than that of scorodite; however release of phosphorus was also observed. This implies that hydrated aluminum phosphate is not an effective coating material, as the coating will eventually dissolve and expose scorodite to the environment. Arsenic release from the coated material under reducing conditions (pH = 7, E_h = 100 mV) was also significantly reduced with respect to scorodite, but the aluminum phosphate coating is nonetheless insufficiently robust for long term arsenic fixation.

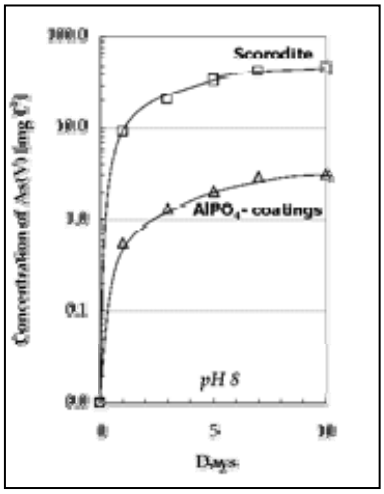

Figure 3: Arsenic release from scorodite and aluminum phosphate coated scorodite at pH 8 [5].

2.3.3 Calcium Phosphate Coatings

Lagno [5] also investigated the encapsulation of scorodite with calcium-deficient hydroxyapatite ($Ca_{10-x}(HPO_4)_x(PO_4)_{6-x}(OH)_{2-x}$, $x<2$) and the metastable zone for the system at 25˚C is depicted in Figure 4. The initial solution contained 60 mg/L Ca(II) and 28 mg/L P(V) at pH 7.6, which was allowed to equilibrate for 30 minutes at 25˚C before the addition of scorodite seed particles. The level of supersaturation was regulated by continuous addition of NaH_2PO_4 and $CaCl_2$ stock solutions at constant pH and the presence of seed particles promoted heterogeneous growth of a hydroxyapatite coating.

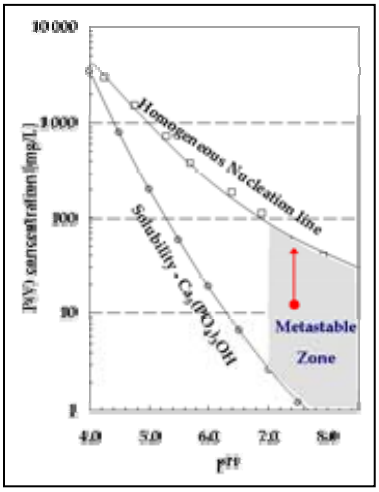

Figure 4: Metastable region for calcium-deficient hydroxyapatite, $Ca_{10-x}(HPO_4)_x(PO_4)_{6-x}(OH)_{2-x}$, x<2, at 25˚C [5].

The synthesized calcium-deficient hydroxyapatite has a molar ratio of calcium to phosphorous of 1.58 and *Lagno* found that the freshly prepared material had a highly soluble surface layer that needs to be removed prior to stability testing. The dissolution of calcium-deficient hydroxyapatite is near congruent at low pH with a slight excess in calcium release. At pH greater than 8, the release of soluble calcium and phosphorus is below stoichiometric amounts, indicating incongruent dissolution. A SEM image of calcium-deficient hydroxyapatite coated scorodite is included in Figure 5 (BSE image), where a thin coating that is well adhered to the scorodite particle is evident. XRD analysis showed that the precipitated material is hydroxyapatite, with no evidence of other calcium-phosphate phases.

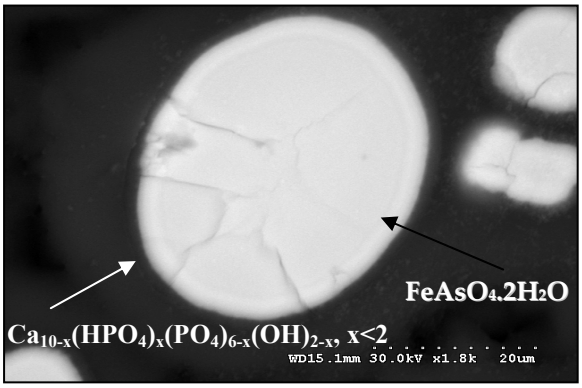

Figure 5: Scanning Electron Microscope image of the cross section of a calcium-deficient hydroxyapatite coated scorodite particle [5].

The long term arsenic release from calcium-deficient hydroxyapatite-coated scorodite, along with uncoated scorodite, is shown in Figure 6 at pH 8. Arsenic release from the coated material is not significantly less than for pure scorodite and release of soluble phosphorus once again indicates that the coating will eventually disappear. Of the two coating materials investigated by *Lagno*, the calcium-deficient hydroxyapatite one appears to be the least effective for controlling arsenic release from scorodite.

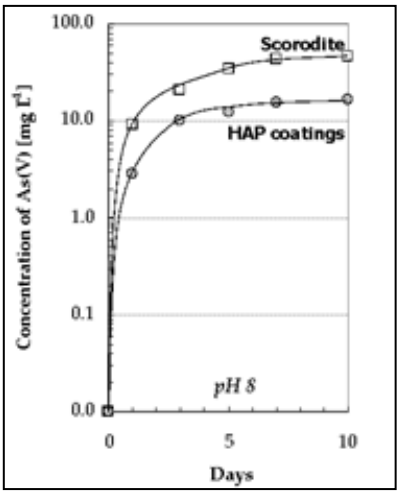

Figure 6: Arsenic release from scorodite and calcium-deficient hydroxyapatite coated scorodite at pH 8 [5].

2.4 Amorphous Aluminum Gels

Another possible material for the stabilization of scorodite type solids may be aluminum (hydroxy)gels. In general, a gel can be defined as a uniform substance that comprises a liquid phase containing solid particles too small for microscopic observation. These particles can be either finely dispersed or form a network within the substance and the gel character can range from jellylike in the case of gelatins to rigid for materials such as silica gel [35]. The aluminum gel material was observed to form during the work of *Gella* [36] who studied the precipitation of aluminum (oxy)hydroxides from chloride solutions by neutralization. It was noted during that study that at certain hydrolysis ratios an amorphous gel-like substance was produced. By mixing aluminum gels with scorodite particles and ageing under different conditions, it was hypothesized that the gels would crystallize and encapsulate scorodite with an aluminum hydroxide coating.

2.4.1 Formation of Aluminum Gels

Aluminum hydroxy gels are of interest to a wide range of industries such as water treatment and pharmaceutical applications due to the reactive nature of the colloidal particles [37]. During base hydrolysis of aluminum salt solutions, a number of species are present, including $Al(H_2O)_6^{3+}$ (monomeric), $Al_2(OH)_2^{4+}$ (dimeric) and the Al_{13} species $Al_{13}O_4(OH)_{24}(H_2O)_{12}^{7+}$ (polymeric). The Al_{13} is of special interest, since it plays an important role in the formation of aluminum hydroxides during base hydrolysis in aqueous systems. The species referred to as Keggin Al_{13} consists of one tetrahedral aluminum molecule (AlO_4) surrounded by 12 aluminum molecules in octahedral positions [38]. This species is depicted schematically in Figure 7.

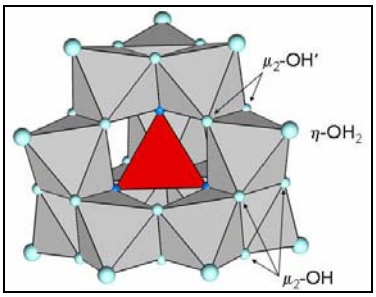

Figure 7: Schematic representation of the Keggin Al_{13} species [39].

If the hydrolysis ratio is less than 0.2 moles OH^- per mole of Al at room temperature, and the solution pH is approximately 4.1 in chloride media, monomeric aluminum is the predominant species in solution. As the ratio is increased from 0.2 to 2.5, there is minimal increase in pH to 4.6 and mononuclear aluminum combines with OH^- to form progressively larger polymer species. These are characterized as small/middle size polymers, which can range in size from Al_2 to Al_{12} and are either linear polymers (Al_2 – Al_5) or have a single / double ring structure (Al_6 – Al_{12}). Large polymers ranging from Al_{13} to Al_{54} form at hydrolysis ratios between 2.5 and 3, which is associated with a rapid increase in pH due to the slow rate of polymerization. The transient Al_{13} species features a triple ring panel structure, which will transform to the symmetric Keggin Al_{13} structure given sufficient ageing time [40]. The transformation process is accelerated if ageing is conducted at higher temperatures or in the presence of excess sulphate ions. However, high temperatures are only beneficial if the hydrolysis ratio exceeds 1.8 otherwise it is

detrimental to the formation of Keggin Al_{13} [37]. The speed of neutralization is an important factor in the formation of the Keggin Al_{13} structure, which is promoted at slow base addition rates for high concentration Al salt solutions and high base addition rates for low concentrations of Al. Local supersaturation can occur if the rate of base addition is excessively high, which leads to the formation of amorphous aluminum hydroxide and only minor quantities of Keggin Al_{13}. The polymeric aluminum species are only stable in acidic conditions and once the hydrolysis ratio exceeds 3, the polymers begin to dissolve with the formation of $Al(OH)_4^-$ [40].

At hydrolysis ratios approaching 2.3 moles OH^- per mole of aluminum, Al_{13} is the predominant species and polymerization starts to occur with the aggregation of these species. In chloride salt solutions, this is associated with progressive removal of Cl^- and the net positive charge decreases as water molecules are replaced by OH^-. The resulting product is an amorphous aluminum hydroxide solid that is metastable and may transform into a crystalline aluminum hydroxide, given appropriate ageing conditions [41]. The formation of aluminum hydroxy gels is a complex process and involves numerous factors such as type of base, rate of base addition, concentration of base, hydrolysis ratio, temperature and type of mixing employed [40].

The surface area of the produced solids can vary widely and is heavily dependent on initial concentration of the starting reagents, ageing, type of drying and heating. If freshly prepared gels from chloride media are reacted in water for a period of 9 days, then initially high surface areas will decrease and initially low surface areas will increase to a limiting value of 32.4 m^2/g (BET surface area) [42].

2.4.2 Crystallization of Aluminum Gels

According to *Bottero et al.*, Keggin Al_{13} is the prerequisite for the formation of crystalline aluminum hydroxides, which form through a self assembly process [41]. This is a solid state mechanism, where crystalline aluminum hydroxides are formed through re-ordering of the aluminum gel structure and does not require redissolution and crystallization. Other researchers have found evidence to the contrary stating that Keggin

Al_{13} does not directly convert to gibbsite, but decomposes to smaller polymeric species with octahedral structures. These species then serve as a pool of aluminum for the formation of gibbsite, but the rate of formation is determined by the existence of colloidal Al species [37]. It has also been reported that the use of high intensity ultrasound during the conversion process is detrimental to the formation of the crystalline aluminum hydroxide bayerite [43].

Through Mass Adsorption Spectroscopy – Nuclear Magnetic Resonance (MAS-NMR) studies of $GaAl_{12}$ gels, a possible model was proposed for the formation of crystalline phases from aluminum gels [44]. During ageing the consolidation of aluminum tridecamers and other species present in solution would result in the initial formation of a pseudo – spinel structure referred to as pseudo – boehmite (AlOOH). The subsequent cleavage of Al – O – Al bonds yields a boehmite phase with defects, the number of which depends on the degree of order in the aluminum gel. Further ageing allows time for structural rearrangement and the aluminum hydroxide bayerite is the resulting phase [44]. The three aluminum hydroxide polymorphs are bayerite, gibbsite and Nordstrandite, and they differ only in the stacking sequence of the Al – OH layers [37].

The rate of crystallization from amorphous aluminum gels to crystalline aluminum hydroxides greatly varies in the literature and depends on factors such as Al^{3+} concentration, hydrolysis ratio, ageing temperature and ageing time. At low aluminum concentrations (0.02M) and at a hydrolysis ratio of 2.5, gibbsite was observed after 6 months ageing at room temperature but only after 20 days ageing at 60˚C [40]. When neutralizing a 0.5M aluminum chloride solution to a hydrolysis ratio of 3, the short-range order of bayerite was observed after only 24 hours [41]. A separate study confirmed the presence of crystalline bayerite after ageing a gel produced from 0.1M aluminum chloride solution at a hydrolysis ratio of 3 for 4 days [44].

2.4.3 Arsenic Adsorption on Aluminum Hydroxide

In addition to ferrihydrite, aluminum hydroxides are also well known for adsorbing a number of ions including arsenic. Aluminum hydroxides are effective adsorbents for arsenate ions, but perform poorly at adsorbing arsenite species [45-48]. Although iron hydroxide or ferrihydrite has been shown to be more effective for arsenic adsorption than aluminum hydroxides [46], there is the risk of reductive dissolution of arsenic-adsorbed ferrihydrite and release of arsenic to the environment. When aluminum is substituted in the structure of iron oxides the adsorption capacity for both arsenate and arsenite species is decreased. However, the rate of reductive dissolution of arsenic-adsorbed ferrihydrite is reduced when aluminum has been substituted in the structure [46]. It has also been reported that the presence of the inorganic species SiO_3^{2-} and PO_4^{3-} increase arsenic release from arsenic adsorbed Al-ferrihydrite [49].

Anderson et al. [50] studied the adsorption of arsenate ion on amorphous aluminum hydroxides. The kinetics of adsorption are extremely fast; over 90% of the adsorption reaction took place before sampling could be conducted and the system reached equilibrium after 48 hours. Conversely, the adsorption of arsenite species on gibbsite has been found to be relatively slow [45]. Adsorption is a complex function of pH [51] and concentration of arsenate in solution, with maximum adsorption of arsenate occurring at the isoelectric point. The pH of the isoelectric point for a suspension of pure aluminum hydroxide is 8.5, but decreases to a limiting value of 4.6 as progressively more arsenate is added to solution [46, 50]. Adsorption of arsenate was shown to increase with pH up to the isoelectric point after which it reached a maximum and then decreased with further increases in pH [46, 50]. Adsorption of arsenate on amorphous aluminum hydroxides is attributed to two mechanisms, namely coulombic forces and chemical adsorption and surface complexation. At pH values less than that of the isoelectric point, the surface charge of the aluminum hydroxide particles are positive and coulombic attraction assists in the adsorption of arsenate anions. When pH is higher than that of the isoelectric point (> 4.6), the surface charge is negative and chemical adsorption is in competition with repulsion by the surface charge [46].

Chapter 3: Experimental

3.1 Introduction

The experimental work described in this thesis is broken down into four major sections, which comprise (1) synthesis of scorodite particles; (2) production of aluminum gels; (3) ageing of scorodite with aluminum gels; and (4) long term stability evaluation. Scorodite was first produced homogeneously in an autoclave, which was used as seed in atmospheric precipitation experiments to produce large batches of scorodite particles. The production of aluminum gel involved looking at different factors that affect the gel formation in order to develop a procedure to consistently produce gels of acceptable quality. For the purpose of this study, a gel of acceptable quality is defined as one that is sufficiently viscous to enable solid particles to be blended with the gel without subsequently settling. Ageing tests involved blending together scorodite with aluminum gels and ageing under various conditions. Following ageing, the mixtures were washed and subjected to stability evaluation by equilibrating them with de-ionized water at pH 8 for extended periods of time.

3.2 Chemicals

The chemicals used for synthesis of scorodite, production of aluminum gels and stability testing are listed in Table 2. Water purified by a Biolab 2200 portable reverse osmosis system was used in all procedures.

Table 2: List of chemical reagents used.

Name	Formula	Supplier	Grade
Arsenic(V) Oxide Hydrate	$As_2O_5 \bullet xH_2O$	Aldrich	Reagent (A.C.S.)
Iron(III) Sulphate Hydrate	$Fe_2(SO_4)_3 \bullet xH_2O$	Aldrich	Reagent (A.C.S.)
Iron(III) Nitrate Nonahydrate	$Fe(NO_3)_3 \bullet 9H_2O$	A&C	Reagent (A.C.S.)
Aluminum Chloride	$AlCl_3 \bullet 6H_2O$	Fisher	Reagent (A.C.S.)
Aluminum Sulphate Octadecahydrate	$Al_2(SO_4)_3 \bullet 18H_2O$	Fisher	Reagent (A.C.S.)
Sulphuric Acid	H_2SO_4	Fisher	Reagent (A.C.S.)
Nitric Acid	HNO_3	Fisher	Reagent (A.C.S.)
Hydrochloric Acid	HCl	Fisher	Reagent (A.C.S.)
Sodium Hydroxide, 5 N	NaOH	Fisher	Reagent (A.C.S.)
Calcium Oxide	CaO	Fisher	Reagent (A.C.S.)
Magnesium Oxide, Light	MgO	Aldrich	Reagent (A.C.S.)
Silver Nitrate	$AgNO_3$	A&C	Reagent (A.C.S.)

3.3 Chemical Analysis

The concentrations of arsenic, iron, sulphur, aluminum and sodium in aqueous samples were analyzed using a Thermo Jarell Ash IRIS Inductively Coupled Plasma – Atomic Emission Spectrometer (ICP-AES). Analysis was conducted in a 4% nitric acid matrix and a multi point calibration was performed with standards containing 0, 0.5, 5 and 50 mg/L As, Fe, S, Al and Na. Standards were prepared from 1000 µg/mL PlamsaCAL ICP standards from SCP Science. Accuracy of the arsenic analysis results from ICP-AES were confirmed on select samples via analysis by hydride generation atomic adsorption (AA). Chemical analysis of solids was performed by dissolving solids in either nitric acid or a nitric/hydrochloric acid mixture prior to analysis by ICP, as outlined in Appendix A.

For determination of the chloride content in aqueous samples, the AgCl gravimetric technique was employed where silver nitrate was added to the sample. The resulting solids were subsequently collected, dried and weighed in order to calculate the

total amount of chlorine in the sample. This number was then reported as a concentration in the aqueous sample.

3.4 Characterization

Various characterization techniques were employed to examine the physical characteristics of the scorodite particles and aluminum gels, as well as determine their interaction in aged samples.

- **X-Ray Powder Diffraction Analysis (XRD):** Powders were analyzed by a Philips PW 1710 X-Ray Diffractometer with a 1.5405 Å CuKα radiation source to determine the major crystalline phases in the sample. Samples were scanned from 2 to 100 (2θ) at a step size of 0.1 (2θ) and a time of 3 seconds per scan step.

- **Particle Size Analysis (PSA):** Particle size distributions of scorodite materials were determined with a Horiba LA-920 Laser Scattering Particle Size Analyzer in an isopropanol medium.

- **BET Surface Area Determination:** BET surface area was determined using a Micromeritics TriStar Surface Area and Porosity Analyzer for aluminum hydroxide, dried aluminum gel and scorodite samples. Prior to analysis, samples were degassed with a Micromeritics FlowPrep 060 Sample Degass System.

- **Thermogravimetric Analysis (TGA):** Thermogravimetric analysis was conducted on a TA Instruments Q500 TGA from room temperature to 900˚C at a ramp rate of 20˚C/min and using nitrogen gas for dried aluminum gel and scorodite samples.

- **Scanning Electron Microscopy (SEM):** Scorodite and aluminum gel particles were placed on double sided carbon tape and subsequently coated with a gold/palladium layer before being examined in a Hitachi S-4700 Field Emission Scanning Electron Microscope (FE-SEM) for particle morphology. Elemental mapping of particle cross sections was achieved by mounting particles in cold setting epoxy resin, polishing the

samples and coating with a gold/palladium layer before obtaining x-ray maps with a Hitachi S-3000N Variable Pressure Scanning Electron Microscope (VP-SEM).

- **Attenuated Total Reflectance Infrared (ATR-IR) Spectroscopy:** ATR-IR spectra were obtained with a Perkin Elmer (Spectrum BX model) Fourrier Transform Infrared (FTIR) spectrometer with a Miracle single bounce diamond ATR cell from PIKE Technologies for dried pure gel, scorodite and gel/scorodite samples.

- **Raman Microscopy:** Raman spectra were collected on a Renishaw Invia microscope with a 50x short distance objective and a polarized argon laser at 514 nm operating at 10% power at the microscope exit for dried pure gel, scorodite and gel/scorodite samples.

- **Magic Angle Spin Nuclear Magnetic Resonance (MAS-NMR) Spectroscopy:** ^{27}Al Nuclear Magnetic Resonance spectra were obtained with a Chemagnetics CMX-300 spectrometer operating at 78.07 MHz. Dried aluminum gel samples were packed in a 7.5 mm rotor and spun at the magic angle at 4.5 kHz. Typical spectra were the result of 256 transients acquired with a 1.6 microsecond pulse and an acquisition time of 200 ms.

3.5 Synthesis of Scorodite

3.5.1 Laboratory Set-up

The homogeneous production of scorodite used as seed in the atmospheric precipitation tests required high temperatures, for which a 2 L Parr titanium autoclave was used. This is a glass-lined bomb autoclave with a mechanical impeller capable of agitation of 10 to 600 rpm and reaction temperature is attained through the use of heating coils.

Atmospheric precipitation tests were conducted in a 1 L Pyrex glass beaker with a custom lid and agitation was achieved with a PVC marine-type impeller. The custom lid was manufactured out of CPVC and had five holes that were plugged with rubber stoppers during operation to prevent heat loss and evaporation. These holes provided a simple means of access during reaction for reagent addition and sampling, as well as pH

and temperature measurement. With this setup, heating the solution to the required reaction temperature was accomplished simply by placing the beaker on a Cole Parmer Model 4658 Stirrer/Hot Plate and manually monitoring the reaction temperature. A picture of the setup is presented in Figure 8.

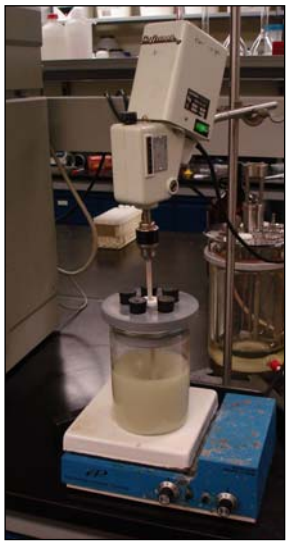

Figure 8: Experimental setup used for the atmospheric precipitation tests.

Large batches of scorodite used in the ageing tests were produced in a 3 L Applikon® bioreactor adapted for inorganic aqueous precipitation research, which is shown in Figure 9.

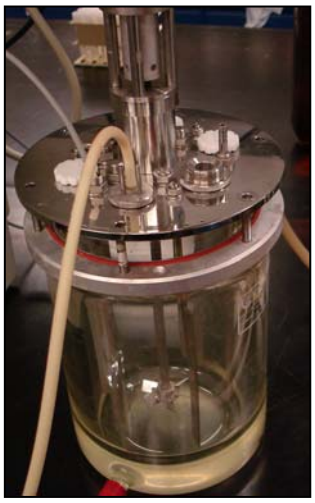

Figure 9: Applikon® reactor used for the atmospheric production of large batches of scorodite.

Included in the setup was the ADI 1010 BioController, which has the capability to measure and control pH, agitation speed and reaction temperature. For the purpose of scorodite production, the control unit was only used to monitor pH and adjustments were conducted manually through one of the inlet ports. The reactor is a double walled vessel with baffles and reaction temperature (95˚C) was maintained with a 3 L HAAKE DC30-B3 Heating Circulator oil bath. The progress of precipitation was monitored by drawing slurry samples from the sampling port with the aid of a plastic syringe.

3.5.2 Procedure

Scorodite seed was produced in the 2 L Parr titanium autoclave at 160˚C with an initial arsenic concentration of 0.3M and an iron(III) to arsenic(V) molar ratio of one [21]. The As(V)-Fe(III)-HNO_3 solution was prepared by dissolving appropriate amounts of reagent grade arsenic pentoxide (As_2O_5) and iron(III) nitrate nonahydrate ($Fe(NO_3)_3 \bullet 9H_2O$) in de-ionized water. Upon heating the solution to reaction temperature, precipitation was allowed to proceed for 24 hours and the slurry was subsequently filtered on a vacuum filter with Whatman No. 5 qualitative filter paper. The solids were re-pulped with acidified (pH = 2, HNO_3) de-ionized water and stirred for 24 hours in four separate contacts in order to remove any soluble material. The solids were then dried in an oven at 50˚C until a constant mass was achieved. The autoclave produced scorodite was subsequently used as seed during atmospheric precipitation tests.

Atmospheric precipitation of scorodite was conducted in sulphate (SO_4^{2-}) media at a reaction temperature of 95˚C, following the supersaturation-controlled procedure previously established in this laboratory [25]. The stock As(V)-Fe(III)-H_2SO_4 solution was prepared by dissolving arsenic pentoxide and ferric sulphate ($Fe_2(SO_4)_3$) in 250 mL de-ionized water and the investigated arsenic concentrations were 10, 20 and 40 g/L. The molar ratio of iron to arsenic was maintained at one for all experiments. Upon heating to the reaction temperature in the 1 L beaker setup a cloud was observed to form signaling the spontaneous (homogeneous) nucleation of an amorphous ferric arsenate phase. This cloud was observed to appear at increasingly higher temperature as the concentration of arsenic was raised from 10 g/L (~57˚C) to 20 g/L (~90˚C) to 40 g/L (~95˚C). Upon

attainment of the target temperature (95˚C) sufficient sulphuric acid was added to the solution to clear the amorphous phase that formed. This ensured that the supersaturated solution was in a sufficiently metastable state to promote heterogeneous growth and 5 g/L of the autoclave produced scorodite seed was subsequently added. The reaction was allowed to proceed for 3 to 6 hours and the final slurry was filtered on Whatman No. 5 qualitative filter paper. During precipitation, samples were taken at regular intervals, filtered, acidified with nitric acid and analyzed for iron and arsenic to monitor precipitation with time.

The scorodite solids were subjected to several washing steps in order to remove any soluble material prior to stability tests. Solids were mixed with 400 mL acidified de-ionized water (pH = 2.5, HNO_3) and stirred for 4 consecutive periods of 24 hours and re-pulped twice with 60˚C acidified de-ionized (pH = 2, HNO_3) water between each step. The final solids were dried in an oven at 50˚C and the wash solutions were analyzed for iron and arsenic content. Following washing, the solids were subjected to 8 consecutive TCLP-type contact steps in order to rapidly determine the relative leachability of the produced scorodite. For each step, 2 g solids were combined with 80 mL de-ionized water in a 125 mL Erlenmeyer flask and agitated for 24 hours on an orbital shaker. The solution from each TCLP-type step was acidified with nitric acid and analyzed for iron and arsenic concentration.

Based on batch yield and TCLP-type leachability response from the atmospheric precipitation tests, two large batches of scorodite were produced in the Applikon® reactor for use in the ageing tests. In this vessel, 1.5 L As(V)-Fe(III)-H_2SO_4 solutions containing 20 and 40 g/L arsenic(V) and iron to arsenic molar ratio of one were produced in the same manner as for the initial atmospheric precipitation tests. For each batch production, the stock solution was placed in the reactor and heated to 95˚C. Reaction was allowed to proceed for 6 hours for the 20 g/L batch (Batch 1) and 9 hours for the 40 g/L batch (Batch 2), after which the slurry was filtered on a vacuum filter with Whatman No. 5 qualitative filter paper. Solids from each batch were mixed with 1.5 L acidified de-ionized water (pH = 2.5, HNO_3) and stirred for 4 consecutive periods of 24 hours and re-pulped twice with 60˚C acidified de-ionized (pH = 2, HNO_3) water between each step.

Subsequent to washing, 2 g solids were subjected to 7 consecutive TCLP-type leachability steps as per the atmospheric precipitation tests.

3.6 Production of Aluminum Gel

Aluminum gels were prepared through the base hydrolysis of aqueous aluminum solutions with reagent grade 5.0N sodium hydroxide (NaOH). Two experimental set-ups were used, including the custom set-up from the atmospheric scorodite precipitation tests and 125 mL Erlenmeyer flasks placed on magnetic stirring/hot plates. The beaker set-up was abandoned early on in favor of the Erlenmeyer flask setup, as the flasks permitted numerous quick tests to be performed in a short period of time when rapid base hydrolysis was employed.

Stock 0.1, 0.5, 1 and 2M Al^{+3} salt solutions were prepared by dissolving appropriate amounts of either aluminum chloride ($AlCl_3$) or aluminum sulphate ($Al_2(SO_4)_3$) salts in de-ionized water. The hydrolysis ratio was varied from 0.5 to 3.0 (mol OH^- per mol of Al) and reaction temperatures of 20, 60 and 95˚C were investigated. For the majority of tests the entire volume of sodium hydroxide was added to the aluminum salt solution all at once, followed by mixing. Mixing was achieved with either magnetic stirrers or by manually shaking the flask if the mixture became excessively viscous for magnetic stirring. Manual mixing with a glass stir rod was another technique used, as it allowed good control over the extent of mixing. This is an important consideration, as the extent of mixing has an effect on the viscosity of the resulting aluminum gel.

For the current study, an aluminum gel of acceptable quality for ageing tests is one that is sufficiently viscous to enable solid particles to be blended with the gel without subsequently settling. It was observed that quality gels were produced from 2M Al^{3+} salt solutions (50 mL) at room temperature and at a hydrolysis ratio of 2.5 (50 mL NaOH). Mixing was achieved manually with a stir rod and care was taken to ensure that the gel did not thin out due to excessive stirring. In addition to sodium hydroxide as neutralizing agent, 5 wt.% calcium oxide (CaO) slurry was also investigated as an alternative.

3.7 Ageing of Scorodite with Aluminum Gels

The general flow sheet employed in this work is presented in Figure 10 and can be broken down into five steps, namely (1) atmospheric production of the crystalline ferric arsenate, scorodite; (2) production of amorphous aluminum gels; (3) blending and ageing of scorodite with aluminum gel; (4) washing followed by solid / liquid separation; and (5) TCLP-type pretreatment and long term stability evaluation. The procedures for the first two steps have been outlined in detail in sections 3.5 and 3.6, respectively. The ageing conditions and washing of the aged products are discussed here and stability testing is covered in section 3.8.

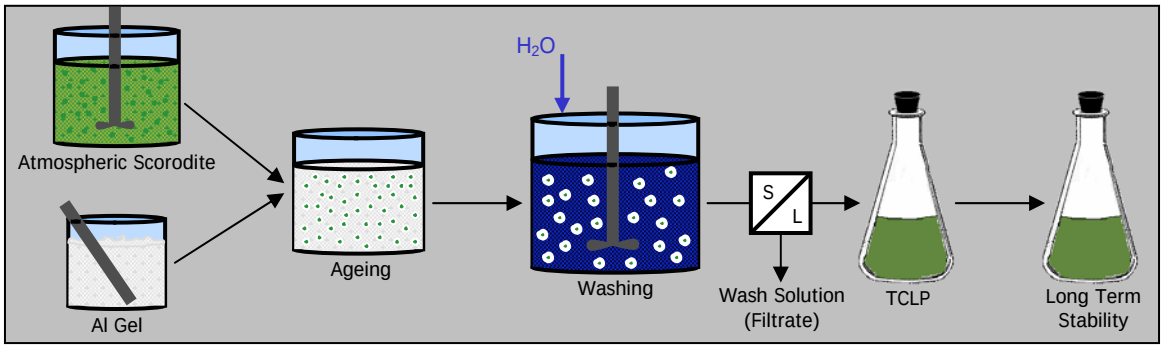

Figure 10: General flow sheet for preparation of aluminum gel / scorodite mixtures.

The various ageing procedures investigated in the present work are summarized in Table 3. The variables related to the blending and ageing procedure include Al:As ratio in the blended product, type of gel used, open vs. closed system ageing, ageing temperature and ageing time. The Al:As molar ratio in the blended mixture is a measure of how much gel is used in the stabilization process. Higher ratios were generally employed during the initial developmental work and lower ratios were applied during the optimization phase, when practical application issues became a consideration. Gel type refers to gels that were produced by the base hydrolysis of either aluminum chloride or sulphate salt solutions with sodium hydroxide. In open system ageing, the gel/scorodite mixture was exposed to the atmosphere and water evaporation occured over time, as opposed to closed system ageing where the mixture was placed in a sealed container. Ageing temperature was investigated mainly in closed system ageing tests, where the mixture was maintained at a specific temperature by placing the sealed container in a water bath. The one

exception was the open system test where the sample was placed in an oven (Test ID 6). Finally, ageing time refers to the period of time that the mixture was kept before washing and subsequent stability testing was conducted. Tests 3 to 6 were performed with scorodite from Batch 1 solids, while tests 13 to 20 were executed with Batch 2 solids.

Table 3: Different ageing procedures investigated.

Test ID	Al:As	Gel Type	Open vs. Closed	Temperature (˚C)	Ageing Time (Days)
3	1.54	Cl^-	Open	22	21
4	0.96	Cl^-	Closed	40	54
5	0.96	Cl^-	Closed	70	1
6	0.96	Cl^-	Open (in oven)	50	1
7	1.5	SO_4^{2-}	Open	22	28
13	1	Cl^-	Open	22	21
14	1	Cl^-	Closed	22	21
15	0.1	Cl^-	Open	22	21
16	0.1	Cl^-	Open	22	7
17	0.1	Cl^-	Open	22	1
18	0.1	Cl^-	Open	22	1
19	0.1	SO_4^{2-}	Open	22	1
20	0.1	SO_4^{2-}	Open	22	1

A single washing step was employed prior to stability testing in order to remove the bulk soluble material from the aged samples. This step was by no means intended to remove all soluble species prior to stability testing, but as an initial look at how the aged samples reacted when introduced to a relatively large quantity of water. The procedure involved placing a measured amount of aged material in a Pyrex glass beaker and adding de-ionized water to a 10:1 liquid/solid ratio. The mixture was then stirred for 24 hours before filtering the entire suspension on a vacuum filter with Whatman No. 5 qualitative filter paper. The filtrate was acidified with nitric acid and analyzed for Fe, As and Al content by ICP-AES. Select filtrates were also analyzed for sulphur and sodium concentration. One portion of the washed solids was used for stability testing, while the rest was reserved for chemical digestion and characterization. In addition to the aged gel/scorodite mixtures, one sample each of aluminum sulphate and chloride gel were aged under open conditions for 2 weeks before washing the resulting solids. This served

as a basis for comparison when conducting mass balances around the washing step for the aged gel/scorodite material and for characterization of pure gels.

3.8 Stability Testing

Prior to long term stability testing, samples were subjected to numerous leaching steps of a TCLP-type procedure in an effort to remove any remaining soluble material. This method involved placing 2 grams of solids from each gel-scorodite ageing test in a 125 mL Erlenmeyer flask and adding 80 mL de-ionized water (40:1 ratio of liquid to solids). The flasks were agitated with an orbital shaker for 24 hours before filtering the slurry on a vacuum filter with qualitative filter paper to separate the solid and liquid phases. The liquid component was acidified with nitric acid for chemical analysis (Fe, As, Al) and the solids were mixed with 80 mL de-ionized water in preparation for another 24 hour contact. A total of 6 contacts were conducted prior to the long term stability tests, the number of which was based on the number of contacts required to achieve the same level of soluble species as in the previous contact. In addition to the aged gel/scorodite samples, autoclave produced scorodite (Test ID 2) seed as well as Batch 1 (Test ID 1) and Batch 2 (Test ID 8) scorodite were subjected to this type of pretreatment to remove any soluble amorphous material resulting from the precipitation tests as was previously reported by *Bluteau and Demopoulos* [4]. Typical soluble metal trends for this TCLP-type pretreatment procedure are shown in Figure 11 for the aluminum chloride gel/scorodite blend (Al/As = 0.1) aged under open conditions for 21 days at room temperature (Test ID 15). It is evident that the concentration of metals stabilized after 6 TCLP-type contacts, indicating that any highly soluble species that may have skewed long term stability results have been removed.

Similarly, physical mixtures of 1 wt% and 10 wt% each of amorphous aluminum hydroxide and bayerite with Batch 2 scorodite were subjected to TCLP-type pretreatment (Test ID 9-12). These tests served as a simple means of verifying whether reduction in arsenic release from the aged gel/scorodite mixtures could be attributed to adsorption by aluminum hydroxide. These solids were produced by the base hydrolysis of aluminum

chloride salt solutions and the procedure is adapted from *Gela's* [36] work, described in Appendix B.

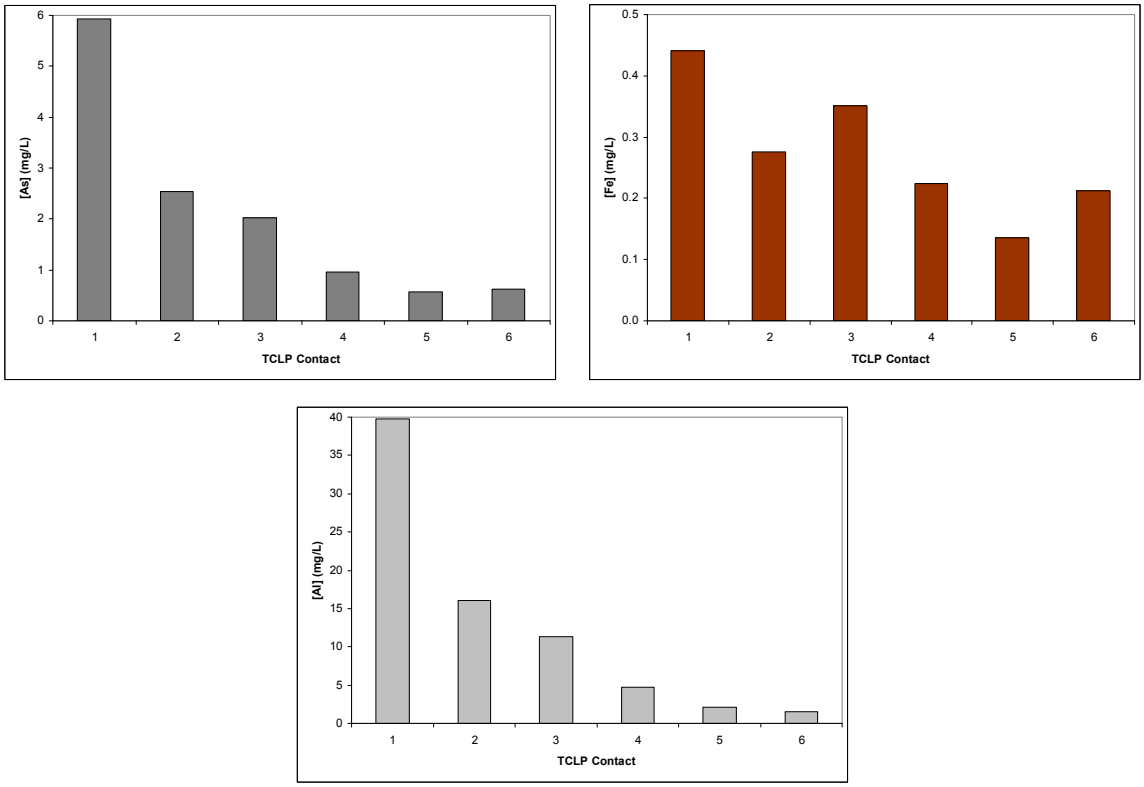

Figure 11: Levels of arsenic, iron and aluminum observed during the TCLP-type pretreatment of the chloride gel/scorodite mixture (Al/As = 0.1) aged under open conditions for 21 days (Test ID 15).

Solids from the final pretreatment step were placed in sealed 125 mL flasks with 80 mL de-ionized water and agitated with an orbital shaker for long term stability evaluation. Samples were taken on a regular basis with 10 cc plastic syringes, which were filtered on Whatman Anotop 25 0.02 μm pore size syringe filters and diluted with acidified (HNO_3) de-ionized water in preparation for chemical analysis.

Measurement of solution pH was conducted using an Orion 720A pH meter employing three point calibration with pH = 4.0, 7.0 and 10.0 buffers for all long term stability evaluations. Numerous electrodes were used to ensure consistent accuracy of measurements, which include (1) a Corning high performance refillable combination electrode; (2) a Cole-Parmer AcutupH refillable double-junction electrode (general purpose); and (3) a Cole-Parmer sealed double-junction KNO_3 gel electrode. The pH of

test ID 1-7 and 13a were adjusted to 8 with 1 M sodium hydroxide on a weekly basis for the first month, after which it was only adjusted if the pH value dropped excessively. This combination of pH drift and control technique was adopted since it was realized that frequent pH control resulted in system upsets that made the attainment of equilibrium difficult and longer to achieve. Based on these observations, 0.5 M magnesium oxide (MgO) slurry was used to adjust the pH of the remaining tests (Test ID 8-12, 13b, 14-20). The pH of the samples was first measured and a few drops of magnesium oxide slurry (~2 wt.%) was added. A period of at least 3 hours was allowed between adjustments to ensure a steady value was reached and that the set point was not exceeded. After the target of pH 8 was reached, the stability evaluation was allowed to operate in a pH drift mode.

Chapter 4: Results and Discussion

The results from the present research study are presented and discussed in this chapter. The chapter is divided into four main sections, namely (1) synthesis of scorodite; (2) production and characterization of aluminum gels; (3) ageing of aluminum gel/scorodite mixtures; and (4) stability testing. In the synthesis of scorodite section, the effect of arsenic concentration on the quality of scorodite is examined and optimum conditions for its production are identified. In section 2, the nature of the produced aluminum gels and hydroxides is investigated followed in section 3 with a review of the ageing procedures and characterization of the aged gel/scorodite mixtures. In the final section, the stability of the aged gel/scorodite samples is measured in a series of long-term tests (pH = 7-8) and compared to gel-free scorodite and aluminum hydroxide/scorodite mixtures.

4.1 Synthesis of Scorodite

The production of scorodite by precipitation at ambient pressure (95˚C) via the use of seed and supersaturation control has been described previously in a series of papers by *Demopoulos* and co-workers [9, 23, 25, 28]. This technique was adopted here for the synthesis of crystalline scorodite.

4.1.1 Characterization of Scorodite Seed

The scorodite seed was prepared by reacting a $Fe(NO_3)_3 \bullet 9H_2O - As_2O_5$ solution at 160 ˚C for 24 hours as per the method of *Dutrizac and Jambor* [21]. Here a detailed characterization of this material is presented. Chemical digestion of the autoclave produced scorodite revealed a composition of 31.4 wt.% As and 24.3 wt.% Fe, which is in good agreement with the theoretical values for scorodite of 32.5 wt.% As and 24.2 wt.% Fe. Thermo gravimetric analysis of the same scorodite (refer to Figure 12) found it to undergo a steep mass loss between 150˚C to 200˚C of 15.6 wt.%, which corresponds exactly to removal of its two waters of crystallization from scorodite. It should be noted

that further loss of mass observed above 800˚C is due to release of arsenic in the form of As_2O_5 [52].

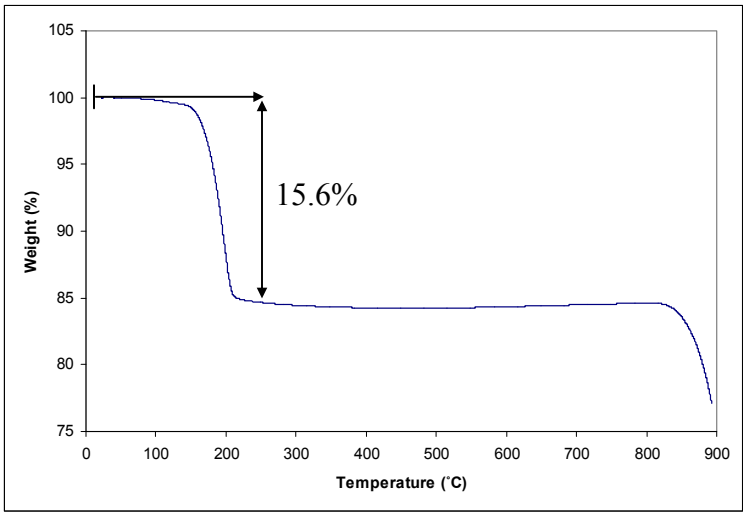

Figure 12: TGA analysis of autoclave produced scorodite seed; heating rate 20 ˚C/min.

The X-Ray Diffraction pattern obtained for autoclave-produced scorodite is shown in Figure 13. Combined with compositional and thermo gravimetric analysis, it can be concluded that the autoclave produced seed material was pure and highly crystalline scorodite ($FeAsO_4 \bullet 2H_2O$).

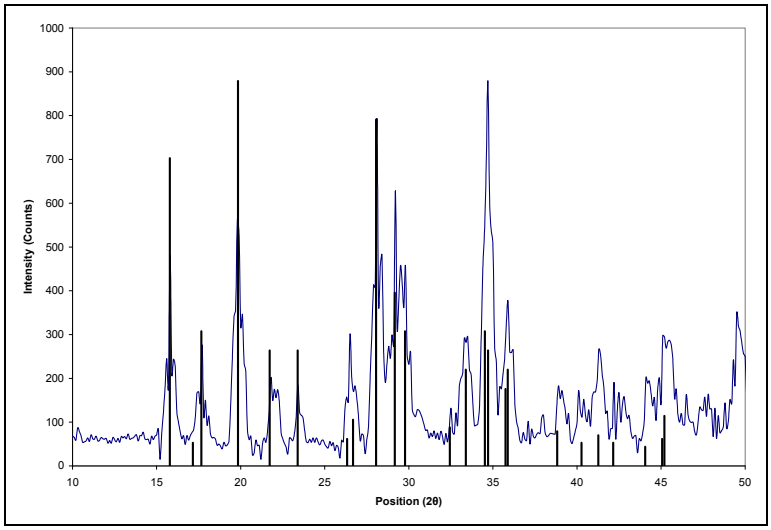

Figure 13: XRD pattern for scorodite produced in an autoclave from an initial arsenic concentration of 0.3M, an iron to arsenic molar ratio of one and reaction temperature of 160˚C (ref #070-0825).

In terms of physical properties, its particle size and morphology were determined. As per the particle size distribution shown in Figure 14, a bi-modal distribution was observed apparently indicating that precipitation occurred through a combination of homogeneous nucleation and heterogeneous growth. The mean particle size was 9 µm with a standard deviation of 4.5 µm and the particle size mode was 9.5 µm in diameter. Scanning electron microscope examination of the scorodite particles (refer to Figure 15) concluded that growth had occurred through aggregation of sub-micron crystallites, hence confirming the particles size distribution data. BET surface area measurements revealed that the autoclave produced scorodite had a specific surface area of 3.63 m^2/g. By applying the formula presented in Equation 4.1 it was determined this surface to correspond to isometric dense particles of 0.51 µm. This suggests that the scorodite aggregates of Figure 15 are porous.

$$d_p = \frac{6\times10^4}{\rho\times S} = \frac{6\times10^4}{(3.27 g/cm^3)\times(3.63\times10^4 cm^2/g)} = 0.51\mu m \qquad \text{Eqn. 4.1}$$

Where: d_p = Equivalent particle size (µm)
ρ = Density (g/cm^3)
S = Specific surface area (cm^2/g)

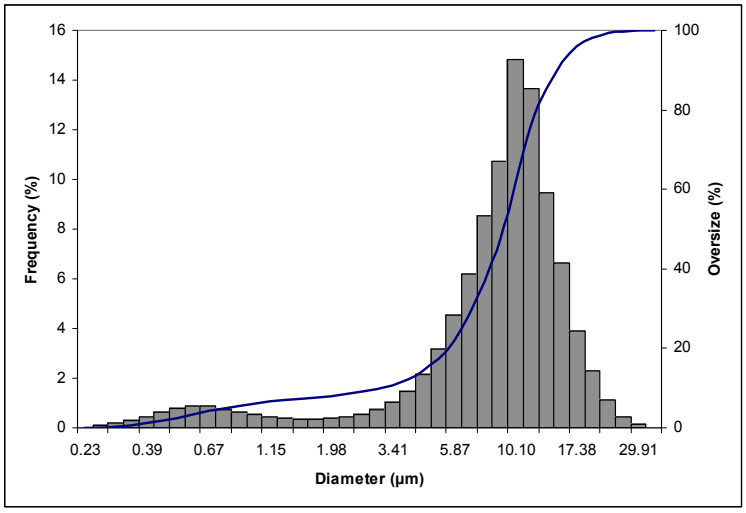

Figure 14: Volume based particle size distribution of autoclave produced scorodite. median = 9.02 µm, mean = 9.0 µm, mode = 9.56 µm.

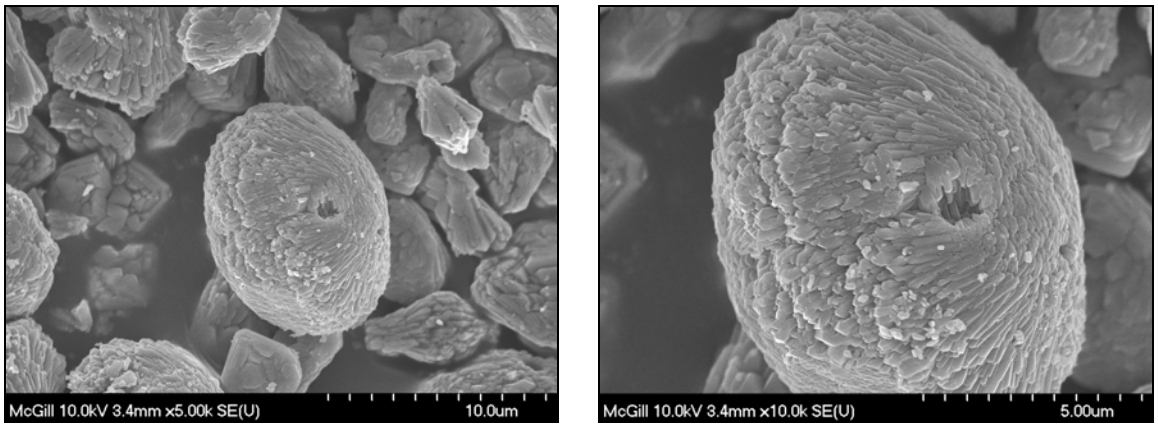

Figure 15: Scanning Electron Microscope (SEM) images of autoclave produced scorodite.

4.1.2 Atmospheric Production of Scorodite

Effect of arsenic concentration: Tests at various initial arsenic concentrations (10, 20, 40 g/L As) were performed in order to determine optimum conditions for the production of large batches of scorodite to be used in the encapsulation tests. It was previously mentioned in the experimental procedure (section 3.5.2) that an amorphous phase (as was evidenced by the appearance of a cloud) was observed to form upon heating the As(V)-Fe(III)-H_2SO_4 solution to reaction temperature (95˚C). This required addition of sulphuric acid to clear the precipitate (upon reaching 95˚C) prior to the addition of scorodite seed. It is interesting to note that the temperature at which this phase formed was dependent on arsenic concentration. At 10 g/L arsenic (initial pH ~ 1) the amorphous phase formed at 60˚C, but at 20 g/L (initial pH ~ 0.8) and 40 g/L arsenic (initial pH ~ 0.3) the precipitate was observed at 90˚C and 95˚C respectively. This may initially seem counterintuitive, however higher arsenic concentrations corresponded to lower solution pH at room temperature as reported above. Hence it is speculated that the lower pH necessitated a higher temperature to be attained for spontaneous nucleation to occur with elevation of arsenic concentration. Important considerations when selecting conditions for the production of scorodite included the batch yield, kinetics and particle morphology.

The observed precipitation curves from the three tests are plotted in Figure 16 in the form of percent arsenic remaining in solution vs. time. The kinetics of the

precipitation reaction (Equation 4.2) may be described by the general heterogeneous rate equation (Equation 4.3).

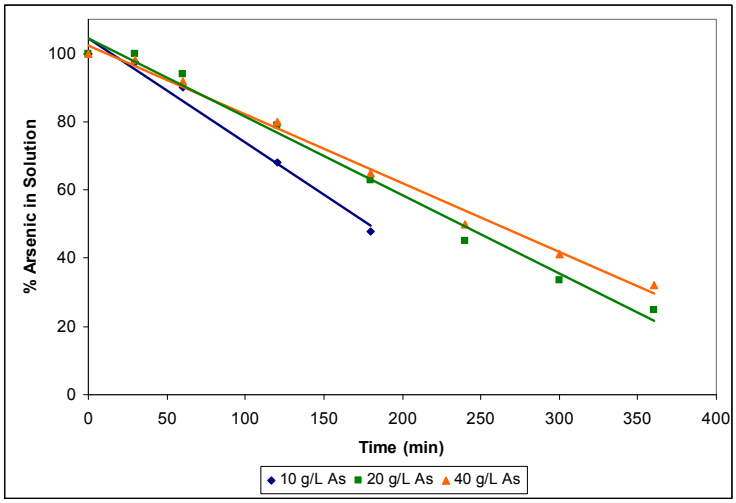

Figure 16: Scorodite precipitation curves at different initial arsenic concentrations.

$$Fe(SO_4)_{1.5(aq)} + H_3AsO_{4(aq)} + 2H_2O \rightarrow FeAsO_4 \bullet 2H_2O_{(s)} + 1.5H_2SO_4 \qquad \text{Eqn. 4.2}$$

$$r_{As} = k_p \times S_A \times C_{As}^{\ a} \quad \text{or,} \qquad \text{Eqn. 4.3a}$$

$$r_{As}' = k_p \times C_{As}^{\ a} \qquad \text{Eqn. 4.3b}$$

Where:
r_{As} = Rate expressed as g As•L^{-1}•min^{-1}
r_{As}' = Rate expressed as g As•L^{-1}•m^{-2}•min^{-1}
k_p = Apparent rate constant
S_A = Seed particle surface area
C_{As} = Concentration of arsenic in solution in g/L
a = Order of the reaction

By using the initial reaction rate for the three precipitation curves, an apparent reaction order of 1.2 was determined via the differential method of analysis (refer to Figure 17). That is, there is a first order dependency of the reaction rate on arsenate concentration. This implies the higher the initial concentration of arsenic the higher the precipitation rate. More specifically, precipitation from an initial arsenic concentration of 10 g/L over 3 hours reaction time resulted in 52% arsenic removal from solution. The post-wash solids contained 55% of the initial arsenic in solution, in good agreement with the 52% arsenic removal. Tests with initial arsenic concentrations of 20 g/L and 40 g/L were allowed to proceed for 6 hours reaction time and arsenic removal from solution was

75% and 69%, respectively. These are reasonable precipitation yields given the rather small mass of seed (5 g/L) used in these tests. As *Singhania et al.* [25] have previously demonstrated, the kinetics of the process accelerates with increasing seed loading and finer particle size.

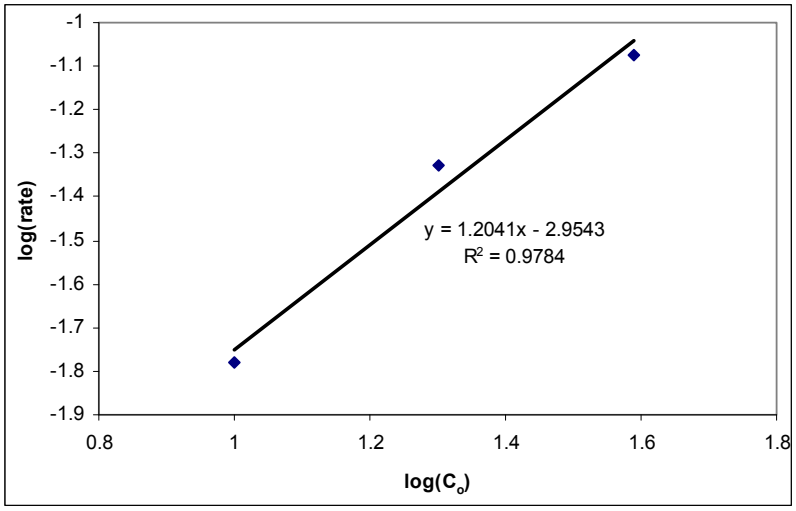

Figure 17: Determination of reaction order using the differential method of analysis.

Scanning electron images of the three scorodite products obtained with a Secondary Electron detector are presented in Figure 18. In contrast to the autoclave produced scorodite, the atmospherically produced scorodite particles consisted of over-grown dense agglomerates reflecting the different nucleation-growth mode of precipitation. As the initial arsenic concentration in solution was raised, the resulting scorodite particles were smoother and denser. Cracks that are evident on some particle surfaces arose from the drying the solids (at 50˚C in an oven) in preparation for analysis. Given the better morphology of the solids observed at higher initial arsenic concentrations and the higher precipitation yield, it was decided to retain the 20 g/L and 40 g/L arsenic solutions for the production of scorodite used in the subsequent encapsulation test work.

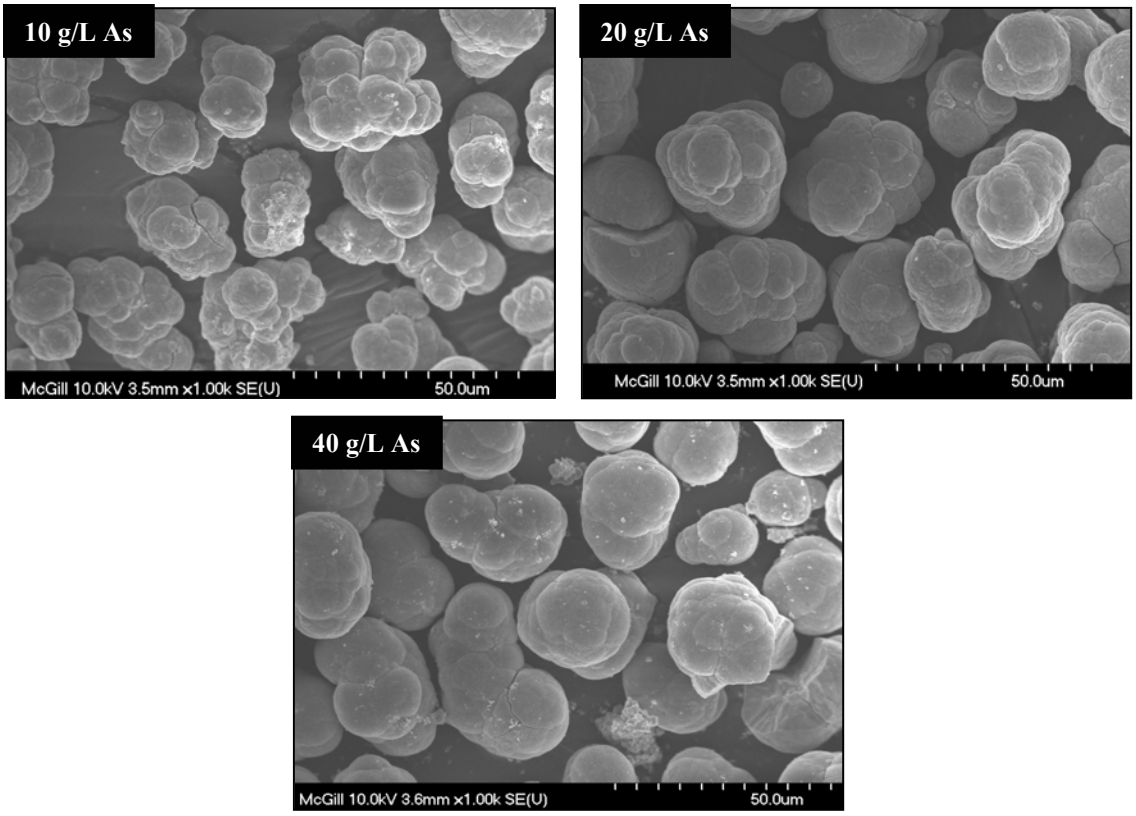

Figure 18: Scanning Electron Microscope (SEM) images of atmospherically produced scorodite from initial concentrations of 10, 20 and 40 g/L arsenic.

Characterization of Batches 1 and 2: The two batches of scorodite used in the encapsulation tests were atmospherically produced at 95˚C from solutions containing 20 g/L (Batch 1) and 40 g/L (Batch 2) arsenic at reaction times of 6 and 9 hours, respectively. Charts of arsenic removal as a function of time are shown in Figure 19 for production of both Batch 1 and Batch 2 solids. The arsenic removal for Batch 1 was 81.9% over 6 hours (compared with 75% in Figure 16) and the precipitation yield was 82 g of solids after washing, corresponding to 81.2% of the initial arsenic in solution after excluding the amount of scorodite used as seed. Arsenic removal for Batch 2 was 64% after 6 hours (compared with 69% for the equivalent test on Figure 16) or 79.8% over 9 hours. The corresponding yield was 196 g post-wash solids representing 76% of the initial arsenic in solution. The 1-4% discrepancy in precipitation yield is attributed at least partly to a small amount of scorodite deposited on the reactor walls as evidenced by the presence of brownish scale. Alternatively, this may have been due to small amount of amorphous co-precipitate that was removed during washing.

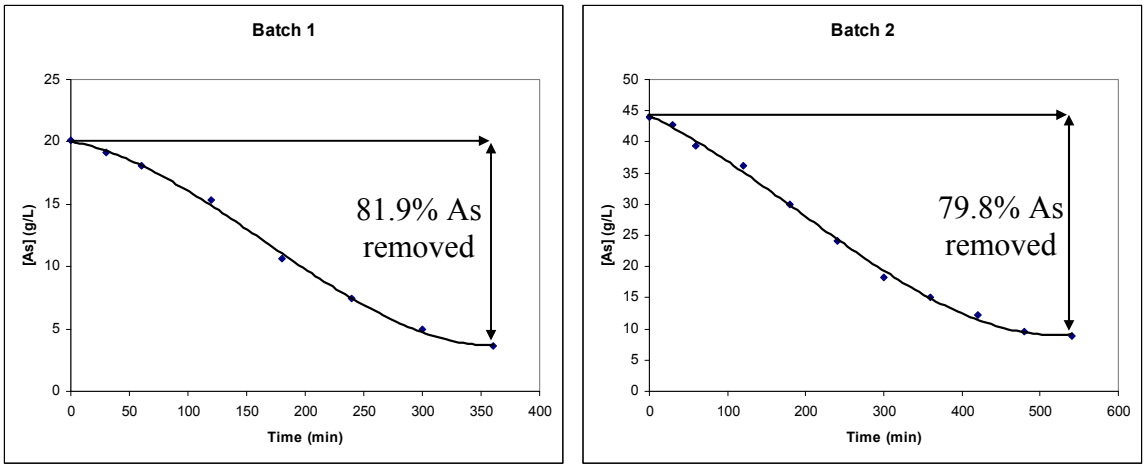

Figure 19: Arsenic removal with time during atmospheric precipitation of Batch 1 (left) and Batch 2 (right) solids.

Chemical digestion revealed a composition of 33.7 wt.% As and 24.6 wt.% Fe for Batch 1 solids, as well as 30.0 wt.% As and 23.0 wt.% Fe for Batch 2 solids. Both of these compositions are relatively close to the theoretical composition of scorodite, which is 32.4 wt.% As and 24.2 wt.% Fe. A minor amount of sulphate was also present in the solids (2.9 Wt. % SO_4^{2-} Batch 1, 3.0 wt.% SO_4^{2-} Batch 2) most likely incorporated into the scorodite structure similar to the findings of *Singhania et al.* [28]. The results from thermo gravimetric analysis of Batch 1 and Batch 2 solids are plotted on the same chart and presented in Figure 20.

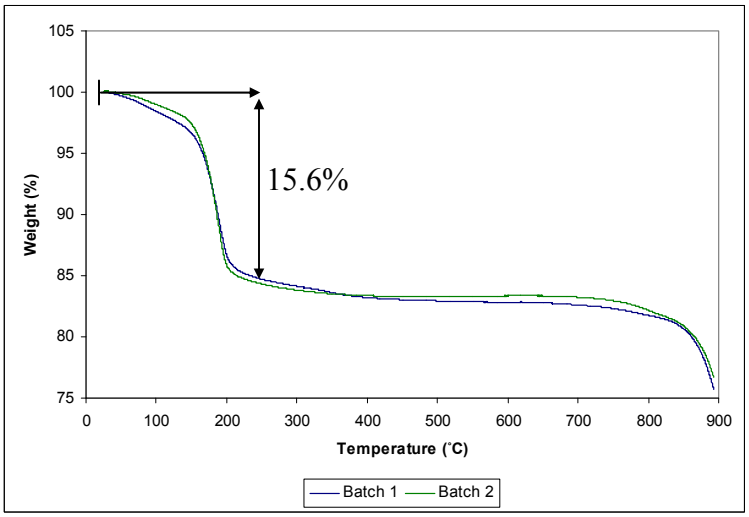

Figure 20: TGA of Batch 1 and Batch 2 atmospherically produced scorodite; heating rate 20˚C/min.

Similar to the autoclave-produced scorodite, there was a mass loss of 15.6% between 150˚C and 200˚C, representing the removal of the two crystallization waters from the scorodite structure. X-Ray Diffraction analysis (pattern shown in Figure 21) confirmed that both Batch 1 and Batch 2 (pattern not shown) solids to be scorodite with excellent crystallinity.

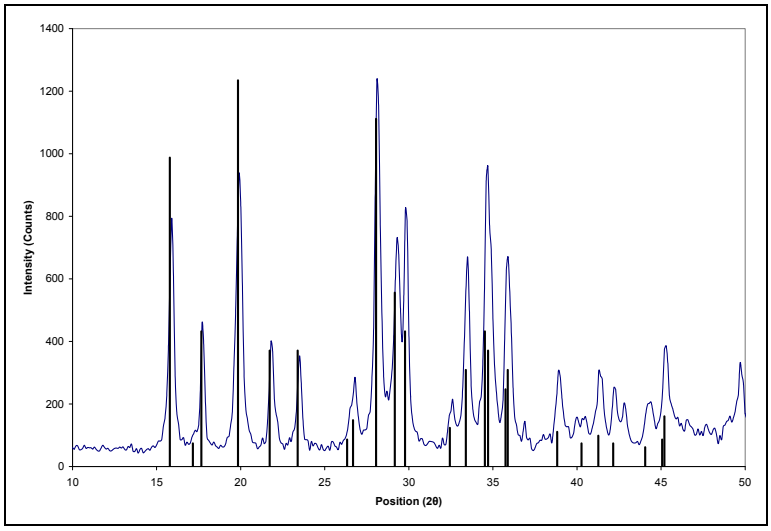

Figure 21: XRD pattern for Batch 1 solids produced from initial arsenic concentration of 20 g/L, compared with the reference (ref #070-0825).

Particle size analysis (shown in Figure 22) revealed that both batches were similar in terms of mean size and distribution. Batch 1 solids had a mean particle size of 23 µm with a standard deviation of 5.9 µm and Batch 2 solids had a mean particle size of 22 µm with standard deviation of 6.2 µm. There was a very small portion of particles for each batch that were significantly smaller than the bulk sample, which indicates that the distribution was slightly bi-modal. This implies that a small amount of homogeneous nucleation occurred in addition to heterogeneous precipitation on the seed particles. As a result of the heterogeneous deposition that was the dominant precipitation mode the mean particle size increased from ~ 9 µm for the initial seed (refer to Figure 14) to > 22 µm.

It may have been expected that the particle size of Batch 2 to be larger than that of Batch 1 because of the larger amount of scorodite material deposited on the otherwise same mass of seed. Since both batches had the same particle size this suggests that the product obtained from the 40 g/L arsenic solution (Batch 2) consisted of higher density

particles; that is particles with less porosity. This was indeed confirmed by BET surface area measurements. Thus, particles from Batch 1 solids appeared to be somewhat irregularly shaped with significant surface porosity (Figure 23), while Batch 2 particles were more uniformly spherical with smooth surface and higher density appearance (Figure 24). Cracks appearing in the particle surface from oven drying appeared to be more prominent in Batch 1 scorodite. Finally, surface area analysis revealed a BET surface area of 3.15 m^2/g for Batch 1 scorodite and 2.16 m^2/g for Batch 2 scorodite.

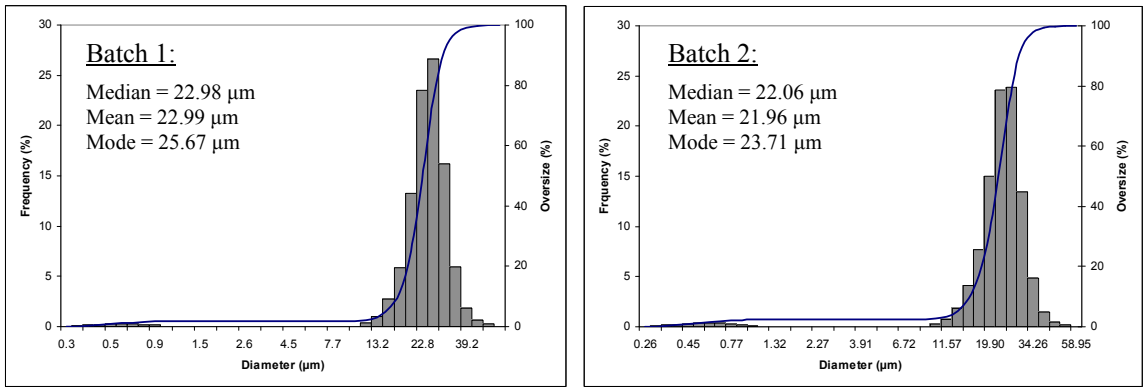

Figure 22: Particle size distribution of Batch 1 (left) and Batch 2 (right) atmospherically produced scorodite.

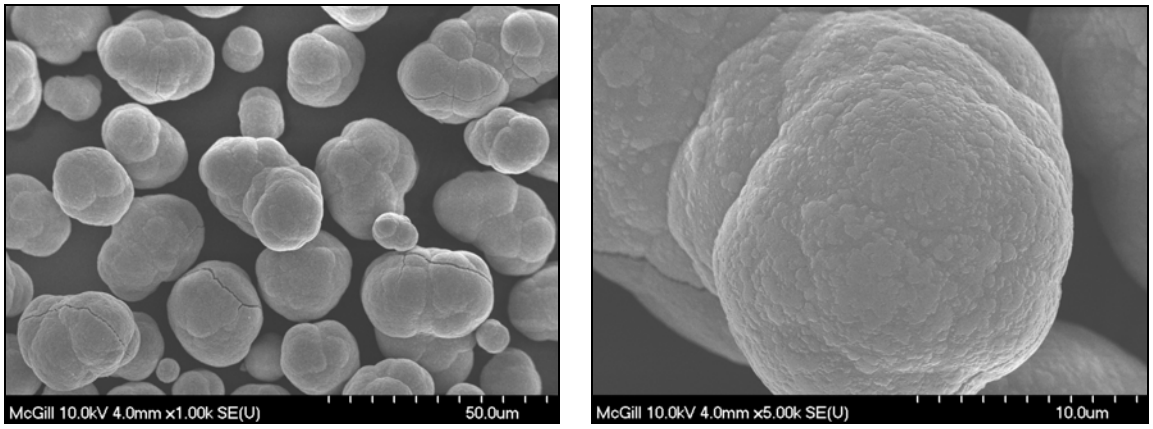

Figure 23: Scanning Electron Microscope (SEM) image of Batch 1 atmospherically produced scorodite.

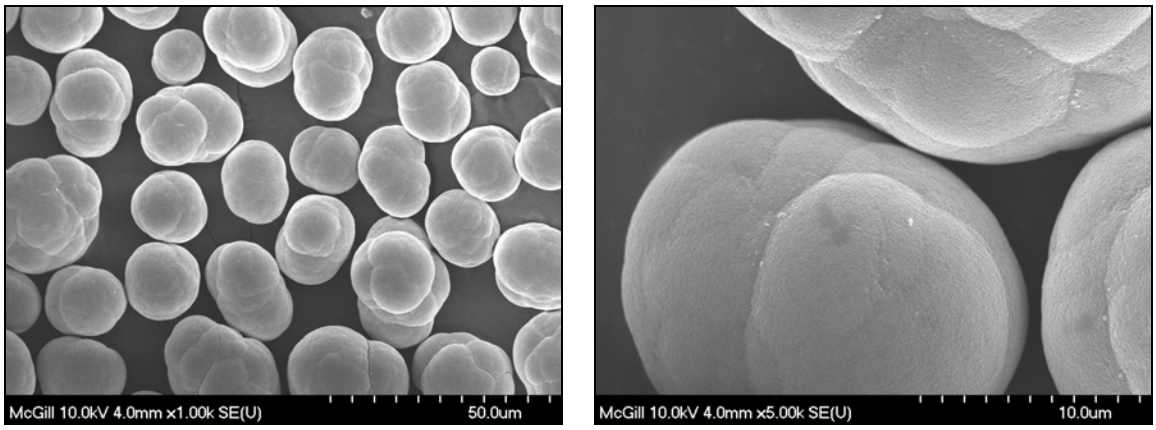

Figure 24: Scanning Electron Microscope (SEM) image of Batch 2 atmospherically produced scorodite.

In terms of short term arsenic release as determined by sequential TCLP-type leachability testing, the two batches of scorodite were found to be equivalent (refer to Figure 25). The relatively high arsenic release during the first two TCLP contacts is attributed to trace amounts of co-precipitated amorphous ferric arsenate. Similar observations were made by *Bluteau and Demopoulos* [4] for autoclave produced scorodite.

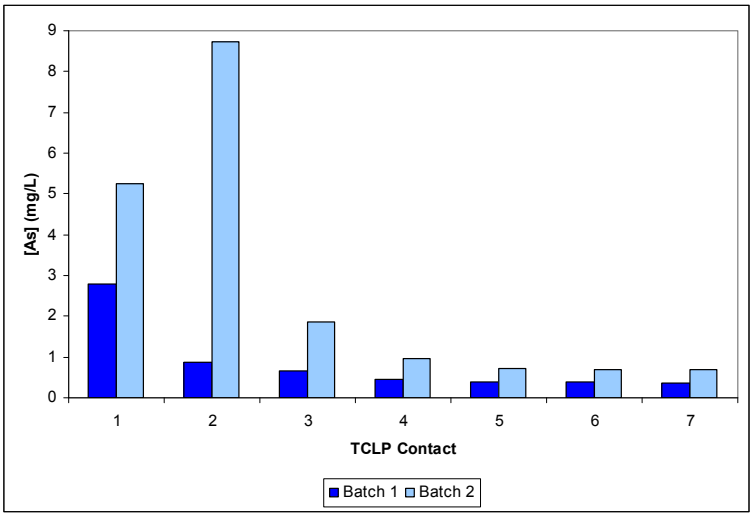

Figure 25: TCLP-type leachability response of Batch 1 and Batch 2 atmospherically produced scorodite.

Arsenic release reached a limiting value after 5 TCLP-type contacts. This limiting value was 0.4 mg/L and 0.7 mg/L arsenic for Batch 1 and Batch 2 scorodite, respectively. These are lower than the values reported by *Singhania et al.* [28] apparently reflecting the

higher inherent stability of the scorodite produced from higher arsenic concentration solutions (10 g/L in the case of *Singhania et al.* vs. 20 or 40 g/L in this work). The use of the Applikon® reactor, which is equipped with baffles and therefore has a better mixing system than a simple kettle reactor, could have potentially further contributed to the better scorodite material produced in this work. Preliminary tests performed by this author with a Pyrex beaker reactor without baffles and with the same elevated arsenic concentrations (20 and 40 g/L) yielded 2x – 3x (1 – 1.5 mg/L As) higher TCLP leachabilities (not included in the thesis).

4.2 Production and Characterization of Aluminum Gels

4.2.1 Production

In the experimental section of this thesis (Chapter 3) reference was made to a typical test; 50 mL of 2M aluminum salt solution was neutralized with 50 mL 5N sodium hydroxide solution. The neutralization reaction in a simplified form is given below (Equation 4.4), where $Al_n(OH)_{3n}$ represents the polymerized aluminum hydroxide species.

$$nAlCl_3 + 2.5nNaOH + 0.5H_2O \rightarrow Al_n(OH)_{3n} + 2.5nNaCl + 0.5nHCl \quad \text{Eqn. 4.4}$$

Neutralization of aluminum salt solutions was mainly effected with 5N sodium hydroxide solution at room temperature. Various tests were carried out in order to define the production conditions for aluminum hydroxyl-gels suitable for encapsulation of scorodite. The selected conditions included partial neutralization (OH/Al = 2.5) of 2M $AlCl_3$ or $Al(SO_4)_{1.5}$ solutions at room temperature using manual stirring. The resultant gel had a viscous consistency as pictured in Figure 26 and a measured pH of 4 and 5.4 for the chloride and sulphate gels, respectively. The type of gel pictured below was retained for characterization and encapsulation testing.

Figure 26: Typical appearance of the aluminum gel obtained by partial hydrolysis of 2M aluminum salt solutions with 5N NaOH (OH/Al 2.5).

In addition to sodium hydroxide, calcium hydroxide slurry of equivalent molar strength was investigated as an alternative neutralizing agent. In this case though, the onset of gel formation was not observed immediately upon the addition (all at once) of $Ca(OH)_2$ slurry as with sodium hydroxide. Typically, while it was less than a minute for the NaOH produced gel it required over 3 hours for the $Ca(OH)_2$ produced gel. This is believed to be due to the slower release of OH^- by the lime slurry in comparison to NaOH. The resultant gel from neutralization of 2 M aluminum chloride solution with calcium oxide slurry had a more translucent look than the one produced using sodium hydroxide. The gel was also more viscous without thinning out with excessive stirring, as occurred with the product pictured in Figure 26. In contrast to aluminum chloride, no gel was produced when aluminum sulphate (2 M solution) was neutralized with calcium oxide slurry, but rather the entire mixture transformed to a solid mass. This was due to the formation of gypsum, effectively blocking the formation of an aluminum hydroxide gel network. For all gel/scorodite encapsulation tests, only gels produced with sodium hydroxide as the neutralizing agent were employed.

4.2.2 Characterization

Composition: Both types of gels produced from either $AlCl_3$ or $Al(SO_4)_{1.5}$ solutions completely dried out after two weeks ageing at ambient pressure (22˚C), losing 77% of their weight. This loss is believed to represent the water contained in the gel that

evaporated over the ageing period. The dry gels were washed with water to remove the residual soluble material, dried and subsequently dissolved with acid and analyzed to determine their chemical composition. The aluminum chloride-generated gel contained 24 wt.% Al and 4.7 wt.% Cl, while the aluminum sulphate-generated gel contained 21.2 wt.% Al and 17.6 wt.% SO_4^{2-}. Assuming aluminum being present as $Al(OH)_3$ these numbers translate to 68 wt.% (or 74 wt.% by including Cl^-) and 62 wt.% (or 80 wt.% when SO_4^{2-} is included) for the chloride and sulphate gels, respectively. The balance of 20 – 26 wt.% is taken to be water. This is in line with the up to 30 wt.% water content that has been reported for similar materials like gelatinous (pseudo) boehmite [53]. The respective molar ratios of aluminum to matrix anion were Al/Cl = 6.8 and Al/SO_4 = 4.4.

The amount of chloride and sulphate present in the solid samples represented 33 wt.% and 12 wt.% of the input amounts respectively, indicating that either anion washing efficiency was relatively low or that these anions form part of the gel network. In such an eventuality the gel formation reaction (Equation 4.4) can be rewritten as shown below (Equation 4.5).

$$nAlCl_3 + 2.5nNaOH \rightarrow Al_n(OH)_{2.5n}(Cl)_{0.5n} + 2.5nNaCl \qquad \text{Eqn. 4.5}$$

It is interesting to note that the wash water from the chloride gel contained 110 mg/L aluminum, while the filtrate from the sulphate gel contained less than 1 mg/L aluminum. This indicates that the character of the gels is likely different depending on the type of aluminum salt solution used and can have different effects on the stabilization of scorodite. Both post-wash gels contained only minor amounts of sodium (0.1 wt.% Na), indicating very high cation washing efficiency. The marked difference between cation and anion washing efficiency may be attributed to greater affinity of the anion towards the surface of aluminum hydroxide particles. It has been previously shown that several washing cycles are required to effectively remove chloride ions from aluminum gel samples [54].

Thermo gravimetric analysis (TGA) of the post-wash aluminum chloride and aluminum sulphate gels produced the weight loss vs. temperature curves shown in Figure 27. The weight loss up to 120˚C (~20 wt.%) is attributed to surface or pore water retained

by the amorphous structure of these materials (in agreement with the estimated amounts of water from the chemical analysis). The further weight loss beyond 120˚C and up to 800˚C is postulated to reflect the transformation of the amorphous $Al(OH)_3$ to crystalline aluminum oxyhydroxides such as boehmite (γ-AlOOH) or diaspore (α-AlOOH) as shown in Equation 4.6.

$$Al(OH)_3 \rightarrow AlOOH + H_2O \qquad \text{Eqn. 4.6}$$

The theoretical weight loss for the above transformation is 23 wt.%, reflecting the loss observed on the TGA graph of Figure 27. The further decrease in mass above 800˚C may reflect the loss of the anion as Cl_2 or SO_3 gases and/or the further transformation to alumina.

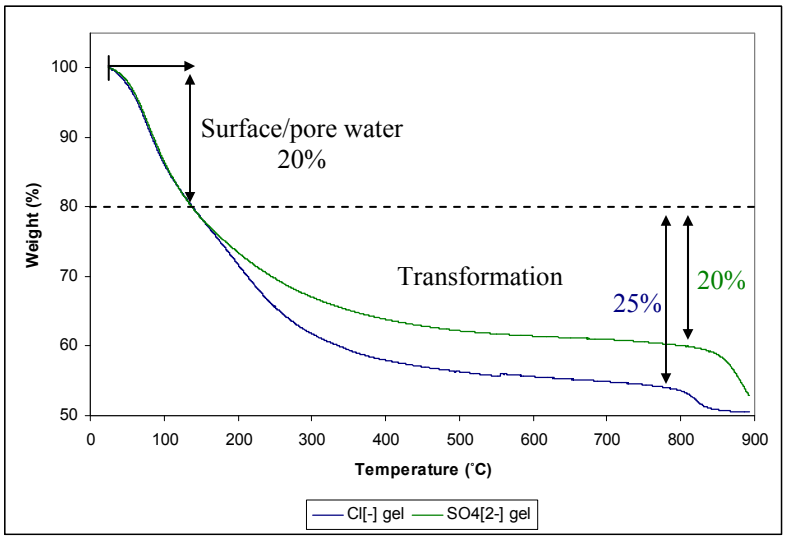

Figure 27: TGA of aluminum chloride (Bottom) and aluminum sulphate (Top) gels produced by rapid hydrolysis (2.5 OH/Al) of 2M aluminum solutions; heating rate 20˚C/min.

Surface Area and Morphology: The post-wash gels after drying were subjected to surface area analysis and SEM examination of their morphological features. The BET surface area measurements are summarized in Table 4. On the same table, the surface area of the amorphous aluminum hydroxide and bayerite samples used in the adsorption tests is reported (refer to Appendix B). Samples were run in duplicate to ensure accuracy. The two dry gel samples were found to have relatively similar surface areas, but the bayerite and amorphous aluminum hydroxide samples were markedly different. While

the surface area of the amorphous aluminum hydroxide material is 0.5 m^2/g, the bayerite material surface area was over an order of magnitude larger with an average of 110 m^2/g. This was unexpected as amorphous materials tend to possess higher surface areas in general than their crystalline counterparts. This implies that bayerite makes for a better sorbent for arsenic since adsorption depends on the number of available surface sites on the particle. As the gels were found to have intermediate surface areas (18 and 37 m^2/g respectively for the chloride and sulphate gels) between the respective areas of amorphous AlOOH and bayerite, their ability to retain arsenic should be lower than that of bayerite if the mechanism is solely adsorption. This however, as it will be reported in section 4.4 (stability testing) is not the case, which implies that other features of the gels than simply their surface area favour arsenic retention-stabilization. Hence, further detailed characterization of these unusual materials was undertaken. It is worth mentioning at this point that the BET surface area of the aluminum chloride gel is similar to the value of 12.6 m^2/g previously reported for unwashed amorphous aluminum hydroxides produced from 1.5M aluminum chloride solution by base hydrolysis with sodium hydroxide (OH/Al 2.67) [42].

Table 4: BET surface area of aged aluminum gels and aluminum (oxy)hydroxides.

Sample	Precipitation Conditions	BET Surface Area (m^2/g)
$Al(OH)_3$ (Bayerite)	0.5M $AlCl_3$, 3.15 OH/Al, T=60 ˚C, 24 hr	88.6 - 132.2
Amorphous AlOOH	0.5M $AlCl_3$, 2.85 OH/Al, T=60 ˚C, 24 hr	0.40 - 0.64
Aluminum Gel - Cl^-	2M $AlCl_3$, 2.5 OH/Al, T=22 ˚C, 2 weeks	18.2 - 18.6
Aluminum Gel - SO_4^{2-}	2M $Al_2(SO_4)_3$, 2.5 OH/Al, T=22 ˚C, 2 weeks	36.7 - 38.3

Scanning electron microscope (SEM) images of washed and subsequently dried aluminum chloride and aluminum sulphate gel materials are shown in Figure 28. It is evident that there is a wide range of particle sizes for both materials. It appears that large porous aggregates that had formed broke up during materials handling. This coincides with visual observations that the solids tended to agglomerate during oven drying and were subsequently easily broken apart with a spatula. At this magnification (1000x) there is no difference between the aluminum chloride and aluminum sulphate gel that is immediately evident.

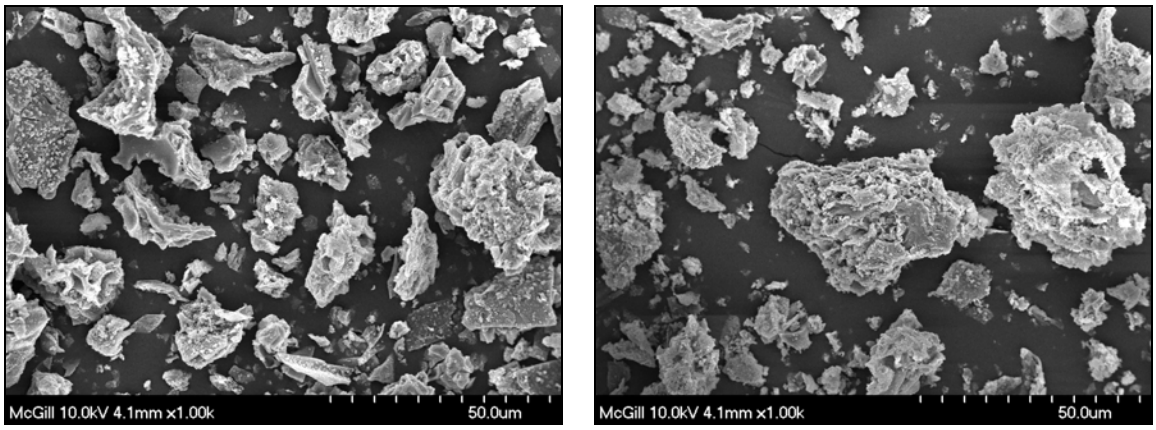

Figure 28: Scanning electron microscope (SEM) images of aluminum chloride (left) and aluminum sulphate (right) gels obtained at 1000x magnification.

In order to verify whether the aluminum chloride and sulphate gels have different morphologies, scanning electron images with the secondary electron detector were obtained at 20000x magnification and are presented in Figure 29. The aluminum chloride-derived gel seems to consist of a highly porous (honeycomb-like) structure formed by aggregates of smaller particles. In contrast, the aluminum sulphate-derived gel material appears of aggregates of a smoother and less porous phase. This observation contrasts the BET surface area measurements (refer to Table 4) that found the sulphate gel material to have twice as much the surface area of the chloride gel. Apparently molecular-scale features have to be considered.

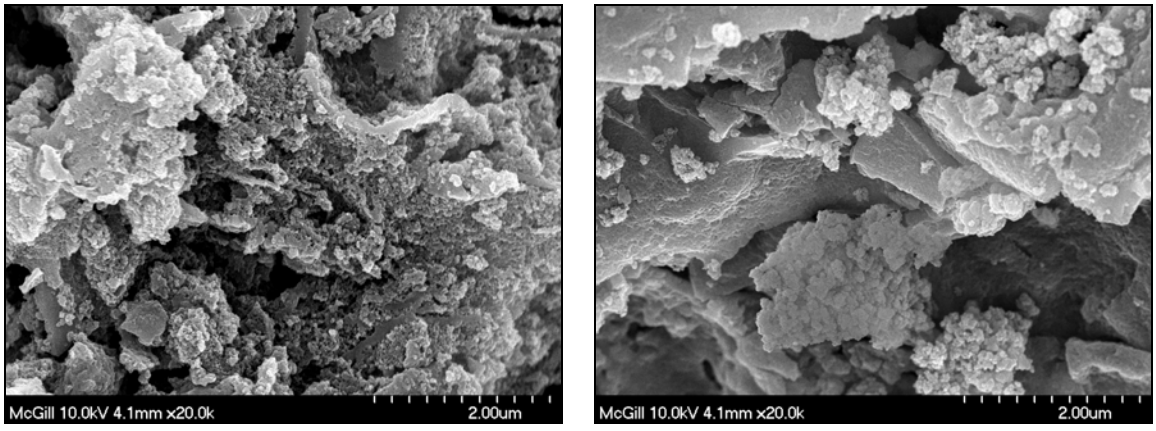

Figure 29: Scanning electron microscope (SEM) images of aluminum chloride (left) and aluminum sulphate (right) gels obtained at 20000x magnification.

XRD Analysis: X-ray diffraction patterns were obtained for the washed aluminum sulphate and aluminum chloride gels, as well as for the amorphous aluminum hydroxide sample. All patterns are plotted on the same chart for comparison and shown in Figure 30. The peaks on the bayerite sample correspond to well crystalline bayerite (ref #020-0011) and the amorphous sample is a poorly crystalline aluminum (oxy)hydroxide sometimes referred to as pseudoboehmite [36].

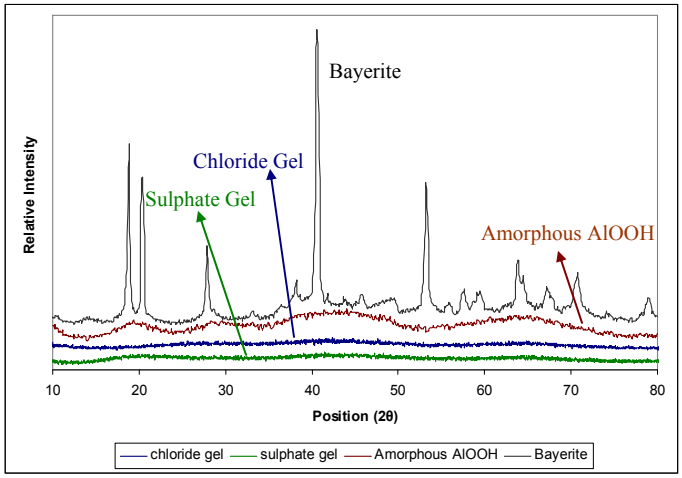

Figure 30: Comparison of X-Ray Diffraction (XRD) patterns for gels produced by rapid hydrolysis (2.5 OH/Al) of 2M aluminum salt solutions to those of amorphous AlOOH and bayerite.

To better enhance the XRD pattern details of the gel materials the low intensity region was considered along that of pseudoboehmite (amorphous AlOOH) as shown in Figure 31.

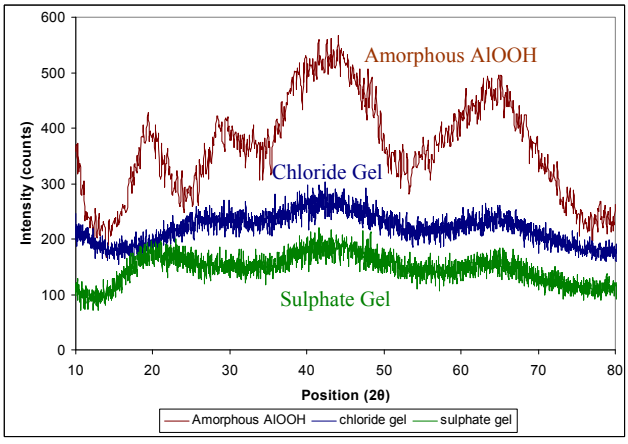

Figure 31: Comparison of X-Ray Diffraction (XRD) patterns for gels produced by rapid hydrolysis (2.5 OH/Al) of 2M aluminum salt solutions to that of amorphous AlOOH.

As it can be seen, both the aluminum chloride and aluminum sulphate-derived gel materials are highly amorphous with the latter to match better the broad peaks of pseudoboehmite. Given the amorphous nature of these materials further characterization was undertaken by employing NMR and vibrational spectroscopy.

NMR Spectroscopy: The ^{27}Al Nuclear Magnetic Resonance (NMR) spectra obtained for washed and subsequently dried aluminum chloride and aluminum sulphate-derived gel samples are shown in Figure 32. Regardless of whether the gels were washed prior to analysis by NMR, the resulting patterns were identical. The large peak at $\delta = 3$ ppm is indicative of octahedrally coordinated aluminum, while the peak at $\delta \sim 60$ ppm denotes aluminum in tetrahedral coordination [44, 55]. While the octahedral peak at $\delta = 3$ ppm may be associated with monomeric species such as $Al(OH)_n(H_2O)_{6-n}^{(3-n)+}$ with $0 \leq n \leq 2$ [37] or the Keggin Al_{13} species ($AlO_4Al_{12}(OH)_{24}(H_2O)_{12}^{7+}$) the chemical shift at $\delta \sim 60$ ppm for both samples may be taken as evidence of the presence of the Al_{13} species. The structure of this polymeric species that was discussed in the literature review chapter consists of a central AlO_4 tetrahedron surrounded by 12 aluminum octahedra. Since Al_{13} is the only species that contains the tetrahedral aluminum moiety in the acidic pH range [37], it is deduced that both gel types produced in this work consist of polymeric Al_{13} tridecamers [44].

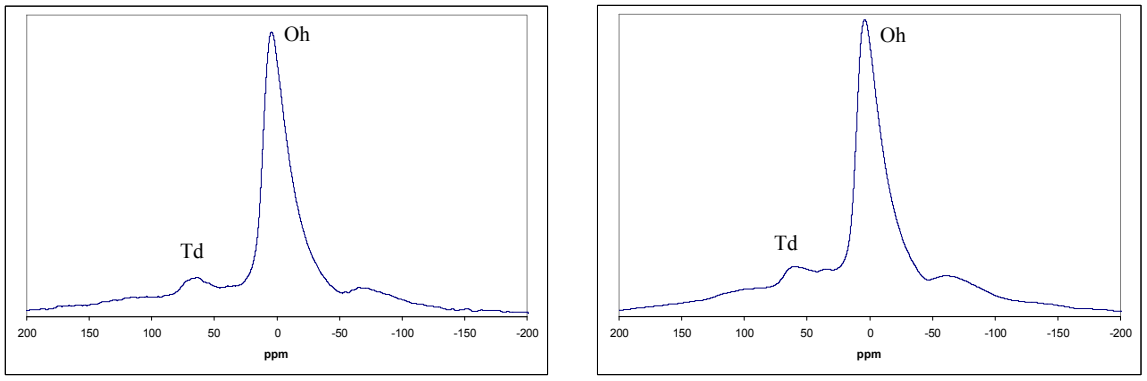

Figure 32: ^{27}Al-NMR spectra of aluminum chloride (left) and aluminum sulphate (right) derived gels produced by rapid hydrolysis (2.5 OH/Al) of 2M aluminum salt solutions.

Vibrational Spectroscopy: Attenuated Total Reflectance Infrared (ATR-IR) spectra obtained for the washed and subsequently dried aluminum chloride and aluminum sulphate derived gels are presented in Figure 31. Table 5 summarizes the known infrared

band assignments from the literature and compares them to the bands observed in spectra for the gels reported in Figure 33. It can be seen from this comparison that in the present synthesized products, the only type of molecular bands observed for the two gel samples are Al-OH and Al-H_2O; no Al-O-Al or Al-O-Al-O bands that are commonly observed for boehmite and monoaluminate materials were present in the obtained spectra [37, 44]. In more detail (refer to Figure 33), the spectrum for the aluminum chloride-derived gel has a broad band at 940 cm^{-1} that is attributed to Al-OH bonding. This band though is not shown in the case of the aluminum sulphate-derived gel because it was masked by the sulphate band [44]. It should be noted that the sulphate band reference of 1105 cm^{-1} is from investigation of gas molecules. However in the solid state, vibrational bands tend to occur at lower frequencies, since there exists strong bonding interactions between the sulphate molecular groups and other elements or groups in the matrix. The broad band observed at 3000 – 3500 cm^{-1} is assigned to both Al-OH and Al-H_2O bonds. The diffuse nature of these peaks is suggestive of a highly disordered structure unlike that observed for other hydrated aluminum oxyhydroxides [56, 57].

Table 5: Relevant infrared band assignments and their observation in aluminum chloride and aluminum sulphate gel spectra.

Band Frequency (cm^{-1})	Assignment	Reference	Observation		Comments
			SO_4^{2-} Gel	Cl^- Gel	
492	Al-OH_2	[44]	No	No	Below investigated range
546	Al-O	[44]	No	No	
627	Al-OH	[44]	Yes	No	-
729	M-O	[44]	No	No	M = Aluminum
760-780	Al-O-Al_{Oh}	[58]	No	No	Boehmite (γ-AlOOH)
800-900	Al-O-Al-O_{Td}	[58]	No	No	Monoaluminates (MAl_2O_4)
940-970	Al-OH	[59, 60]	No	Yes	Masked in SO_4^{2-} Gel by sulphate band
970-1080	Al-OH	[60]	No	Yes	
1105	SO_4^{2-}	[61]	Yes	No	Study of gas molecules
~ 1600	H_2O	-	Yes	Yes	Common observation
2500-3100	Al-OH	[60]	Yes	Yes	Diffuse band includes both assignments
3300-3700	Al-H_2O	[60]	Yes	Yes	

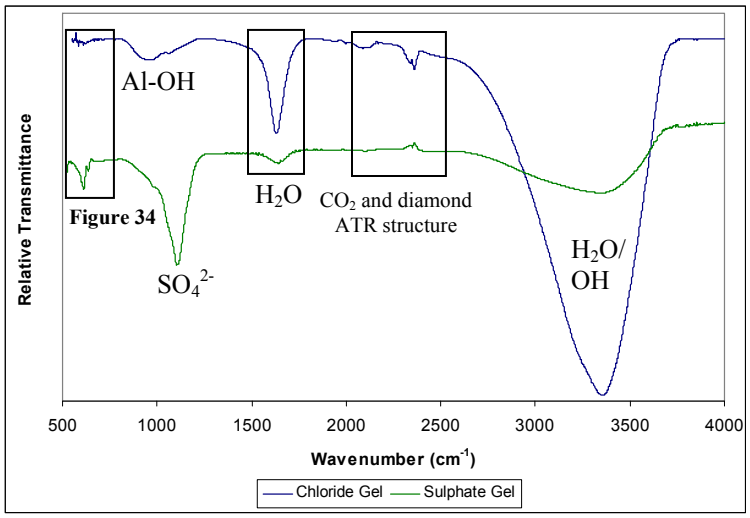

Figure 33: Infrared spectra of aluminum chloride (Top) and aluminum sulphate (Bottom) gels produced by rapid hydrolysis (2.5 OH/Al) of 2M aluminum solutions.

The region below 900 cm^{-1} is rich in structural information as this region has been used to observe Al-O_{Td} and Al-OH_{Oh} vibrations [44]. To be able to better examine this region an expanded version of the infrared spectra between 850 cm^{-1} and 550 cm^{-1} is shown in Figure 34. For comparison the reference spectra for aluminum chloride gels formed at different hydrolysis ratios and that of aluminum sulphate gel reported by *Bradley et al.* are also presented [44]. The spectra obtained for the present work are plotted in decreasing wavenumber and relative absorbance in order to be consistent with the reference work. The Al-OH_{Oh} (octahedral) band is evident in only the aluminum sulphate gel and neither gel sample shows evidence of the Al-O_{Td} (tetrahedral) band. Both spectra lack bands in the 760 - 850 cm^{-1} range indicating that either sample contains the Al-O-Al or Al-O-Al-O bonds present in boehmite or monoaluminate type materials [58]. The similarity between the aluminum sulphate gel spectrum and that of the reference Al_{13} sulphate spectrum suggests that this material has a keggin-like structure (refer to Figure 7 in Chapter 2) with minimal aluminum in tetrahedral coordination as observed from the ^{27}Al NMR studies. The absence of the presence of the AlO_4 tetrahedral group from the IR spectrum is puzzling. It is possible that that another ion such as sulphate (SO_4) has occupied the tetrahedral position in the Al_{13} keggin structure. The aluminum chloride gel spectrum was found not to have similarities with those of Keggin

Al_{13} type gels reported by *Bradley et al.* [44]. This indicates that there exists a basic molecular structure difference between the two types of gels.

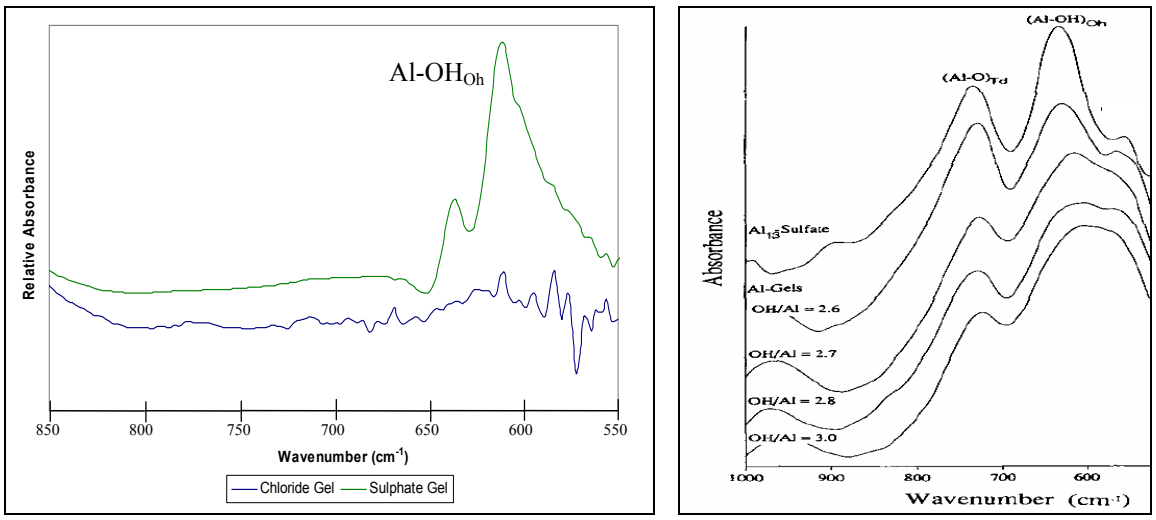

Figure 34: Infrared spectra of aluminum chloride (Bottom) and aluminum sulphate (Top) gel in the 850 cm^{-1} to 550 cm^{-1} region and gel reference spectra from *Bradley et al.* [44].

The Raman spectra obtained for the dried aluminum chloride and aluminum sulphate gels, which are shown in Figure 35, confirmed the different make up of the respective gels. As it can be seen, the spectrum for the chloride gel does not contain many features except for the diffuse band located at 1000 cm^{-1}. This corresponds to an Al-OH vibration bond (for band assignments refer to Table 6) in accordance with the observations from the infrared spectroscopic analysis. The sulphate gel spectrum contained numerous features mainly due to different sulphate vibrations. Again, no Al-OH bands are clearly evident here because they were masked by the 983 cm^{-1} and 1105 cm^{-1} sulphate bands that are located in the same region. Thus there is a clear difference between the vibrational spectra of the two gels giving evidence that at the molecular structural level they are distinct. This is something that was not evident when a comparison of XRD and ^{27}Al NMR spectra was made. It is tentatively concluded that the molecular structure of the aluminum chloride gel is composed of polymerized aluminum octahedra (refer to Figure 36), while that of the aluminum sulphate gel to be made up of polymerized tridecamers (Al_{13}) (refer to Figure 37) that incorporate SO_4 as part of the structure.

Table 6: Relevant Raman band assignments observed in the aluminum chloride and aluminum sulphate gel spectra.

Vibrational Frequency (cm^{-1})	Assignment	Reference
983	SO_4^{2-} v_1	[61]
450	SO_4^{2-} v_2	[61]
1105	SO_4^{2-} v_3	[61]
611	SO_4^{2-} v_4	[61]
970-1080	Al-OH	[60]
2500-3100	Al-OH	[60]
3300-3700	Al-H_2O	[60]

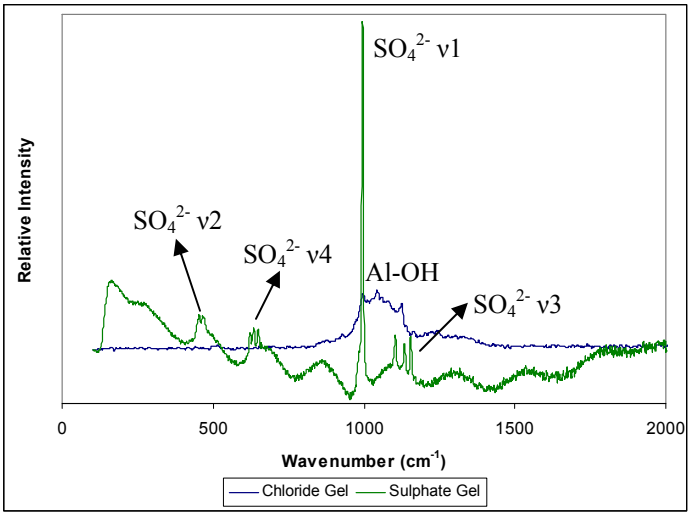

Figure 35: Raman spectra for aluminum chloride (Top) and aluminum sulphate (Bottom) gels produced by rapid hydrolysis (2.5 OH/Al) of 2M aluminum salt solutions in the 0 cm^{-1} to 2000 cm^{-1} region.

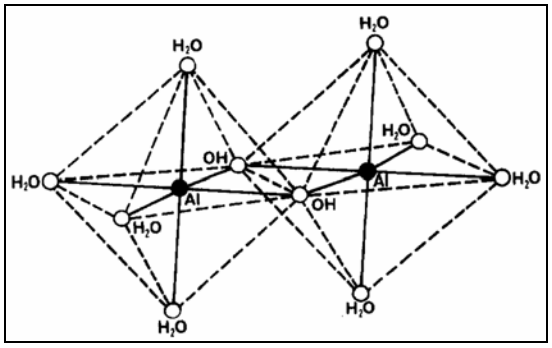

Figure 36: Schematic Representation of aluminum octahedra, the dimer ion $Al_2(OH)_2(H_2O)_8^{4+}$ [60].

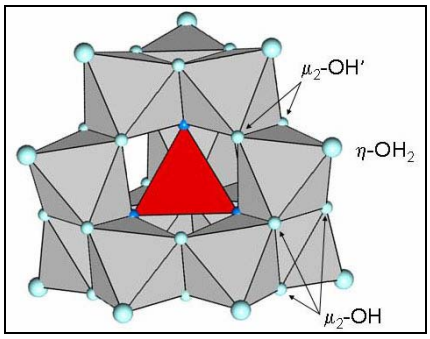

Figure 37: Schematic representation of the Keggin Al_{13} Structure [39].

4.3 Ageing of Gel-Scorodite Mixtures

4.3.1 Process Aspects

Procedure: The general flow sheet used for encapsulating scorodite with aluminum gels that was presented in the experimental procedure chapter is reproduced in Figure 38 for easy reference.

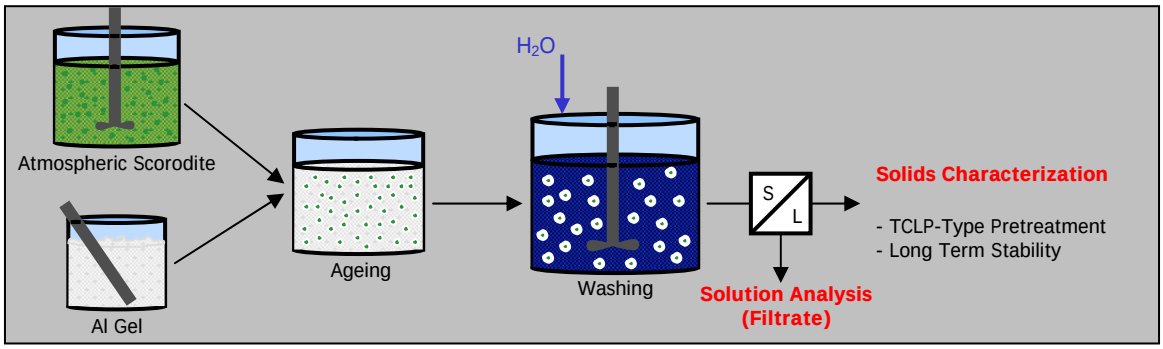

Figure 38: General flow sheet followed for the encapsulation of scorodite with aluminum hydroxide gels.

After synthesis of scorodite and production of aluminum gel, the two products were blended together and subsequently allowed to age under various conditions (unstirred). The aged solids were in general (unless otherwise stated) washed with de-ionized water and then filtered to separate the liquid and solid phases. A portion of the solids was subjected to a TCLP-type pre-treatment prior to long term stability testing and the rest was reserved for characterization by a variety of techniques. The levels of soluble

species in the filtrate were also determined in order to perform a mass balance around the washing procedure.

The various ageing procedures investigated are summarized in Table 7. The experimental parameters applied were outlined in the experimental section (Chapter 3) and can be classified into two categories, namely (1) batch make-up; and (2) ageing conditions. Batch make-up relates to the blending of aluminum gel with scorodite and includes the type of gel used (chloride vs. sulphate) as well as the molar ratio of aluminum to arsenic in the blended product. Ageing conditions refer to the ageing procedure itself and comprises the use of an open vs. closed system, ageing temperature and ageing time. Before the results are presented, it is important to explain the rationale for the different type of ageing tests listed in Table 7.

These tests can be divided into 2 groups. Group 1 tests include ID 3-7. In this first series of tests high aluminum to arsenic (i.e. gel/scorodite) molar ratios were used seeking to identify if the concept of encapsulation of scorodite with aluminum gels had merit for further investigation. During this series of tests (all conducted with the Batch 1 scorodite), emphasis was given to the role of ageing temperature and closed vs. open system type of ageing. It should be noted that the washed solids of group 1 were dried prior to long term stability evaluation. In contrast, the rest of the washed solids were placed directly into stability testing unless otherwise specified. The second series of tests (ID 13-20), all carried out at 22˚C, sought basically to examine the feasibility of lowering the aluminum to arsenic (or gel/scorodite) ratio (Al:As = 0.1 vs. >1) and to select between the chloride and sulphate gels. With the exception of group 1, all tests involved Batch 2 scorodite. Moreover it should be clarified that Batch 1 scorodite was dried before use while Batch 2 scorodite was stored as a wet cake prior to its use in encapsulation tests.

Table 7: Summary of the different ageing procedures investigated.

ID	Al:As	Gel Type	Open vs. Closed	Temp (˚C)	Time (Days)	Comments
3▲	1.54	Cl^-	Open	22	21	Gel dried up
4▲	0.96	Cl^-	Closed	40	54	Partial gel breakdown
5▲	0.96	Cl^-	Closed	70	1	Total gel breakdown
6▲	0.96	Cl^-	Open: oven dried	50	1	Gel dried up
7▲	1.5	SO_4^{2-}	Open	22	28	Gel dried up
13	1	Cl^-	Open	22	21	Gel dried up
14	1	Cl^-	Closed	22	21	Partial water release
15	0.1	Cl^-	Open	22	21	Gel dried up
16	0.1	Cl^-	Open	22	7	Gel thickened up
17▲	0.1	Cl^-	Open	22	1	Gel thickened up
18	0.1	Cl^-	Open	22	1	Gel thickened up
19	0.1	SO_4^{2-}	Open	22	1	Gel thickened up
20▲	0.1	SO_4^{2-}	Open	22	1	Gel thickened up

▲ Washed solids were dried before long term stability evaluation.
* In tests 3-7 Batch 1 scorodite was used as opposed to tests 13-20 in which Batch 2 scorodite was used.

Gel behavior during ageing: During ageing of the aluminum gel/scorodite mixtures a number of qualitative observations were made that are relevant to materials handling considerations. After blending the scorodite particles with the aluminum gel, the mixture was noted to become less viscous than the starting gel, but sufficiently thick to prevent scorodite from settling. The mixture regained its original thickness when ageing under open conditions (at 22˚C) as a result of water evaporation.

The amount of mass loss due to water evaporation was proportional to the molar ratio of aluminum to arsenic. This is so because given that a fixed (2M) aluminum concentration solution was used to make the gel, the higher the mass of aluminum gel used for blending the higher the amount of water contained in the gel/scorodite mixture. The greatest mass loss of 68% was observed for the aluminum chloride gel mixture aged at 50˚C in an oven for 1 day (0.96 Al:As). The mixture was totally dry at the end of this ageing treatment. When ageing at room temperature for 21 days, evaporation accounted for a mass loss of 22% and 67% for mixtures with aluminum to arsenic ratios of 0.1 and 1, respectively. After only one day ageing at low aluminum to arsenic (0.1) molar ratios,

the mass loss was in the order of 5%. As ageing proceeded the mixture became more viscous and eventually yielded a dry cake.

For the sample aged (for 21 days) under closed conditions at room temperature (ID 14), an aqueous phase separated from the gel/scorodite mixture, representing 10% of the original mixture volume. At higher temperatures, the gel began to break down into an aqueous phase with the extent of de-gelation dependent on both ageing time and temperature. Thus, while at 40˚C there was still some evidence of a gel-like substance after 54 days, no gel was present after 1 day ageing at 70˚C.

Post-ageing washing: Following the observations made in the previous section in terms of behavior of the gel/scorodite mixtures during ageing, the washing results (in terms of wash water analysis and washed solids composition) following ageing are reported. For the complete results refer to Appendix C.

(1) The effect of open vs. closed type of ageing on aluminum deportment: By referring to the wash filtrate analysis results in Table 8 it becomes apparent that the closed system (aged at 40˚C) yielded an elevated aluminum concentration (1297 mg/L) in the wash water. This is in agreement with the observation made earlier that the gel broke down during ageing. Analyses of the washed solids (refer to Table 9) were found to contain only 0.5 wt.% aluminum (or, in terms of molar ratio Al:As = 0.05 vs. initial Al:As = 1), which signifies that 95 % (based on mass balance calculations) of the aluminum input reported to the wash water. The composition of the post-wash solids from the closed system ageing at 70˚C was very similar to that from the 40˚C test (results appear in Appendix C).

In contrast to the high temperature closed system tests, the filtrate from washing the open system aged samples contained only 100 – 300 mg/L aluminum. This represents 51% of the input aluminum for the chloride gel test aged at room temperature which corresponds to 7.5 wt.% aluminum content in the post-wash solids.

It was determined above that the type of ageing (closed vs. open) affects the composition and washing behavior of the gel/scorodite mixtures. However, because of

the different temperature at which ageing was effected (40 – 70˚C for the closed system vs. 22˚C for the open system) it was decided to directly compare open vs. closed system ageing but this time at 22˚C for both tests (Test ID 13 and 14 – refer to Table 8 and 9). In this case, no significant difference between the two systems was observed with essentially all aluminum staying with the washed solids independent of whether ageing was done in a closed or open system. Hence, it can be concluded that ageing at elevated temperature in a closed environment results in a mostly 'soluble' gel type. Thus the remainder of the ageing tests was performed at ambient temperature.

Table 8: Reporting of arsenic, iron and aluminum into the filtrate after washing (high Al:As series) – the effect of type of ageing (open vs. closed) and gel type (Cl vs. SO_4).

ID	Description	[As] (mg/L)	[Fe] (mg/L)	[Al] (mg/L)
3	open, Cl^- gel, 1.54 Al:As, 22 ˚C, 21 days	6.5	4.5	297
6	open, Cl^- gel, 0.96 Al:As, 50 ˚C, 1 day (oven)	6.9	5.1	117
7	open, SO_4^{2-} gel, 1.5 Al:As, 22 ˚C, 28 days	4.9	4.6	16
4	closed, Cl^- gel, 0.96 Al:As, 40 ˚C, 54 days	18.5	8	1297
13	open, Cl^- gel, 1 Al:As, 22 ˚C, 21 days	0.3	0.1	118
14	closed, Cl^- gel, 1 Al:As, 22 ˚C, 21 days	0.1	0.2	78

Table 9: Composition of aged gel/scorodite samples (high Al:As series) after washing – the effect of type of ageing (open vs. closed) and gel type (Cl vs. SO_4).

ID	Description	As (wt.%)	Fe (wt.%)	Fe:As (molar)	Al (wt.%)	Al:As (molar)	SO_4^{2-} (wt.%)
1	Batch 1 Scorodite	31.4	24.3	0.98	-	-	2.9
3	open, Cl^- gel, 1.54 Al:As, 22 ˚C, 21 days	24.6	17.5	0.96	7.5	0.84	1.9
6	open, Cl^- gel, 0.96 Al:As, 50 ˚C, 1 day (oven)	23.5	18.4	1.05	5.6	0.66	2
7	open, SO_4^{2-} gel, 1.5 Al:As, 22 ˚C, 28 days	17.3	13.3	1.04	9.0	1.45	26.1
4	closed, Cl^- gel, 0.96 Al:As, 40 ˚C, 54 days	28.9	22.5	1.04	0.5	0.04	2.7
8	Batch 2 Scorodite	30.0	23.0	1.03	-	-	3.0
13	open, Cl^- gel, 1 Al:As, 22 ˚C, 21 days	21.4	17.5	1.10	7.9	1.02	1.4
14	closed, Cl^- gel, 1 Al:As, 22 ˚C, 21 days	21.8	17.7	1.09	8.4	1.06	1.3

(2) The effect of gel type (SO_4 vs. Cl) on aluminum deportment: By considering further the aluminum results from Table 8 it is noted that the amount of aluminum in the filtrate is higher for the chloride gel/scorodite mixture than for the sulphate gel/scorodite mixture (aged under open conditions) suggesting removal of aluminum from the aged solids. This was indeed confirmed from the analysis of the post-wash solids (Table 9). Thus the aluminum content for the chloride test was 7.5 wt.% while that of the sulphate gel was 9 wt.%. However the difference was more dramatic when the aluminum to arsenic ratio in the washed solids is considered (0.85 for the chloride gel vs. 1.45 for the sulphate one). For the chloride gel test this represents approximately half of the aluminum input, with

the remaining aluminum reporting to the wash water. In contrast, aluminum in the washed sulphate gel/scorodite solids accounted for over 95 % of the aluminum used to make the gel. Similar behavior was observed with the tests at low aluminum to arsenic molar ratios. These are summarized in Table 10 and Table 11. Thus for the ageing tests at an initial aluminum to arsenic molar ratio of 0.1 the aluminum content was 0.7 – 0.8 wt.% for the chloride gel samples (ID 15 and 16) and 1.0 wt.% for the sulphate gel sample (ID 20) regardless of ageing time. This represents 75 % of the input aluminum for the chloride gel tests and over 95 % for the sulphate gel test. This is reflected in the aluminum to arsenic molar ratio of the washed solids: 0.07 – 0.08 for the chloride gels vs. 0.1 for the sulphate gel (refer to Table 11). The significant difference in solubilization of aluminum between the two systems may reflect the different molecular make-up of the chloride and sulphate-derived gels respectively as it was detected during the characterization work presented in section 4.2.

Table 10: Reporting of As, Fe, Al, SO_4 and Na in the filtrate after washing (low Al:As series) – the effect of ageing time (open system) and gel type (Cl vs. SO_4).

ID	Description	[As] (mg/L)	[Fe] (mg/L)	[Al] (mg/L)	[S] (mg/L)	[Na^+] (mg/L)
15	open, Cl^- gel, 0.1 Al:As, 22 °C, 21 days	9.7	5.6	30	0.38	194
17	open, Cl^- gel, 0.1 Al:As, 22 °C, 1 day	2.7	1.8	16	0.17	195
20	open, SO_4^{2-} gel, 0.1 Al:As, 22 °C, 1 day	0.1	0.0	2	94.0	185

Table 11: Composition of aged gel/scorodite samples (low Al:As series) after washing – the effect of ageing time (open system) and gel type (Cl vs. SO_4).

ID	Description	As (wt.%)	Fe (wt.%)	Fe:As (molar)	Al (wt.%)	Al:As (molar)	SO_4^{2-} (wt.%)
15	open, Cl^- gel, 0.1 Al:As, 22 °C, 21 days	27.6	22.0	1.07	0.7	0.07	1.8
17	open, Cl^- gel, 0.1 Al:As, 22 °C, 1 day	27.6	23.2	1.12	0.8	0.08	2.2
20	open, SO_4^{2-} gel, 0.1 Al:As, 22 °C, 1 day	28.3	22.1	1.05	1.0	1.05	2.8

(3) The effect of ageing time on aluminum deportment: From an implementation point of view, a shorter ageing time prior to solids disposal of the gel/scorodite mixture is of obvious benefit. In Table 8 and 9 the ageing time varied from 21 to 58 days with no apparent effect. Hence it was decided to examine the effect of shortening the retention time down to one day. The results (Test ID 15 and 17) are shown in Table 10 and Table 11. As it can be seen, the two gels resulted in the same level of aluminum retention and wash water composition. With reference to the latter it is worthy to mention that effectively all sodium after washing reported to the wash water independent of gel type.

(4) The deportment of arsenic and iron: By examining the arsenic and iron concentration data in Table 8 (in particular ID 3, 4, 6 and 7) it can be seen that these elements have reported to the wash water at the level of 5 – 19 mg/L As and 5 – 8 mg/L Fe. These levels exceed the solubility of scorodite (< 0.6 mg/L As) [4] for the pH range of the wash water of 4 to 6. This implies that some scorodite had reacted with the gel. It is suspected that despite the bulk pH of 4 – 6, the gel may have contained some localized high alkalinity spots that resulted in attack of scorodite. However, no such attack was observed in the case of tests with ID 13, 14 and 20 (soluble [As] < 0.3 mg/L). This variable response may be a manifestation of poor homogeneity in some of the gels due to the manual method of mixing used during the production of the gel.

4.3.2 Characterization

SEM: Scanning electron microscope images of the post-wash aged solids produced with aluminum chloride and aluminum sulphate gels (Test ID 3, 7) are shown in Figure 39. The solids from the chloride gel/scorodite mixture show evidence of non-uniform deposits on some scorodite particles, while other particles have no visible coating at all. This suggests that incomplete encapsulation had taken place. It is possible, however, that a very thin coating not visible with this technique may still be present. Post-wash solids from the sulphate gel/scorodite mixture were quite different in morphological features than those from the chloride gel/scorodite mixture. In this case, it can be seen the scorodite particles have small agglomerates spread on a non-uniform fashion on their surface. However, it is unclear to what extent they are ‘bound’ together.

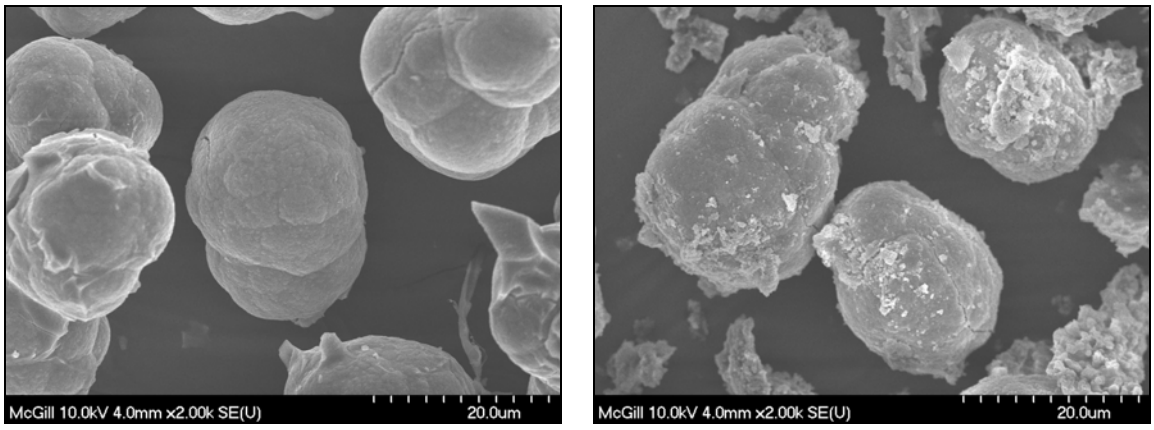

Figure 39: Scanning electron microscope images of gel/scorodite mixtures for samples aged under open conditions with chloride gel (ID 3) (left) and sulphate gel (ID 7) (right).

Select samples were further mounted in a cold setting epoxy resin and subsequently polished in order to examine the particle cross sections. A back-scattered electron image of the washed aluminum sulphate gel/Batch 1 scorodite mixture (Al/As 1.5, ID 7) aged under open conditions for 28 days along with As, Fe and Al elemental x-ray maps is depicted in Figure 40.

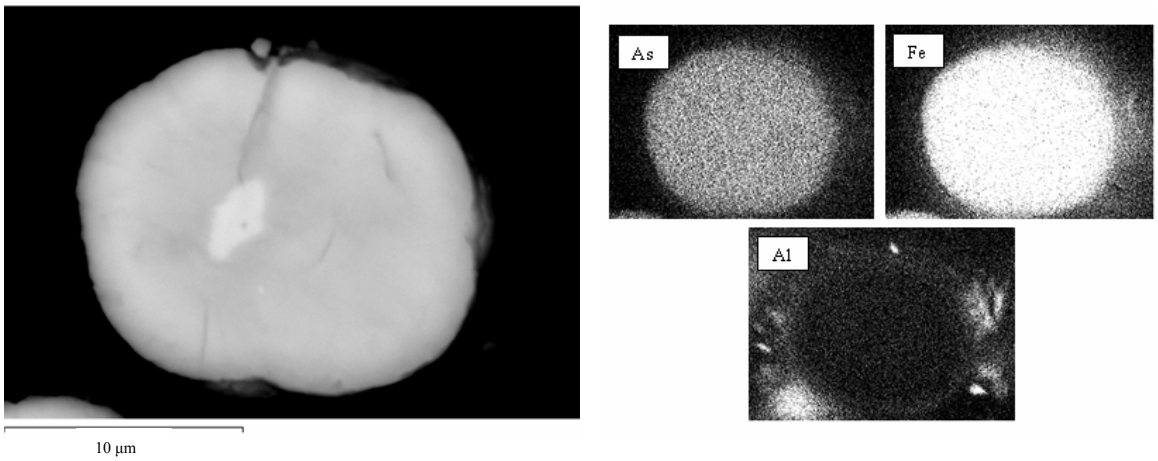

Figure 40: Back-scattered electron (BSE) image of Batch 1 scorodite aged with aluminum sulphate gel (Al:As 1.5) under open conditions for 28 days and elemental x-ray maps – site of interest 1 (5000x, 25 keV).

An interesting feature is the observation of a lighter region in the core of the scorodite particle, which represents the autoclave scorodite seed. But according to BET measurement the autoclave seed had a higher surface area, i.e. it consisted of highly porous aggregates. The arsenic and iron elemental x-ray maps confirmed that the large particle is scorodite. The aluminum x-ray map reveals that there is no aluminum inside

the large particle, but several ‘islands’ of aluminum hydroxide phases are evident to occur on or near the scorodite particle surface.

A second back-scattered electron image along with As, Fe, and Al elemental x-ray maps for another particle from the same sample is shown in Figure 41. This particle appears to have a much larger core than the previous one. It is also evident that the particle has been cracked in numerous places, apparently as a result of the polishing of the specimen. This is an important observation that needs to be taken into account when it comes to materials handling issues in a possible industrial application. The arsenic and iron x-ray maps indicate that the large particle is clearly scorodite. Upon examination of the aluminum x-ray map once more there is no aluminum evident inside the scorodite particle but several aluminum hydroxide ‘islands’ are again observed in the surrounding region.

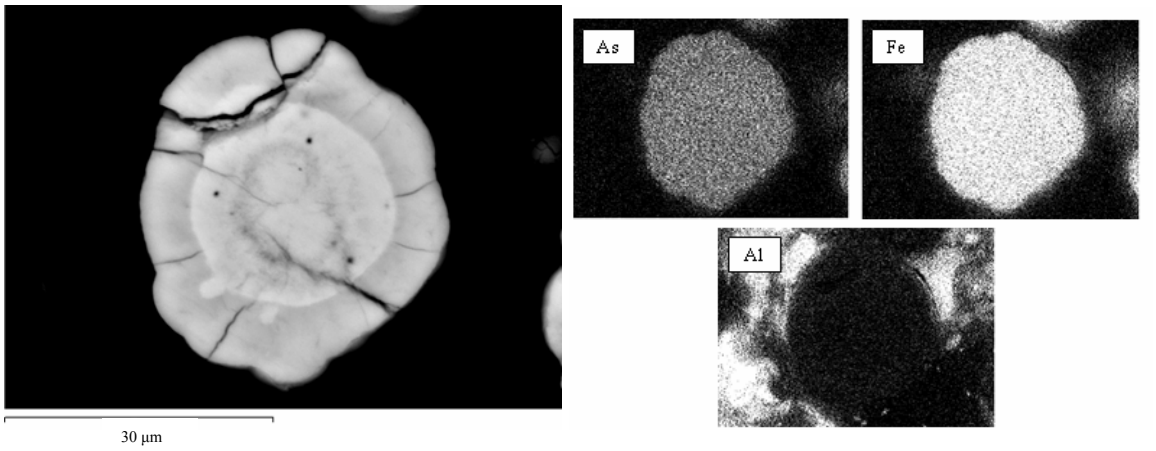

Figure 41: Back-scattered electron image (BSE) of Batch 1 scorodite aged with aluminum sulphate gel (Al:As 1.5) under open conditions for 28 days and elemental x-ray maps – site of interest 2 (2000x, 25 keV).

As noted above, aluminum hydroxide (assumed) islands were evident in the aluminum x-ray map but not in the back-scattered electron image. This was thought to be an artifact of the applied accelerating voltage (25 keV) that led to specimen charging that obscured the light aluminum-containing phase [62]. Hence, a new back-scattered electron image was taken but this time the accelerating voltage was decreased to 7 keV (same site of interest as for Figure 41). The back-scattered electron image along with As, Fe and Al elemental x-ray maps at this reduced accelerating voltage are presented in Figure 42. The

autoclave produced scorodite seed and cracks in the scorodite particle are once again visible, but the surrounding region now contains features not previously visible. X-ray elemental maps were collected over a significantly longer acquisition time due to the reduced signals and the aluminum x-ray map revealed the same features as previously observed. However, these features now correspond with the ones observed in the back-scattered electron image. It appears from the image of Figure 42 that the aluminum hydroxy-gel has formed a matrix around the scorodite particle.

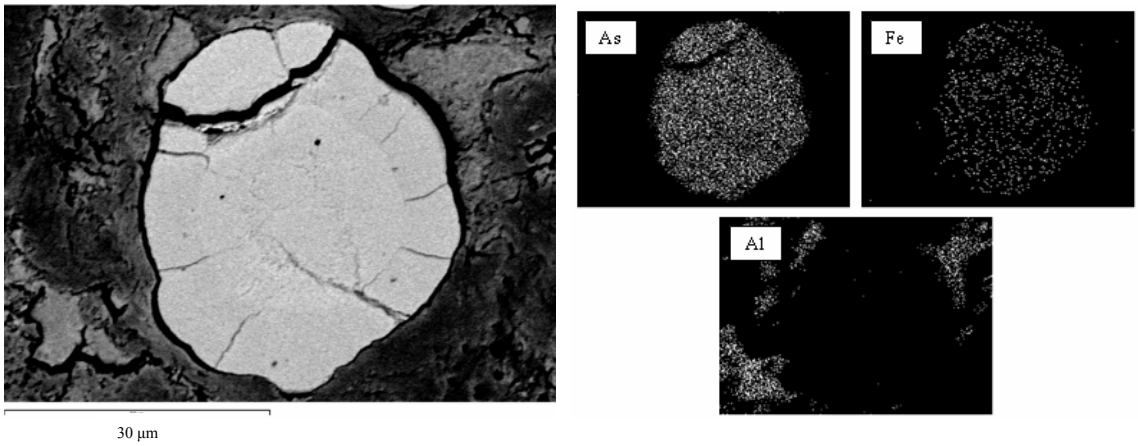

Figure 42: Back-scattered electron image (BSE) of Batch 1 scorodite aged with aluminum sulphate gel (Al:As 1.5) under open conditions for 28 days and elemental x-ray maps – site of interest 2 (2000x, 7 keV).

A back-scattered scanning electron microscope image of the washed aluminum sulphate gel/Batch 2 scorodite mixture (Al/As 0.1, ID 20) aged under open conditions for 1 day along with As, Fe and Al elemental x-ray maps is depicted in Figure 43. The image contains numerous particles and it is evident from the arsenic and iron x-ray maps that the largest particles are scorodite. The aluminum x-ray map shows evidence of aluminum hydroxide rings (albeit diffuse) surrounding the scorodite particles.

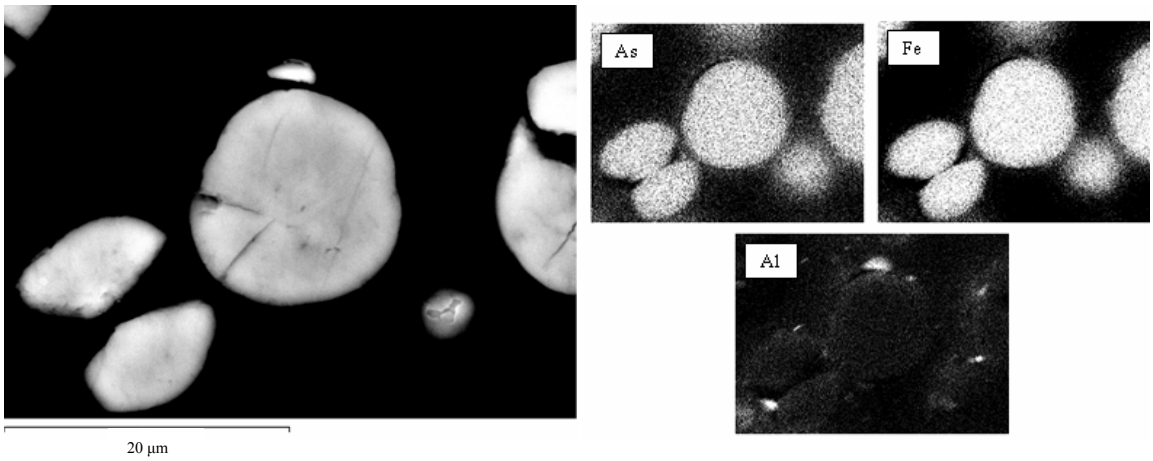

Figure 43: Back-scattered electron (BSE) image of Batch 2 scorodite aged with aluminum sulphate gel (Al:As 0.1) under open conditions for 1 day and elemental x-ray maps (3000x, 25 keV)

Vibrational spectroscopy: Attenuated Total Reflectance Infrared (ATR-IR) spectra were obtained for aged chloride gel/scorodite (Test ID 3) and sulphate gel/scorodite (Test ID 7) samples and compared with those of Batch 1 scorodite as presented in Figure 44.

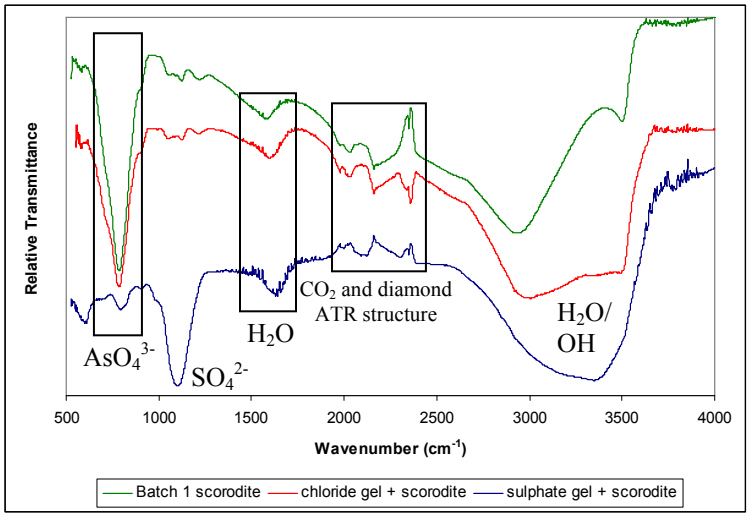

Figure 44: Infrared spectra of aged sulphate gel/scorodite (Bottom) and chloride gel/scorodite (Middle) mixtures in comparison with Batch 1 scorodite (Top).

All spectra exhibit the CO_2 and diamond ATR features. However, while the scorodite and chloride gel/scorodite sample produced essentially identical spectra (especially when it comes to H_2O/OH and AsO_4 bands), the sulphate gel/scorodite sample exhibited some unique features. Thus in addition to the SO_4 band, confirming the presence of SO_4 as determined by chemical analysis, it is evident that the H_2O/OH and

AsO_4 bands are diffuse and repressed respectively. This indicates that the polarization of the As-O bond is modified in the sulphate gel/scorodite sample and further study is required to identify precisely how scorodite is affected by the presence of aluminum sulphate gel.

Raman spectra were also obtained for Batch 1 atmospheric scorodite as well as the aged chloride gel/scorodite and sulphate gel/scorodite materials, but are omitted from the present work as there were no discernable differences observed.

4.4 Stability of Samples

The long term stability of the aged gel/scorodite materials was evaluated by equilibrating these solids in water that was initially adjusted to pH = 8 with NaOH or MgO. The system pH was allowed to drift to pH = 7 or lower and subsequently re-adjusted. This section comprises the results from the long term stability evaluation study.

4.4.1 High Aluminum/Arsenic Series

In this section the stability behavior of the high aluminum gel/scorodite materials (namely those obtained from ageing tests ID 3, 4, 5, 6, 7 – refer to Table 7) is considered by comparing their release of arsenic to that of scorodite (Batch 1). In this series of tests pH adjustment was conducted with 1 M NaOH.

Attainment of equilibrium – pH evolution: Before the stability data for each aged gel/scorodite combination are presented and discussed the evolution of pH with time is presented. The pH vs. time data are plotted in a series of charts in Figure 45. As it can be seen, during the first few weeks significant acid release took place requiring frequent (on a weekly basis) pH re-adjustment with base addition. Such acid release may be interpreted as evidence of some minor surface dissolution of scorodite as described by the following reaction reported by *Bluteau and Demopoulos* [4]:

$$FeAsO_4 \bullet 2H_2O_{(s)} + H_2O \rightarrow Fe(OH)_{3(s)} + H_2AsO_4^- + H^+ \qquad \text{Eqn. 4.7}$$

According to this reaction, some colloidal ferrihydrite (here written as $Fe(OH)_3$) precipitate forms. No iron was detected in the long term stability solution samples while the soluble aluminum was less than 0.5 mg/L. Here it appears that after the last pH adjustment (to pH = 8) at 158 days all systems tended to stabilize in the pH = 7 – 7.5 region essentially reaching near equilibrium after about 250 days. Ultimately, with the exception of the sulphate gel system, all other chloride gel/scorodite systems stabilized at pH = 7 – 7.3. The equilibrium pH of the sulphate gel/scorodite system on the other hand was ~6.6.

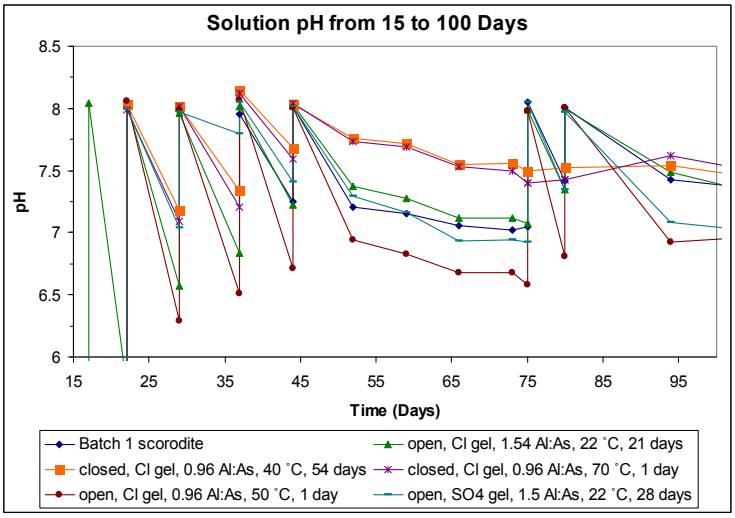

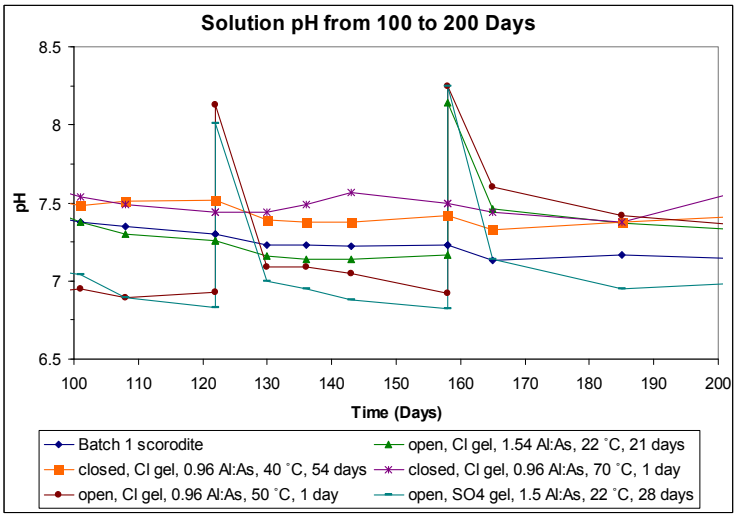

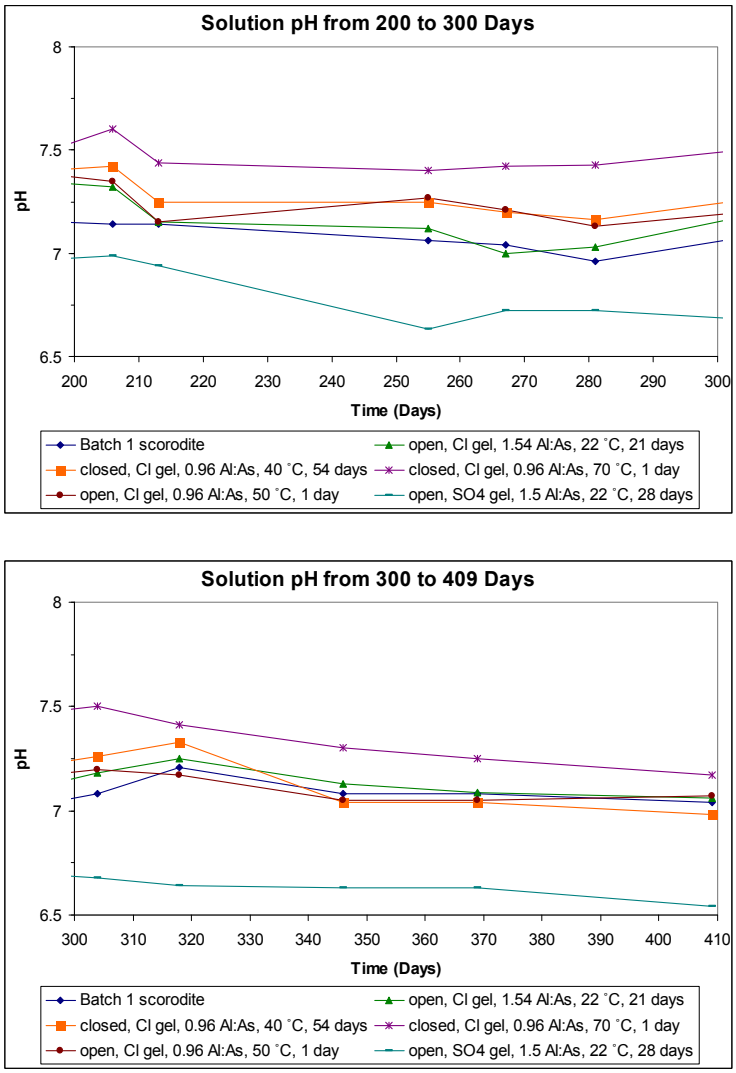

Figure 45: The variation of pH with time during the long term stability testing of the high Al:As system solids.

Arsenic release: The detailed arsenic release data as a function of time for the various aged gel/scorodite systems along that from atmospheric scorodite (Batch 1) are summarized in Appendix E. Plots of these data are presented in Figure 46. As it can be seen, the release of arsenic from Batch 1 atmospheric scorodite was significant in the order of 38 mg/L at pH 7.0 after 409 days. This number is over 6 times the equilibrium value (6 mg/L As at pH = 7) reported for the autoclave synthesized scorodite by *Bluteau and Demopoulos* [4]. This points to possible crystal imperfections as a source for the higher solubility exhibited by the atmospheric scorodite caused partly due to SO_4 incorporation. However, all aged gel/scorodite systems showed significantly improved

stability over that of Batch 1 scorodite, with no arsenic release over 5 mg/L detected in the 6.5 – 7.2 pH range. This implies that some stabilization of scorodite with aluminum hydroxyl-gels took place.

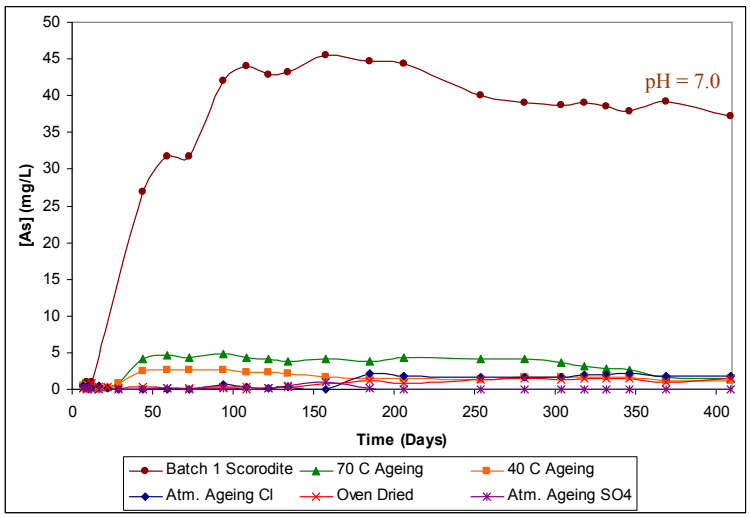

Figure 46: Arsenic release from Batch 1 atmospheric scorodite and aged gel/scorodite systems – high Al:As series (Test ID 3-7).

In order to better differentiate between the stability of aged gel/scorodite systems, the data of Figure 46 are replotted in Figure 47 at a magnified scale by omitting the results from the reference scorodite material. The last of the weekly pH adjustments was conducted after 44 days and initially, the samples aged under closed conditions showed the highest arsenic release. The sample aged at 70˚C exhibited the highest arsenic release of 4 mg/L (pH = 7.5) followed by the sample aged at 40˚C with 2.5 mg/L As (pH = 7.5). The three open system tests all had comparable arsenic release of less than 1 mg/L, but pH was lower in the 6.9 – 7.4 range. Consequently, intermittent pH adjustment of the open system tests was conducted in order to raise the pH to the same range as the closed system tests. Arsenic release is observed to significantly increase after 150 days for the oven dried and atmospherically aged chloride gel/scorodite mixtures to values of 1.5 mg/L and 2 mg/L at pH = 7.1, respectively. The sulphate gel/scorodite mixture aged under open conditions had the lowest arsenic release of 0.02 mg/L, which is promising despite a low pH value of 6.6. The two closed system tests were allowed to proceed in pH drift mode after 44 days and it is interesting to note that arsenic release for both tests decreased significantly with a corresponding drop in pH. After 409 days stability testing,

the 70˚C aged sample had 1.6 mg/L As at pH = 7.2, while the 40˚C aged sample had 1.4 mg/L As at pH = 7.1. Regardless of the observed decrease in arsenic release from the two closed system ageing tests later on, the aluminum sulphate gel by far proved more effective than the aluminum chloride gel in imparting stabilization to scorodite.

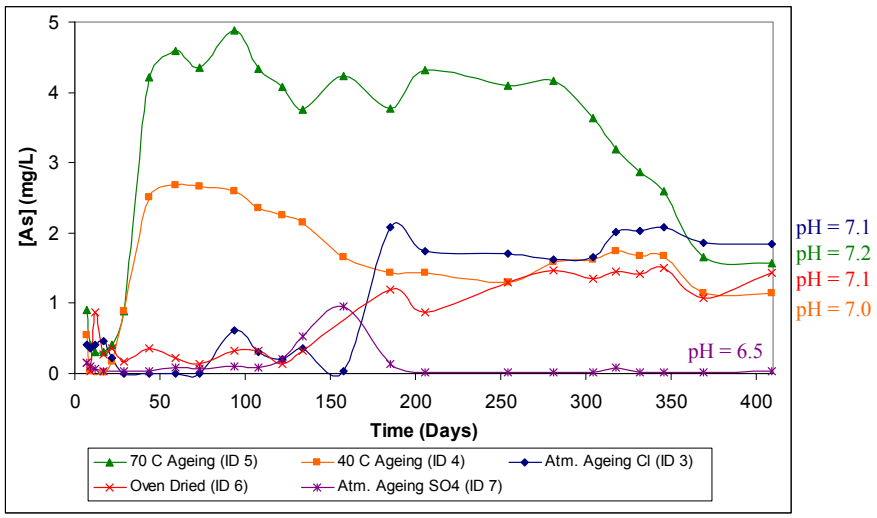

Figure 47: Arsenic release from aged gel/scorodite mixtures (Test ID 3-7) containing batch 1 scorodite.

The essentially equilibrium values of arsenic concentration and pH from Batch 1 scorodite and the aged gel/scorodite systems over an extended period of time are summarized in Table 12.

Table 12: The stability of high Al:As aged gel/scorodite systems (Batch 1 scorodite was used): near equilibrium arsenic concentration data along with corresponding pH values and time periods during which stable values were obtained.

Sample ID	Description	[As] (mg/L)	pH	Time* (days)
1	Batch 1 Scorodite	38.5 ± 0.5	7.0 - 7.1	281 - 409
3	open, Cl^- gel, 1.54 Al:As, 22 ˚C, 21 days	1.85 ± 0.02	7.1 - 7.2	206 - 409
6	open, Cl^- gel, 0.96 Al:As, 50 ˚C, 1 day (oven)	1.42 ± 0.08	7.1	281 - 409
7	open, SO_4^{2-} gel, 1.5 Al:As, 22 ˚C, 28 days	0.03 ± 0.01	6.6 - 6.7	206 - 409
4	closed, Cl^- gel, 0.96 Al:As, 40 ˚C, 54 days	1.4 ± 0.3	7.1 - 7.3	206 - 409
5	closed, Cl^- gel, 0.96 Al:As, 70 ˚C, 1 day	1.60 ± 0.05	7.2	369 - 409

* Time period over which steady [As] and pH was observed.

The near equilibrium pH was fairly similar (7 – 7.3) for all samples excluding the sulphate gel/scorodite system for which a lower pH of 6.6 was noted. All chloride gel systems, independent of the method of ageing, yielded similar arsenic release levels of

~1.6 ± 0.3 mg/L As. On the other hand, arsenic release from the sulphate gel/scorodite system was only 0.03 mg/L As albeit at lower pH ~6.6. However, such a low arsenic level (i.e. 0.03 mg/L As) cannot be explained solely on the basis of pH as it is approximately 100 times lower than the solubility of scorodite (2.97 mg/L As for the autoclave variety) as inferred from the data of *Bluteau and Demopoulos* [4].

The effect of pH: In an effort to more objectively evaluate the pH effect on arsenic release for the different systems, the arsenic concentration for each of them was plotted as a function of solution pH and compared to that of Batch 1 atmospheric scorodite and autoclave scorodite (data taken from *Bluteau and Demopoulos* [4]) in Figure 48.

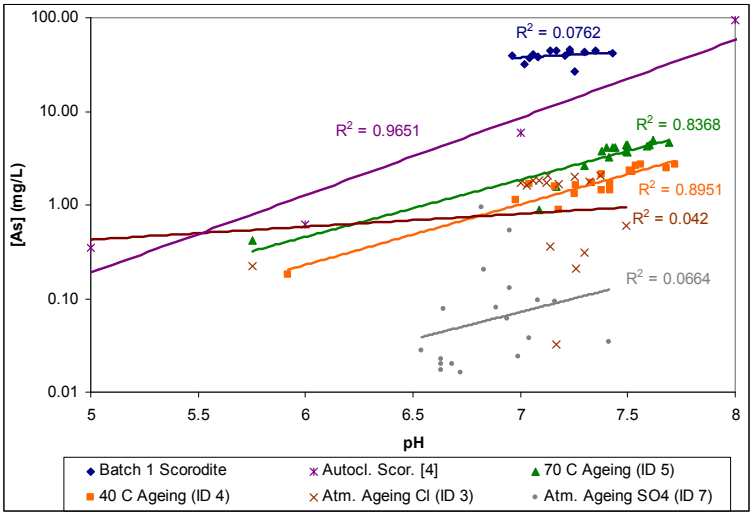

Figure 48: Effect of pH on arsenic release for Batch 1 atmospheric scorodite and aged gel/scorodite systems containing Batch 1 solids in comparison with autoclave produced scorodite [4].

It should be noted that the data plotted in Figure 48 were not necessarily obtained at equilibrium. Examination of the solubility data from *Bluteau and Demopoulos* [4] shows an exponential increase of arsenic release with pH. The Batch 1 atmospheric scorodite data had a fairly low correlation and the absence of a clear trend is attributed to lack of data over a wide pH range. Of the gel/scorodite systems included, only the data from the two closed system ageing tests show acceptable correlations. The regression curves are parallel to the data from autoclave scorodite [4] and show a reduction in arsenic release over these data and the Batch 1 scorodite control sample. However caution should be exercised with this interpretation, as there is only a single point at the

low pH range. The sulphate and chloride gel/scorodite systems aged under open conditions at 22˚C lack any discernable trend and the wide scatter in data renders further quantitative interpretation difficult. Regardless, ageing of scorodite with aluminum gels is clearly seen to reduce arsenic release in the pH range of interest with respect to gel-free scorodite. Moreover, the sulphate gel/scorodite system is by far the most effective. The fact that the open aged gel/scorodite system showed no similar trend in terms of pH effect (parallel curves to that of autoclave scorodite) reflects a different type of stabilization. Thus, it is conceivable that in the case of the closed systems adsorption of soluble arsenic on residual aluminum hydroxides (this is a pH dependent system [46-48, 50]) occurs, while in the case of the open systems other more complex mechanisms may be responsible for arsenic retention.

4.4.2 Physical Mixture of Scorodite and Aluminum (Oxy)Hydroxides

In the previous section reference was made to possible arsenate retention by the aged aluminum hydroxyl-gels via adsorption analogous to that occurring on aluminum hydroxides (refer to section 2.4.3 in Chapter 2). To verify this hypothesis and compare the relative performance of the newly investigated aluminum hydroxyl-gels to that of aluminum (oxy)hydroxides, a series of tests was performed involving physical mixtures of scorodite (Batch 2) with amorphous aluminum hydroxide and bayerite. Arsenic release from these mixtures was monitored over a period of 169 days following an initial single pH adjustment to pH = 8 using 0.5M magnesium oxide slurry. The results from this series of tests are presented in Figure 49 along with the stability response of Batch 2 scorodite. The full set of data is summarized in Appendices F and G.

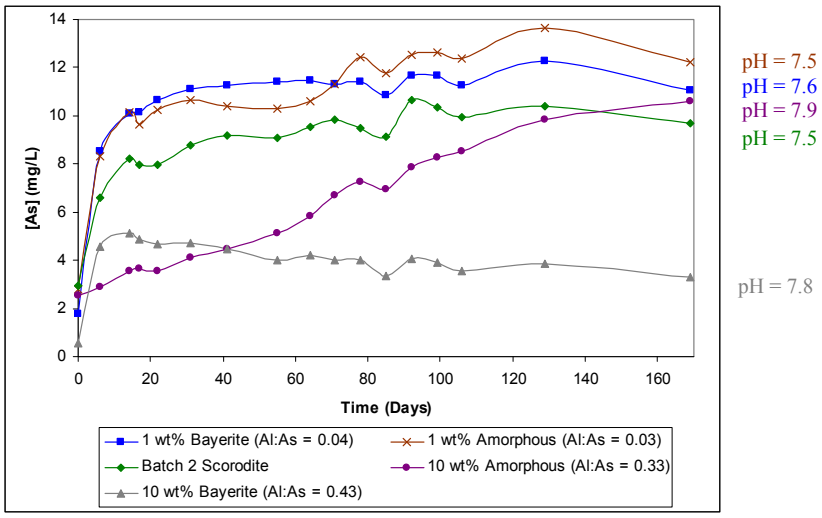

Figure 49: Arsenic release from Batch 2 scorodite and physical mixtures of scorodite/aluminum (oxy)hydroxides (Test ID 9 - 12).

Comparison of Batch 1 to Batch 2 scorodite and NaOH to $Mg(OH)_2$: As it can be seen, arsenic release from Batch 2 atmospheric scorodite after 169 days was 9.7 mg/L at pH 7.5, which is significantly lower than the 38.5 mg/L As observed for Batch 1 scorodite (refer to Figure 50).

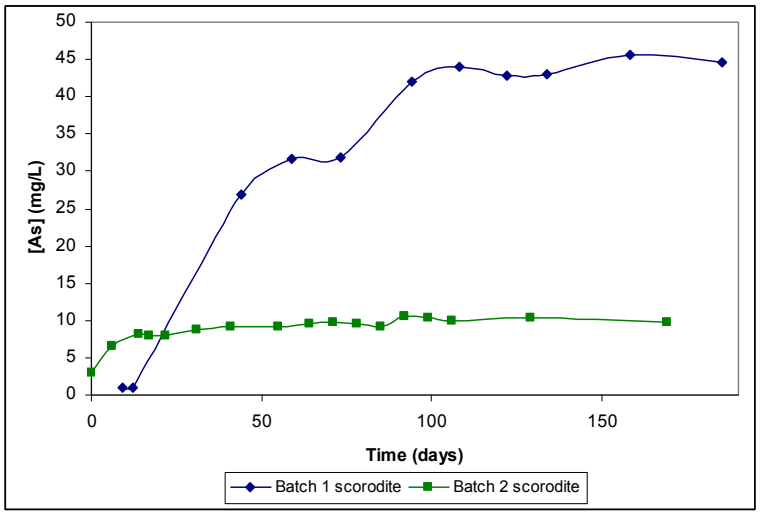

Figure 50: Direct comparison of arsenic release from Batch 1 (NaOH for pH adjustment) and Batch 2 ($Mg(OH)_2$ for pH adjustment) atmospheric scorodite.

This implies that atmospheric precipitation of scorodite from the 40 g/L feed solution produced more stable scorodite than that produced from the 20 g/L feed solution. As discussed in section 4.1 the Batch 2 scorodite possessed a lower specific surface area

(2.16 m^2/g vs. 3.15 m^2/g) than Batch 1 scorodite, i.e. it was denser material which may have contributed to its enhanced stability. It is interesting to note that Batch 2 scorodite exhibited lower solubility than even the autoclave synthesized scorodite by *Bluteau and Demopoulos* [4] so far considered the most stable of all synthetic scorodites. Thus by interpolation from the data published in [4] the solubility of autoclave produced scorodite was calculated to be 16 mg/L at pH 7.5 in comparison to 9.7 mg/L for Batch 2 atmospheric scorodite.

Finally, it is worthy to note that the use of MgO for pH adjustment followed by free pH drift resulted in less sharp pH changes than when NaOH was used (refer to Figure 51). Moreover, with MgO a higher stable solution pH was observed in a shorter period of time. Thus in the case of Batch 1 scorodite an equilibrium pH of 7 was attained after 255 days when NaOH (1 M) was used as base, while in the case of Batch 2 scorodite/MgO system an equilibrium pH of 7.5 was attained after only 30 days. It is deduced from this comparison that pH adjustment with MgO provides more stable pH control stemming apparently from the low solubility of magnesium oxide, thus facilitating the attainment of equilibrium.

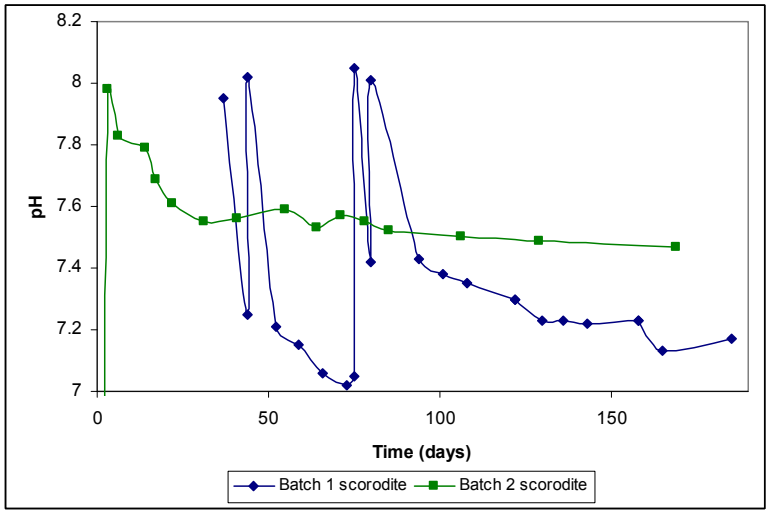

Figure 51: pH evolution with time involving two different bases for pH adjustment: 1.0 M NaOH and 0.5M MgO slurry.

Amorphous aluminum hydroxide vs. bayerite: By returning to Figure 49 it can be seen that with the exception of the 10 wt.% bayerite system (corresponding to Al:As molar

ratio of 0.43), all other mixtures of amorphous aluminum hydroxide (1 wt.% and 10 wt.%) and bayerite (1 wt.%) with scorodite yielded the same level of arsenic release as scorodite (Batch 2). Thus arsenic release was 11.1 mg/L at pH = 7.6 for the sample containing 1 wt.% bayerite and 12.2 ppm at pH = 7.5 for the sample containing 1 wt.% amorphous aluminum hydroxide. For physical mixtures containing 10 wt.% bayerite and 10 wt.% amorphous aluminum hydroxide arsenic release was 3.3 mg/L at pH = 7.8 and 10.6 mg/L at pH = 7.9, respectively. Only the 10 wt.% bayerite system released less arsenic than pure scorodite and it is interesting to note that the mixture containing bayerite achieved equilibrium after 10 days, while the one containing amorphous aluminum hydroxide required over 100 days. This implies that only bayerite is an effective sorbent for arsenic, which is attributed to its significantly higher surface area over that of the amorphous aluminum hydroxide (110 m^2/g vs 0.5 m^2/g) used in this work. But as it will be demonstrated in the following section the sulphate gel material is still superior to bayerite.

4.4.3 Low Al:As (Gel/Scorodite) Series

The stability of a second series of aged gel/scorodite materials in terms of arsenic release over a period of 169 days is discussed in this section. All tests included here involved Batch 2 scorodite and comprised test ID 13 – 20 (refer to Table 7). With the exception of tests 13 and 14 all other tests involved low aluminum to arsenic molar ratios (i.e. Al:As = 0.1).

The effect of Al:As ratio on arsenic release: Figure 52 shows the arsenic release for all chloride gel/scorodite materials in comparison with the Batch 2 atmospheric scorodite control sample. The corresponding pH evolution chart is plotted in Figure 53 while all data involving Batch 2 scorodite are summarized in Appendices F and G. By considering tests 13b (Al:As = 1) and 15 (Al:As = 0.1) it can be seen that lowering the aluminum content to Al:As = 0.1 yielded essentially the same level of arsenic release, i.e. 4.6 mg/L As (at pH = 7.6) vs. 7.9 mg/L As (at pH 7.8). Both systems had been aged for 21 days at 22˚C under open conditions.

The effect of closed vs. open system ageing: With reference to Figure 52 comparison of tests 14 (closed) and 13b (open) – both aged for 21 days at 22˚C with Al:As = 1 – reveals no particular difference in terms of arsenic release. Thus the corresponding stable concentration of arsenic was 5.9 mg/L (at pH = 7.9) for the closed system vs. 4.6 mg/L (at pH = 7.6) for the open system.

The effect of ageing time: Comparison of the arsenic release data from tests 18 (1 day), 16 (7 days) and 15 (21 days) - involving ageing at 22˚C under open conditions for different times (refer to Figure 52) – appears to suggest the longer the ageing time the lower the release of arsenic. Thus the materials aged for 1 day and 7 days exhibit arsenic release of 13.9 mg/L (at pH = 7.9) and 14.2 mg/L (at pH = 8.2) respectively, while the material aged for 21 days released only 4.6 mg/L (at pH = 7.6). The material from test 17 was aged for 1 day as with test 18, except that it was dried after washing prior to stability testing. In this case the arsenic release was only 5.6 mg/L (at pH 7.9). Given the pH sensitivity of arsenic release (discussed in more detail later in this section) no clear connection can be drawn as to the effect of ageing time on arsenic release.

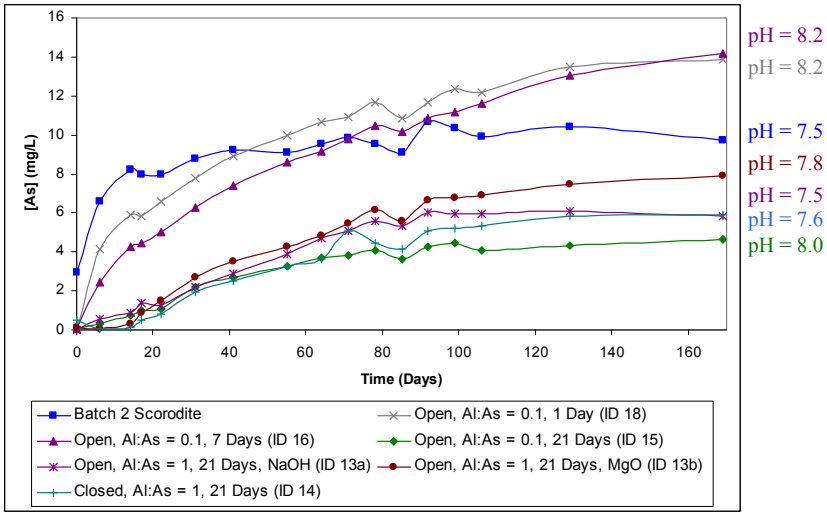

Figure 52: Long term stability of aged chloride gel/scorodite mixtures illustrating the effect of Al:As ratio (Test ID 13b and 15); closed vs. open system ageing (Test ID 13b and 14); and ageing time (Test ID 15, 16, 18).

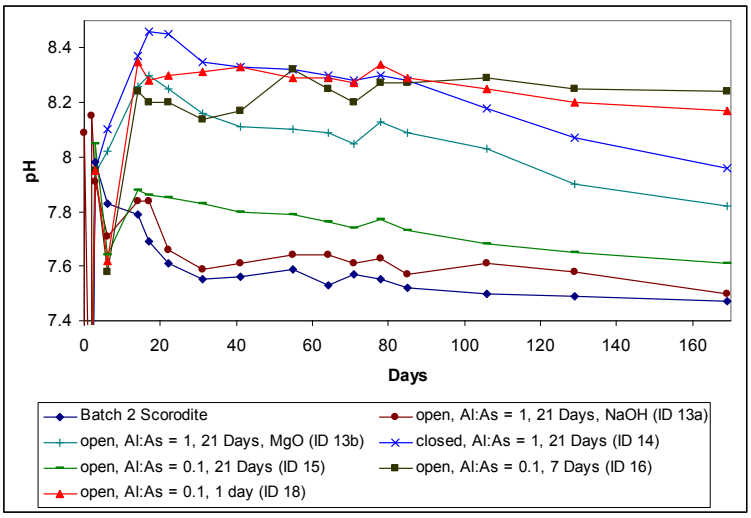

Figure 53: The evolution of pH with time – stability evaluation with single pH adjustment to pH 8 with 0.5M $Mg(OH)_2$ slurry.

The effect of gel type: The effect of aluminum sulphate gel (Test ID 19, 20) vs. aluminum chloride gel (Test ID 17, 18) on arsenic release from scorodite (Batch 2) is shown in Figure 54.

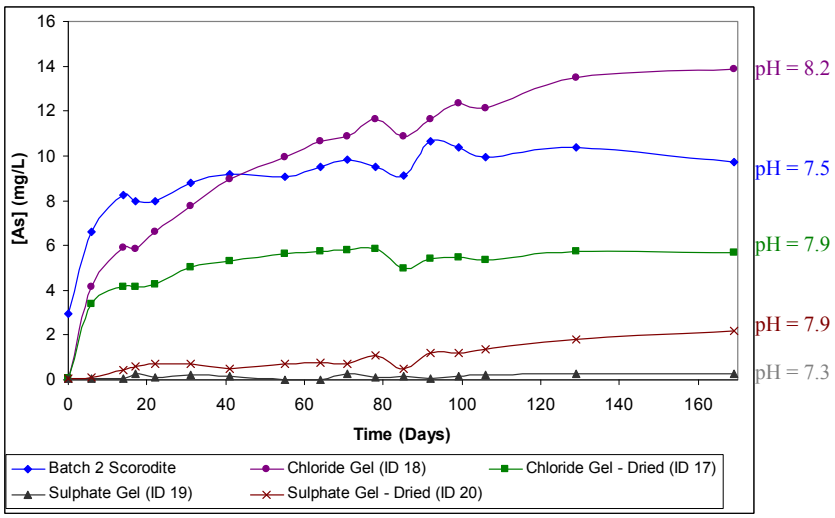

Figure 54: Long term stability of aged gel/scorodite mixtures illustrating the effect of gel type (Test ID 17 - 20) and post-wash drying under open system ageing for one day (0.1 Al:As).

The materials were aged under open conditions for one day and arsenic release from Batch 2 scorodite is also included as a reference. The chloride gel sample has an arsenic release of 13.9 mg/L (at pH = 7.9) after 169 days with ID 18, or 5.6 mg/L As for test 17 (dried prior to stability testing). In contrast, arsenic release from the sulphate gel

mixture was only 0.3 mg/L, which is significantly lower despite the pH value being only 7.3. This confirms the earlier observation that the aluminum sulphate gel is better for arsenic fixation than the equivalent aluminum chloride gel.

The effect of pH: In order to separate the influence of pH from the effect of the aluminum hydroxyl-gel on arsenic release, the data from the sulphate gel/scorodite (Al/As 0.1) and chloride gel/scorodite (Al/As 0.1) systems aged under open conditions for 1 day are plotted in Figure 55 as a function of pH. The data from *Bluteau and Demopoulos* [4] are also plotted for comparison. It is emphasized again (as was done for the chart in Figure 48) that caution should be exercised when interpreting these results as they do not represent true equilibrium conditions especially at the low end of the pH range. Rather, this analysis is used to search for order-of-magnitude type comparisons among the various systems. As it can be seen, in agreement with earlier observations, Batch 2 atmospheric scorodite shows lower arsenic release than the reference data at high pH suggesting that its synthesis from a 40 g/L As solution produces a better crystalline and more stable scorodite variety. Arsenic release from the aged gel/scorodite systems is both below that of Batch 2 scorodite and the reference data, with the aluminum sulphate gel being more effective than the aluminum chloride gel for this treatment.

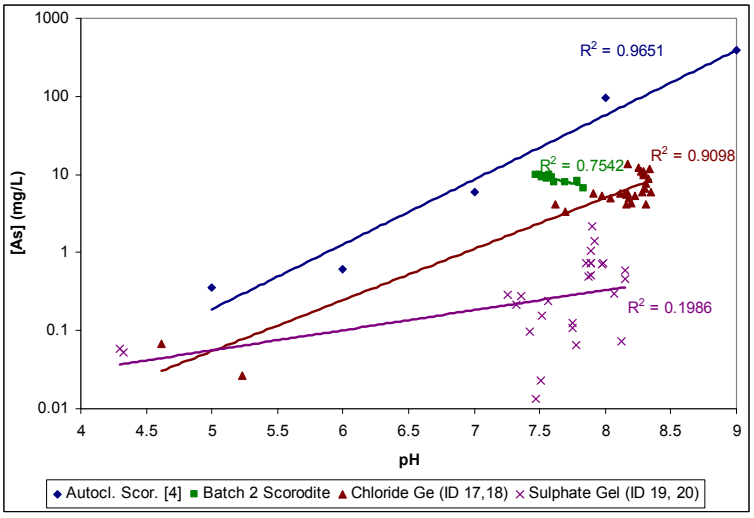

Figure 55: Effect of pH on arsenic release for Batch 2 atmospheric scorodite and aged gel/scorodite systems (Al:As = 0.1, 1 day ageing at 22˚C, ID 17 - 20) containing Batch 2 solids in comparison with autoclave produced scorodite [4].

It should be noted that similar to the previous analysis of arsenic release as a function of pH (refer to Figure 48), the chloride gel system shows pH dependency analogous to that of pure scorodite. This suggests that arsenic retention occurs via an adsorption-type mechanism on the aged gel. On the other hand, the sulphate gel shows no similar pH dependency (R^2 = 0.20) once more pointing to a different (than solely adsorption) mechanism of arsenic control.

Summary: Near-equilibrium arsenic release from Batch 2 scorodite as well as selected aged gel/Batch 2 scorodite materials and aluminum hydroxide/scorodite mixtures are summarized in Table 13 along with the equilibrium pH and time period over which near-equilibrium was observed. Of the physical mixtures of Batch 2 atmospheric scorodite with aluminum hydroxides, only the 10 wt.% $Al(OH)_3$ mixtures are included. Between the two hydroxide materials tested the best result was obtained with 10 wt.% bayerite owing to its significantly higher BET surface area. In this case, it is hypothesized that a fraction of the soluble arsenic in equilibrium with scorodite is removed from solution via adsorption of arsenate ions on the surface of $Al(OH)_3$ [46]. The equivalent molar ratio for this sample is Al/As = 0.43 and since all the tabulated aged mixtures contain less aluminum (Al:As = 0.1) except for Test ID 13a (Al:As = 1), lower arsenic release from the aged samples would indicate an additional mechanism to mere arsenic adsorption by aluminum hydroxide particles. The aluminum sulphate-derived gel/scorodite system (ID 19) with Al/As = 0.1 and BET surface area of 38 m^2/g is calculated to have ~12 times smaller surface area per unit arsenic than the 10 wt.% bayerite/scorodite mixture with Al/As = 0.4 and BET surface area equal to 110 m^2/g. This lends further support to the above theory. None of the chloride gel/scorodite mixtures showed lower arsenic release than the 10 wt.% bayerite sample, which suggests that the mechanism of scorodite stabilization with aluminum chloride gels is by adsorption on the aged gel material (most likely an amorphous precursor to bayerite [41]). It was previously observed that arsenic release from the aged gel chloride/scorodite systems was slow, which may be taken as indication that as arsenic is released from scorodite it is quickly adsorbed by the gels. Once the available surface sites for adsorption become fully occupied, arsenic release levels should attain the same level as for gel-free scorodite. Nonetheless, it appears that

extended ageing of chloride gel/scorodite systems will result in better retention of soluble arsenic possibly because of (at least partially) to crystallization of aluminum hydroxides on the surface of scorodite (refer to SEM characterization in section 4.3.2).

Table 13: Near-equilibrium of arsenic concentration data along with corresponding pH and time over which the values remained stable for selected chloride and sulphate gel/scorodite systems containing Batch 2 atmospheric scorodite. Compared to equivalent data from Batch 2 scorodite alone and in mixtures with 10 wt.% amorphous aluminum hydroxide (Al:As = 0.3) and bayerite (Al:As = 0.43).

Test ID	Description	[As] (mg/L)	pH	Time (Days)
8	Batch 2 atmospheric scorodite	9.7 ± 1	7.5	30 - 169
10	Scorodite + 10 wt% Bayerite	3.5 ± 0.3	7.8	106 - 169
12	Scorodite + 10 wt% Amorphous AlOOH	9.5 ± 1	7.9	106 - 169
13a*	open, Cl^- gel, 1 Al:As, 22 ˚C, 21 days, NaOH	5.9 ± 0.1	7.5	85 - 169
15	open, Cl^- gel, 0.1 Al:As, 22 ˚C, 21 days	4.4 ± 0.2	7.6	106 - 169
18	open, Cl^- gel, 0.1 Al:As, 22 ˚C, 1 day	13 ± 1	8.2	106 - 169
19	open, SO_4^{2-} gel, 0.1 Al:As, 1 day	0.2 ± 0.1	7.3	71 - 169

* pH adjustment for Test 13a was done with 1 M NaOH, while 0.5M $Mg(OH)_2$ slurry was used for the other tests.

The best stabilizing effect was offered by the sulphate gel/scorodite system as is evidenced by near-equilibrium arsenic release of only 0.2 mg/L at pH 7.3 after 72 – 169 days. Considering that this suppressed arsenic release level was observed with low gel/scorodite ratio (Al:As = 0.1) aged under open conditions for one day makes this system a very interesting candidate for further investigation as a potentially effective scorodite encapsulating material. The superior performance of the sulphate gel vis-à-vis the other systems is better appreciated with the aid of Figure 56. The 0.2 mg/L As solubility by the sulphate gel/scorodite system (Al:As = 0.1) is 55 times less than the solubility of unprotected autoclave scorodite for the same pH environment (7.3 at 22˚C).

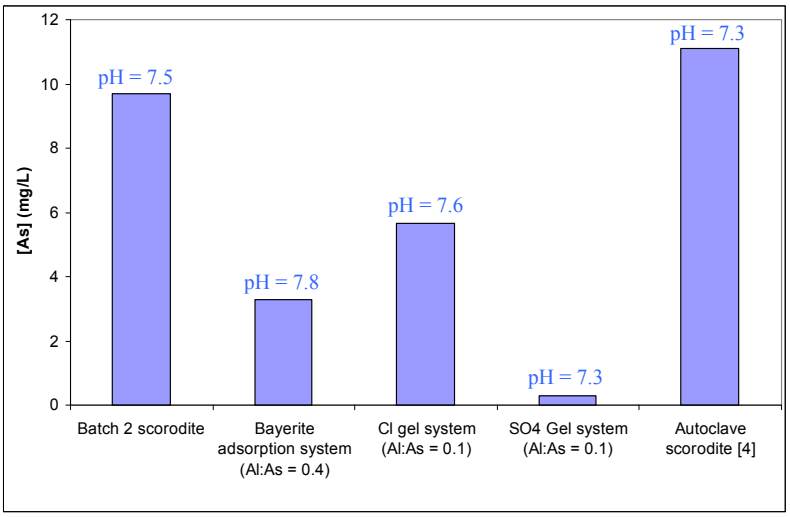

Figure 56: Comparison of near-equilibrium arsenic concentrations for different systems.

4.5 Process Flow Diagram for Industrial Application

Based on the results obtained in this present work, a conceptual process flow diagram for scorodite stabilization with aluminum hydroxyl-gels was prepared and depicted in Figure 57. The process requires two parallel circuits, including one for the preparation of amorphous aluminum gel and another for the atmospheric production of crystalline scorodite. Arsenic solid residue such as flue dust is first leached with sulphuric acid plus an oxidant in the case of As(III) materials [26] and the resultant arsenic rich solution is sent to scorodite precipitation. If the feedstock comprises arsenic-rich plant effluents [9] leaching is redundant but oxidation may still need to be carried out. Precipitation is conducted in stirred tank reactors at 95˚C, where the addition of ferric sulphate, ferrous sulphate or other soluble forms of iron and oxidant (O_2 or SO_2/O_2) [63] is necessary if the liquor does not contain sufficient ferric iron (Fe/As 1.2:1 molar ratio). Part of the scorodite may be recycled as seed. The resultant slurry is transferred to a solid liquid separation stage and the filtrate is recycled back to the leaching step, while the wet scorodite cake is transferred to gel/scorodite blending. Meanwhile, in the gel preparation stage, 2M aluminum sulphate salt solution is partially neutralized (OH/Al = 2.5) via rapid hydrolysis with 5 N sodium hydroxide solution. Other bases such as MgO slurry may be used but not CaO as it results in gypsum formation that leads to a solidified rather than gelatinous product. This is true only for the aluminum sulphate system, as CaO was

found to be equally effective as NaOH in the case of aluminum chloride solution. Equal amounts by weight of atmospheric scorodite and aluminum gel are subsequently blended together, which represents an approximate aluminum to arsenic molar ratio of 0.1. Blending of the two products would likely be done using cement mixing type equipment. The blended mixture is aged (or cured) at ambient temperature for a defined amount of time (at least 1 day) before being transferred either directly as is to waste disposal sites or after washing. The washing step would ideally not be required (requires verification), hence reducing the associated capital and operating costs. If washing is practiced, then some minor (mg/L range) soluble Fe, As and Al may report to the wash water. This will require bleed treatment to control impurity accumulation before returning the aluminum salt solution to gel preparation.

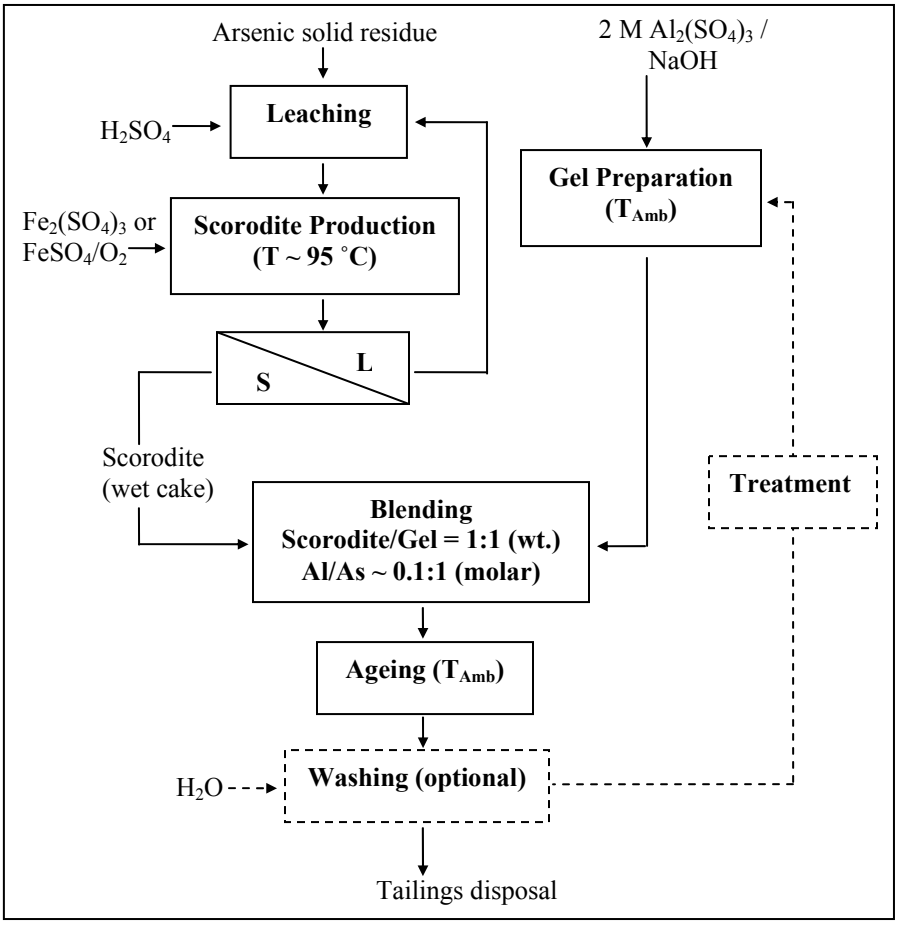

Figure 57: Conceptual process flow diagram for scorodite stabilization with aluminum sulphate hydroxyl-gel.

Chapter 5: Conclusions

The use of amorphous aluminum hydroxyl-gels to stabilize scorodite type solids for disposal under oxidizing conditions at or slightly above the neutral pH has been investigated for the first time. The conducted investigation involved four different type of experiments, namely (1) synthesis of scorodite; (2) production of aluminum hydroxyl-gels; (3) ageing of aluminum gel/scorodite blends; and (4) long term stability evaluation. The major findings from this work are summarized below.

Atmospheric precipitation of scorodite in the presence of seed at 95˚C from ferric sulphate solutions of variable initial arsenic concentrations of 10, 20 and 40 g/L and an iron(III) to arsenic(V) molar ratio of one was found to follow first order kinetics in terms of initial arsenic concentration. Moreover, it was noted for the first time that the morphology of the resultant scorodite particles improved with increasing arsenic concentration. Thus the best scorodite produced from 40 g/L As(V) solutions was found to consist of smooth and dense spherical particles with mean particle size of 22 ± 6.2 μm and specific surface area of 2 m^2/g. Long term stability tests (> 169 days at pH = 7 – 7.5) found the scorodite produced from the 40 g/L As(V) solution to be yet the most stable variety of synthetic scorodite. This scorodite had an 'equilibrium' solubility of ~ 10 mg/L As at pH = 7.5 in comparison with 38.5 mg/L As for the atmospheric scorodite produced from 20 g/L feed solution and 16 mg/L As for the autoclave (from nitrate solution) produced scorodite.

It was determined that sufficiently viscous aluminum hydroxyl-gels could be prepared through the partial neutralization of 2M aluminum sulphate or aluminum chloride salt solutions with 5 N sodium hydroxide at a hydrolysis ratio of OH/Al = 2.5 and at room temperature. Characterization of aged and subsequently washed aluminum hydroxyl-gels revealed them to be predominantly amorphous in nature consisting of 60 – 70 wt.% $Al(OH)_3$, 5 wt.% Cl or 18 wt.% SO_4 (depending on type of aluminum salt solution) and ~20 wt.% surface water. The $Al(SO_4)_{1.5}$-derived gel was found to differ significantly from the $AlCl_3$-derived gel both in terms of surface area (38 m^2/g vs. 18 m^2/g) and chemical features. Thus it was detected from ATR-IR and Raman spectra that

the aluminum chloride gel material is likely composed of chains of aluminum octahedra ($Al_n(OH)_{2.5}Cl_{0.5n}(H_2O)_{3n}$) with no long range order, while the aluminum sulphate gel comprises a Keggin Al_{13}-type structure: $AlO_4Al_{12}(OH)_{24}(SO_4)_{3.5}(H_2O)_{12}$.

The gels were blended with atmospherically produced scorodite at different Al:As molar ratios, aged under various conditions and subsequently washed. Ageing at elevated temperature (40 – 70˚C) in a closed system resulted in breakdown of the gel releasing most of the aluminum into the wash water. In contrast, ageing under either open or closed conditions at 22˚C for up to 3 weeks resulted in a paste or partially dry material that was less soluble to water upon washing. Of the two gels produced, the sulphate one was the most stable with < 5% of its aluminum content reporting to the wash water, while the chloride gel released between 25 – 50% of its aluminum to the wash water. This points to significant differences in the molecular make-up between the two types of gel. Back-scattered electron images and x-ray elemental mapping of particle cross sections revealed evidence that a sulphate-derived aluminum hydroxyl-gel had formed a diffuse-type matrix around the scorodite particles. ATR-IR spectra showed the chloride gel/scorodite samples resemble physical mixtures with no chemical interaction between the aluminum gel and scorodite. This is in contrast to the sulphate gel/scorodite sample, as judged from an alteration of the arsenate band interaction. Further study is required to determine the exact nature of this interaction.

Long term stability tests (up to 400 days) involving infrequent pH adjustment in the range 6.5 to 8 with either NaOH or $Mg(OH)_2$, which essentially reached pseudo-equilibrium, found the aged aluminum hydroxy-gel/scorodite blends to release less arsenic under oxidizing conditions than pure scorodite. Equilibrium was achieved earlier when $Mg(OH)_2$ was used as base. Satisfactory results were obtained with as low as 0.1 Al/As molar ratio and as short an ageing time as 1 day at room temperature. Of the two types of gels, the $Al(SO_4)_{1.5}$-derived one proved the most effective. Thus there was only 0.03 mg/L As with the sulphate gel sample/scorodite system (Al/As = 1.5) equilibrated at pH = 6.6; that is 100 times lower than the solubility of the autoclave produced scorodite. This increased to 0.2 ± 0.1 mg/L As at pH – 7.3 (Al/As = 0.1) compared to 11 mg/L As for the autoclave produced scorodite and 6 mg/L As for the chloride gel/scorodite system.

Comparison with physical mixtures of bayerite/scorodite (Al/As = 0.4) possessing higher surface area (110 m^2/g) than the sulphate-derived gel (38 m^2/g) and analysis of the pH dependency of arsenic release led to the conclusion that the retention of arsenic by the sulphate gel is not based on simple adsorption.

Further research is required to delve into the underlying mechanism and develop this interesting stabilization system into a practical application. Among the aspects that need to be investigated is the effect of washing the aged gel/scorodite mixture prior to stability evaluation/disposal. Other aspects worthy of investigation are the use of MgO as base to make the gel and the stability evaluation of the aged gel/scorodite blends under reducing conditions.

References

1. Riveros, P. A.; Dutrizac, J. A.; Spencer, P., Arsenic Disposal Practices in the Metallurgical Industry. *Canadian Metallurgical Quarterly* **2001,** *40*, (4), 395-420.
2. Environmental Protection Agency, Technical Assistance Document for Complying with the TC Rule and Implementing the Toxicity Characteristic Leaching Procedure (TCLP). **1994**; EPA-902-B-94-001.
3. Harris, G. B. *The Removal of Arsenic from Process Solutions: Theory and Industrial Practice*, Hydrometallurgy 2003: Electrometallurgy and Environmental Hydrometallurgy; Young, C. A.; Alfantazi, A. M.; Anderson, C. G.; Dreisinger, D. B.; Harris, B.; James, A., Eds. The Minerals, Metals & Materials Society: Warrendale, PA, **2003**; pp 1889-1902.
4. Bluteau, M.-C.; Demopoulos, G. P., The Incongruent Dissolution of Scorodite - Solubility, Kinetics and Mechanism. *Hydrometallurgy* **2007,** *87*, 163-177.
5. Lagno, F. Encapsulation of Scorodite Particles with Phosphate Coatings. Ph.D., McGill University, Montreal, **2005**.
6. Escobar-Gonzales, V. L.; Monhemius, A. J. *The Mineralogy of Arsenates Relating to Arsenic Impurity Control*, Arsenic Metallurgy Fundamentals and Applications; Reddy, R. G.; Hendrix, J. L.; Queneau, P. B., Eds. The Minerals, Metals & Materials Society: Warrendale, PA, **1988**; pp 405-453.
7. Piret, N. L.; Melin, A. E. *An Engineering Approach to the Arsenic Problem in the Extraction of Non-Ferrous Metals*, Productivity and Technology in the Metallurgical Industries; Koch, M.; Taylor, J. C., Eds. The Minerals, Metals & Materials Society: Warrendale, PA, **1989**; pp 735-814.
8. Weeks, T.; Wan, R. Y., Behaviour of Arsenic in Refractory Gold Ore Processing - A Case Study. *Minor Elements 2000*, Young, C. A., Ed. Soc. Min. Met. Expl: Littleton, CO, U.S.A., **2000**; pp 125-134.
9. Filippou, D.; Demopoulos, G. P., Arsenic Immobilization by Controlled Scorodite Precipitation. *JOM* **1997,** *49*, (12), 52-55.
10. Monhemius, A. J.; Swash, P. M., Removing and Stabilizing As from Copper Refining Circuits by Hydrothermal Processing. *JOM* **1999A,** *51*, (9), 30-33.

11. Swash, P. M.; Monhemius, A. J.; Schaekers, J. M. *Solubilities of Process Residues from Biological Oxidation Pretreatments of Refractory Gold Ores*, Minor Elements 2000; Young, C. A., Ed. Soc. Min. Met. Expl: Littleton, CO, **2000**; pp 115-122.
12. Gomez, M. A.; Becze, L.; Bluteau, M.-C.; Le Berre, J. F.; Cutler, J. N.; Demopoulos, G. P. *Autoclave Precipitation and Characterization of Fe(III)-AsO4-SO4 Phases*, Hydrometallurgy 2008, Young, C.A., Ed.; Soc. min. Met. Expl., **2008**.
13. Paktunc, A. D.; Szymanski, J. T.; Lastra, R.; Laflamme, J. H. G.; Enns, V.; Soprovich, E., Assessment of Potential Arsenic Mobilization from the Ketza River Mine Tailings, Yukon, Canada. *Waste Characterization and Treatment*, Petruk, W., Ed. Soc. Min. Met. Expl.: Littleton, CO, U.S.A., **1998**.
14. Harrington, J. M.; Fendforf, S. E.; Rosenzweig, R. F., Biotic Generation of Arsenic(III) in Metal(loid)-Contaminated Lake Sediment. *Environ. Sci. Technol.* **1998,** *32*, 2425-2430.
15. Environment Canada Status Report on Water Pollution Prevention and Control in the Canadian, Metal Mining Industry 2001. http://www.ec.gc.ca/nopp/docs/rpt/waterpollution/mining2001/en/toc.cfm
16. Khoe, G. H.; Carter, M.; Emett, M. T.; Vance, E. R.; Zaw, M., The Stability and Immobilization of Iron Arsenate Compounds. *Sixth AusIMM Extractive Metallurgy Conference*, The Australasian Institute of Mining and Metallurgy: Carlton, Victoria, Australia, **1994**.
17. Jia, Y.; Demopoulos, G. P. *Coprecipitation of As(V) with Fe(III) in Sulfate Media: Solubility and Speciation of Arsenic*, Arsenic Metallurgy; Reddy, R. G.; Ramachandran, V., Eds. The Minerals, Metals & Materials Society: **2005**; pp 137-148.
18. DeKlerk, R. J. Investigating the Continuous Circuit Coprecipitation of Arsenic(V) with Ferric Iron in Sulphate Media. M.Eng. thesis McGill Univerity, Montreal, **2008**.

19. Jia, Y.; Demopoulos, G. P., Coprecipitation of arsenate with iron(III) in aqueous sulfate media: Effect of time, lime as base and co-ions on arsenic retention. *Water Research* **2008,** *42*, (3), 661-668.

20. Swash, P. M.; Monhemius, A. J. *Hydrothermal Precipitation From Aqueous Solutions Containing Iron(III), Arsenate and Sulphate*, Hydrometallurgy '94, London, UK, **1994**; pp 177-190.

21. Dutrizac, J. E.; Jambor, J. L., The Synthesis of Crystalline Scorodite, $FeAsO_4.2H_2O$. *Hydrometallurgy* **1987,** *19*, 377-384.

22. Harris, G. B.; Monette, S., The Disposal of Arsenic Solid Residues. *Productivity and Technology in the Metallurgical Industries*, Koch, M.; Taylor, J. C., Eds. The Minerals, Metals and Materials Society: Warrendale, PA, **1989**; pp 545-560.

23. Demopoulos, G. P., On the Preparation and Stability of Scorodite. In *Arsenic Metallurgy*, The Minerals, Metals & Materials Society: Warrendale, PA, **2005**.

24. Demopoulos, G. P.; Droppert, D. J.; Van Weert, G., Precipitation of crystalline scorodite ($FeAsO_4 \bullet 2H_2O$) from chloride solutions. *Hydrometallurgy* **1995,** *38*, (3), 245-261.

25. Singhania, S.; Wang, Q.; Filippou, D.; Demopoulos, G. P., Temperature and Seeding Effects on the Precipitation of Scorodite From Sulfate Solutions Under Atmospheric-Pressure Conditions. *Metallurgical and Materials Transactions B* **2005,** *36B*, 327-333.

26. Dabekaussen, R.; Droppert, D. J.; Demopoulos, G. P., Ambient Pressure Hydrometallurgical Conversion of Arsenic Trioxide to Crystalline Scorodite. *CIM Bulletin* **2001,** *94*, (1051), 116-122.

27. Fujita, T.; Taguchi, R.; Abumiya, M.; Matsumoto, M.; Shibata, E.; Nakamura, T., Novel Atmospheric Scorodite Synthesis by Oxidation of Ferrous Sulfate Solution. Part I. *Hydrometallurgy* **2008,** *90*, (2-4), 92-102.

28. Singhania, S.; Wang, Q.; Filippou, D.; Demopoulos, G. P., Acidity, Valency and Third Ion Effects on the Precipitation of Scorodite from Mixed Sulfate Solutions Under Atmospheric-Pressure Conditions. *Metallurgical and Materials Transactions B* **2006,** *37B*, 189-197.

29. Environmental Protection Agency, EPA Test Method 1311 - Toxicity Characteristic Leaching Procedure (TCLP). **1992**; p 38.
30. Zhang, Y. L.; Evangelou, V. P., Formation of Ferric Hydroxide-Silica Coatings on Pyrite and its Oxidation Behavior. *Soil Science* **1998,** *163*, (1), 53-62.
31. Paraskeva, C. A.; Charambous, P. C.; Stokka, L.-E.; Klepetsanis, P. G.; Koutsoukos, P. G.; Read, P.; Ostvold, T.; Payatakes, A. C., Sandbed Consolidation with Mineral Precipitation. *Journal of Colloid and Interface Science* **2000,** *232*, 326-339.
32. Sijstermans, L. F. J. Pellet Production from Concentrated Solutions with a Pellet Reactor. M.Eng. Thesis, Delft University of Technology, Delft, 1992.
33. Lagno, F.; Demopoulos, G. P., Synthesis of Hydrated Aluminum Phosphate, $AlPO_4 \bullet 1.5H_2O$ ($AlPO_4$-H_3), by Controlled Reactive Crystallization in Sulfate Media. *Industrial and Engineering Chemical Research* **2005,** *44*, 8033-8038.
34. Lagno, F.; Demopoulos, G. P., The Stability of Hydrated Aluminum Phosphate, $AlPO_4 \bullet 1.5H_2O$. *Environmental Technology* **2006,** *27*, 1217-1224.
35. Gel. In *Encyclopedia Britannica Online*, Britannica, E. Ed., **2008**.
36. Gella, V. Precipitation of Aluminum (Oxy)hydroxides From Concentrated Chloride Solutions by Neutralization. M.Eng. Thesis, McGill University, Montreal, **2007**.
37. Wang, S. L.; Wang, M. K.; Tzou, Y. M., Effect of Temperatures on Formation and Transformation of Hydrolytic Aluminum in Aqueous Solutions. *Colloids and Surfaces A* **2003,** *231*, 143-157.
38. Bottero, J. Y.; Cases, J. M.; Flessinger, F.; Poirier, J. E., Studies of Hydrolyzed Aluminum Chloride Solutions. 1. Nature of Aluminum Species and Composition of Aqueous Solutions. *Journal of Physical Chemistry* **1980,** *84*, 2933-2939.
39. Phillips, B.L. http://www.geosciences.stonybrook.edu/people/faculty/phillips/phillips.html (accessed on May 27, **2008**).
40. Bi, S.; Wang, C.; Cao, Q.; Zhang, C., Studies on the mechanism of hydrolysis and polymerization of aluminum salts in aqueous solution: correlations between the "Core-links" model and "Cage-like" Keggin-Al13 model. *Coordination Chemistry Reviews* **2004,** *248*, (5-6), 441-455.

41. Bottero, J. Y.; Axelos, M.; Tchoubar, D.; Cases, J. M.; Fripiat, J. J.; Fiessinger, F., Mechanism of formation of aluminum trihydroxide from keggin Al13 polymers. *Journal of Colloid and Interface Science* **1987,** *117*, (1), 47-57.

42. Goldberg, S.; Lebron, I.; Suarez, D. L.; Hinedi, Z. R., Surface Characterization of Amorphous Aluminum Oxides. *Soil Sci. Soc. Am. J.* **2001,** *65*, 78-86.

43. Enomoto, N.; Choi, H. L.; Katsumoto, M.; Nakagawa, Z., Effect of Ultrasound on Crystallization From Amorphous Gels in Solution. *Transactions of the Materials Research Society of Japan* **1994,** *14*, (A), 777-780.

44. Bradley, S. M.; Kydd, R. A.; Howe, R. F., The Structure of Al Gels Formed Through the Base Hydrolysis of Al^{+3} Aqueous Solutions. *Colloid and Interface Science* **1993,** *159*, 405-412.

45. Weerasooriya, R.; Tobschall, H. J.; Wijesekara, H. K. D. K.; Arachchige, E. K. I. A. U. K.; Pathirathne, K. A. S., On the Mechanistic Modeling of As(III) Adsorption on Gibbsite. *Chemosphere* **2003,** *51*, 1001-1013.

46. Masue, Y.; Loeppert, R. H.; Kramer, T. A., Arsenate and Arsenite Adsorption and Desorption Behavior on Coprecipitated Aluminum:Iron Hydroxides. *Environ. Sci. Technol.* **2007,** *41*, 837-842.

47. Hering, J. G.; Chen, P.-Y.; Wilkie, J. A.; Elimelech, M., Arsenic Removal from Drinking Water During Coagulation. *Journal of Environmental Engineering* **1997,** *123*, 800-807.

48. Goldberg, S.; Johnston, C. T., Mechanisms of Arsenite Adsorption on Amorphous Oxides Evaluated Using Macroscopic Measurements, Vibrational Spectroscopy, and Surface Complexation Modeling. *Journal of Colloid and Interface Science* **2000,** *234*, 204-216.

49. Mohapatra, D.; Singh, P.; Zhang, W.; Pullammanappallil, P., The effect of citrate, oxalate, acetate, silicate and phosphate on stability of synthetic arsenic-loaded ferrihydrite and Al-ferrihydrite. *Journal of Hazardous Materials* **2005,** *124*, (1-3), 95-100.

50. Anderson, M. A.; Ferguson, J. F.; Gavis, J., Arsenate adsorption on amorphous aluminum hydroxide. *Journal of Colloid and Interface Science* **1976,** *54*, (3), 391-399.

51. Gulledge, J. H.; O'Connor, J. T., Removal of Arsenic (V) From Water by Adsorption on Aluminum and Ferric Hydroxides. *Journal of American Water Works Association* **1973,** *65*, 548-552.

52. Savage, K. S.; Bird, D. K.; O'Day, P. A., Arsenic Speciation in Synthetic Jarosite. *Chemical Geology* **2005,** *215*, 473-498.

53. Wefers, K.; Misra, C. *Oxides and Hydroxides of Aluminum*; Alcoa Laboratories: 1987.

54. Green, R. H.; Hem, S. L., Effect of Washing on Physicochemical Properties of Aluminum Hydroxide Gel. *Journal of Pharmaceutical Sciences* **1974,** *63*, (4), 635-637.

55. Ashbrook, S. E.; MacKenzie, K. J. D.; Wimperis, S., 27Al Multiple-Quantum MAS NMR of Mechanically Treated Bayerite (alpha-Al(OH)3) and Silica Mixtures. *Solid State Nuclear Magnetic Resonance* **2001,** *20*, 87-99.

56. Nail, S. L.; White, J. L.; Hem, S. L., Structure of Aluminum Hydroxide Gel III: Mechanism of Stabilization by Sorbitol. *Journal of Pharmaceutical Sciences* **1976,** *65*, (8), 1195-1198.

57. Nail, S. L.; White, J. L.; Hem, S. L., IR Studies of Development of Order in Aluminum Hydroxide Gels. *Journal of Pharmaceutical Sciences* **1976,** *65*, (2), 231-234.

58. Kolesova, V. A., A Spectroscopic Criterion for the Coordination of Aluminum in the Anionic Body. *Otdelenie Khimicheskikh Nauk* **1962,** *11*, 2082-2084.

59. Phambu, N., Characterization of Aluminum Hydroxide Thin Film on Metallic Aluminum Powder. *Materials Letters* **2003,** *57*, 2907-2913.

60. Riesgraf, D. A.; May, M. L., Infrared Spectra of Aluminum Hydroxide Chlorides. *Applied Spectroscopy* **1978,** *32*, (4), 362-366.

61. Nakamoto, K., Infrared and Raman Spectra of Inorganic and Coordination Compounds, Part A: Theory and Applications in Inorganic Chemistry. 5 ed.; John Wiley & Sons Inc.: New York, **1997**; p 387.

62. Gauvin, R., Charging of Aluminum Gel/Scorodite Sample Cross Sections. Private Communication, McGill University, Montreal, **2008**.

63. Wang, Q.; Nishimura, T.; Umetsu, Y. *Oxidative Precipitation for Arsenic Removal in Effluent Treatment*, Minor Elements 2000; Young, C., Ed. Society for Mining, Metallurgy, and Exploration: **2000**; pp 39-52.

Appendix A – Chemical Digestion and Analysis of Solids

In order to determine the chemical composition of the produced solid materials, chemical digestion was applied followed by ICP-AES analysis. The general analysis procedure was outlined in section 3.3. Here the chemical digestion is described:

- Into a 100 mL volumetric flask place ~ 0.25 g solids and record the exact weight.
- Add approximately 20 mL de-ionized water to the flask followed by 6.5 mL nitric acid (HNO_3) and 24.7 mL hydrochloric acid (HCl). For samples where chloride analysis is required the volume of hydrochloric acid can be replaced by nitric acid.
- In order to increase the rate of dissolution, the flask can be put on a hot plate to heat the solution (~ 90 ˚C). The flask can be gently shaken by hand to promote mixing and care should be taken to ensure the liquid does not boil. More acid can be added if necessary.
- After all the solids have dissolved, allow the solution to cool if required and fill the remaining volume of the volumetric flask with de-ionized water. Shake thoroughly.
- Pipette 1 mL of the mixture into another 100 mL volumetric flask and fill the remaining volume with 4 % nitric acid solution (required for analysis by ICP).
- Determine the concentration by Inductively Coupled Plasma – Atomic Emission Spectroscopy (ICP-AES).
- The percent of each element in the solids can be determined with the following equation:

$$M(wt.\%) = \frac{C_M(mg/L) \times 0.1L \times 100:1}{W(mg)} \times 100\% = \frac{C_M(mg/L)}{W(g)}$$

Where: M = Weight percent of metal in sample

C_M = Concentration of metal in dilute sample (mg/L)

W = Mass of sample dissolved in mg or g

Appendix B – Production of Amorphous Aluminum Hydroxide and Bayerite Used in the Adsorption Tests

Amorphous aluminum hydroxide and Bayerite samples were mixed with atmospherically produced scorodite (Batch 2) and subjected to long term stability evaluation, as discussed in section 3.8. This was used as a simple means to verify whether low arsenic release from the aged gel/scorodite mixtures could be attributed to adsorption by aluminum hydroxide. The procedure used to synthesize the amorphous aluminum hydroxide and bayerite materials, which is adapted from *Gella's* [36] work is presented below.

The experimental setup was identical to the one described in section 3.5.1 for the atmospheric scorodite precipitation tests. In addition, a peristaltic pump with tubing going into one of the holes in the reactor lid was used for measured addition of sodium hydroxide (NaOH).

- 300 mL of 0.5 M aluminum chloride salt solution was prepared by dissolving an appropriate amount of $AlCl_3 \bullet 6H_2O$ in de-ionized water, which was subsequently placed in the reactor.
- Solutions were heated to 60˚C with the aid of a programmable hot plate with thermocouple for the production of both bayerite and amorphous aluminum hydroxide samples.
- Once the solution had attained the target temperature, the peristaltic pump was used to add 5 N NaOH at a rate of 1 mL/min up to hydrolysis ratios of 3.15 and 2.85 for the production of bayerite and amorphous aluminum hydroxide materials, respectively. The total time of base addition was typically ~ 1.5 hours.
- The resulting slurry was agitated for 24 hrs at reaction temperature before being filtered through a 0.1 μm membrane with a pressure filter at 50 psi.
- The solids were re-pulped with de-ionized water and filtered during several washing steps and the final solids were dried in an oven between 40˚C and 60˚C.

Appendix C – Solids Composition and Soluble Species Contained in the Wash Filtrate for Scorodite and Aged Gel/Scorodite Materials

Subsequent to ageing the gel/scorodite materials a washing step was employed to remove the bulk of soluble species from the resulting solids, as outlined in section 3.7. The solids composition and concentration of soluble species in the filtrate is summarized for all tests below.

Solids Composition:

ID	Description	As (wt.%)	Fe (wt.%)	Fe:As (molar)	Al:As (molar)	Al (wt.%)	SO_4^{2-} (wt.%)
2	Autoclave Scorodite	31.4	24.3	1.04	-	-	-
1	Batch 1 scorodite	33.7	24.6	0.98	-	-	2.9
8	Batch 2 scorodite	30.0	23.0	1.03	-	-	3.0
3	open, Cl^- gel, 1.54 Al:As, 22 ˚C, 21 days	24.6	17.5	0.96	0.84	7.45	1.9
4	closed, Cl^- gel, 0.96 Al:As, 40 ˚C, 54 days	28.9	22.5	1.04	0.04	0.45	2.7
5	closed, Cl^- gel, 0.96 Al:As, 70 ˚C, 1 day	29.1	22.8	1.05	0.04	0.40	2.5
6	open, Cl^- gel, 0.96 Al:As, 50 ˚C, 1 day	23.5	18.4	1.05	0.66	5.58	2.0
7	open, SO_4^{2-} gel, 1.5 Al:As, 22 ˚C, 28 days	17.3	13.4	1.04	1.45	9.03	23.3
13	open, Cl^- gel, 1 Al:As, 22 ˚C, 21 days	21.4	17.5	1.10	1.02	7.85	1.4
14	closed, Cl^- gel, 1 Al:As, 22 ˚C, 21 days	21.8	17.7	1.09	1.06	8.35	1.3
15	open, Cl^- gel, 0.1 Al:As, 22 ˚C, 21 days	27.6	22.0	1.07	0.07	0.71	1.8
16	open, Cl^- gel, 0.1 Al:As, 22 ˚C, 7 days	27.7	22.8	1.11	0.07	0.69	1.8
17	open, Cl^- gel, 0.1 Al:As, 22 ˚C, 1 day	27.6	23.2	1.12	0.08	0.75	1.8
18	open, Cl^- gel, 0.1 Al:As, 22 ˚C, 1 day	27.6	23.2	1.13	0.08	0.75	1.8
19	open, SO_4^{2-} gel, 0.1 Al:As, 22 ˚C, 1 day	28.6	23.0	1.08	0.11	1.11	2.7
20	open, SO_4^{2-} gel, 0.1 Al:As, 22 ˚C, 1 day	28.3	22.1	1.05	0.10	0.97	2.6

Soluble Species in the Filtrate:

ID	Description	$V_{Filtrate}$ (L)	[As] (mg/L)	[Fe] (mg/L)	[Al] (mg/L)	[S] (mg/L)	$[Na^+]$ (mg/L)
3	open, Cl^- gel, 1.54 Al:As, 22 ˚C, 21 days	0.630	6.53	4.45	297.2	*	*
4	closed, Cl^- gel, 0.96 Al:As, 40 ˚C, 54 days	0.620	18.55	7.99	1297.1	*	*
5	closed, Cl^- gel, 0.96 Al:As, 70 ˚C, 1 day	0.242	96.53	39.11	3760.3	*	*
6	open, Cl^- gel, 0.96 Al:As, 50 ˚C, 1 day	0.572	6.94	5.08	116.6	*	*
7	open, SO_4^{2-} gel, 1.5 Al:As, 22 ˚C, 28 days	0.554	4.94	4.55	16.4	*	*
13	open, Cl^- gel, 1 Al:As, 22 ˚C, 21 days	0.975	0.29	0.13	118.30	0.06	152.5
14	closed, Cl^- gel, 1 Al:As, 22 ˚C, 21 days	1.017	0.11	0.22	77.93	0.06	171.3
15	open, Cl^- gel, 0.1 Al:As, 22 ˚C, 21 days	1.058	9.67	5.59	30.32	0.38	194.3
16	open, Cl^- gel, 0.1 Al:As, 22 ˚C, 7 days	1.029	0.23	0.02	12.39	0.07	185.5
17	open, Cl^- gel, 0.1 Al:As, 22 ˚C, 1 day	0.975	2.71	1.84	15.85	0.17	194.8
18	open, Cl^- gel, 0.1 Al:As, 22 ˚C, 1 day	1.021	0.34	0.02	14.67	0.16	194.4
19	open, SO_4^{2-} gel, 0.1 Al:As, 22 ˚C, 1 day	1.027	0.14	0.02	2.78	94.04	191.8
20	open, SO_4^{2-} gel, 0.1 Al:As, 22 ˚C, 1 day	1.017	0.12	0.01	1.58	94.04	185.3

* Sodium and sulphur content of the wash filtrate was not determined for these samples.
** Sample ID 3 – 7 are with Batch 1 scorodite, sample ID 13 – 20 are with Batch 2 scorodite.

Appendix D – Post-Ageing Washing Step Mass Balance

The solids compositions along with the soluble species content in the filtrate permit a mass balance to be conducted around the post-ageing washing step. The percent distribution of arsenic, iron and aluminum between the solids and wash filtrate are summarized for all aged gel/scorodite materials containing Batch 1 and Batch 2 atmospheric scorodite. The percent of material not accounted for in the mass balance is also included, where a negative value denotes that more than all the input material was accounted for by these two streams.

ID	Description	Filtrate			Solids			Unaccounted		
		% As	% Fe	% Al	% As	% Fe	% Al	% As	% Fe	% Al
3	open, Cl^- gel, 1.54 Al:As, 22 ˚C, 21 days	0.69	0.66	51.16	75.6	72.4	41.4	23.9	27.1	15.3
4	closed, Cl^- gel, 0.96 Al:As, 40 ˚C, 54 days	0.51	0.28	95.85	82.6	86.0	3.7	17.0	13.8	10.4
5	closed, Cl^- gel, 0.96 Al:As, 70 ˚C, 1 day	1.01	0.52	96.61	84.9	89.2	3.4	14.2	10.3	-0.6
6	open, Cl^- gel, 0.96 Al:As, 50 ˚C, 1 day	0.41	0.38	22.43	94.9	100.1	65.3	4.7	-0.4	15.8
7	open, SO_4^{2-} gel, 1.5 Al:As, 22 ˚C, 28 days	0.35	0.41	2.16	88.3	91.6	85.2	11.4	8.0	12.9
13	open, Cl^- gel, 1 Al:As, 22 ˚C, 21 days	0.01	0.01	10.07	92.5	101.4	94.4	7.4	-1.4	-4.4
14	closed, Cl^- gel, 1 Al:As, 22 ˚C, 21 days	0.00	0.01	8.44	78.1	85.0	83.0	21.9	15.0	8.6
15	open, Cl^- gel, 0.1 Al:As, 22 ˚C, 21 days	0.42	0.33	36.97	88.2	94.4	62.9	11.4	5.3	0.2
16	open, Cl^- gel, 0.1 Al:As, 22 ˚C, 7 days	0.01	0.00	16.52	85.2	94.1	59.2	14.8	5.9	24.3
17	open, Cl^- gel, 0.1 Al:As, 22 ˚C, 1 day	0.13	0.12	21.82	81.9	92.2	62.0	17.9	7.7	16.2
18	open, Cl^- gel, 0.1 Al:As, 22 ˚C, 1 day	0.02	0.00	21.01	88.6	100.0	66.8	11.4	0.0	12.2
19	open, SO_4^{2-} gel, 0.1 Al:As, 22 ˚C, 1 day	0.01	0.00	3.85	95.8	103.3	99.6	4.2	-3.3	-3.5
20	open, SO_4^{2-} gel, 0.1 Al:As, 22 ˚C, 1 day	0.01	0.00	2.29	90.0	99.4	89.8	10.0	0.6	7.9

Appendix E – Arsenic Release from Samples Containing Batch 1 Scorodite (Test ID 1-7)

Arsenic release during long term stability testing of Batch 1 scorodite as well as aged gel/scorodite materials containing Batch 1 scorodite were presented in the form of graphs in section 4.3. The raw data is summarized below.

Sample ID	Sample Description \ Time (Days)	9	12	17	22	29	44	59	73
1	Batch 1 scorodite	1.0	0.9	-	-	-	26.9	31.7	31.8
3	open, Cl^- gel, 1.54 Al:As, 22 °C, 21 days	0.36	0.41	0.46	0.22	0.00	0.00	0.00	0.00
4	closed, Cl^- gel, 0.96 Al:As, 40 °C, 54 days	0.03	0.00	0.01	0.18	0.89	2.50	2.68	2.67
5	closed, Cl^- gel, 0.96 Al:As, 70 °C, 1 day	0.40	0.31	0.30	0.41	0.89	4.21	4.59	4.36
6	open, Cl^- gel, 0.96 Al:As, 50 °C, 1 day	0.03	0.88	0.28	0.36	0.17	0.36	0.23	0.13
7	open, SO_4^{2-} gel, 1.5 Al:As, 22 °C, 28 days	0.10	0.07	0.03	0.00	0.04	0.03	0.09	0.06

Sample ID	Sample Description \ Time (Days)	94	108	122	134	158	185	206	254
1	Batch 1 scorodite	42.0	44.0	42.8	43.1	45.5	44.7	44.3	40.0
3	open, Cl^- gel, 1.54 Al:As, 22 °C, 21 days	0.61	0.31	0.21	0.36	0.03	2.09	1.75	1.70
4	closed, Cl^- gel, 0.96 Al:As, 40 °C, 54 days	2.60	2.35	2.25	2.15	1.66	1.43	1.44	1.30
5	closed, Cl^- gel, 0.96 Al:As, 70 °C, 1 day	4.89	4.33	4.09	3.75	4.23	3.77	4.31	4.09
6	open, Cl^- gel, 0.96 Al:As, 50 °C, 1 day	0.33	0.32	0.13	0.33	-	1.19	0.86	1.30
7	open, SO_4^{2-} gel, 1.5 Al:As, 22 °C, 28 days	0.10	0.08	0.20	0.53	0.95	0.13	0.02	0.02

Sample ID	Sample Description \ Time (Days)	281	304	318	332	346	369	409
1	Batch 1 scorodite	39.1	38.7	39.0	38.5	37.9	39.3	37.9
3	open, Cl^- gel, 1.54 Al:As, 22 °C, 21 days	1.62	1.66	2.01	2.03	2.08	1.85	1.85
4	closed, Cl^- gel, 0.96 Al:As, 40 °C, 54 days	1.58	1.63	1.74	1.67	1.67	1.15	1.14
5	closed, Cl^- gel, 0.96 Al:As, 70 °C, 1 day	4.16	3.63	3.19	2.86	2.59	1.66	1.58
6	open, Cl^- gel, 0.96 Al:As, 50 °C, 1 day	1.46	1.34	1.46	1.42	1.51	1.08	1.44
7	open, SO_4^{2-} gel, 1.5 Al:As, 22 °C, 28 days	0.02	0.03	0.08	0.05	0.02	0.02	0.03

Appendix F – Arsenic Release from Samples Containing Batch 2 Scorodite (Test ID 8-20)

Arsenic release data during long term stability evaluation of Batch 2 atmospheric scorodite, physical mixtures of Batch 2 scorodite with aluminum hydroxides and aged gel/Batch 2 scorodite materials are summarized below. Adjustment of pH was conducted with 0.5 M magnesium oxide (MgO) slurry with the exception of test 13a, which was adjusted with 1 M sodium hydroxide (NaOH).

Sample ID	Sample Description \ Time (Days)	0	6	14	17	22	31	41	55	64
8	Batch 2 scorodite	2.94	6.59	8.22	7.97	7.98	8.78	9.20	9.08	9.52
9	Scorodite + 1 wt% Bayerite	1.76	8.53	10.09	10.14	10.63	11.09	11.24	11.41	11.45
10	Scorodite + 10 wt% Bayerite	0.55	4.55	5.12	4.86	4.65	4.71	4.45	3.99	4.20
11	Scorodite + 1 wt% amorphous	2.79	8.34	10.16	9.65	10.24	10.66	10.39	10.31	10.63
12	Scorodite + 10 wt% amorphous	2.51	2.87	3.55	3.63	3.53	4.10	4.47	5.14	5.84
13a	open, Cl^- gel, 1 Al:As, 22 ˚C, 21 days	0.02	0.54	0.90	1.37	1.26	2.18	2.86	3.89	4.69
13b	open, Cl^- gel, 1 Al:As, 22 ˚C, 21 days	0.15	0.09	0.34	0.86	1.51	2.68	3.50	4.27	4.85
14	closed, Cl^- gel, 1 Al:As, 22 ˚C, 21 days	0.50	0.05	0.14	0.53	0.79	1.97	2.50	3.28	3.66
15	open, Cl^- gel, 0.1 Al:As, 22 ˚C, 21 days	0.06	0.31	0.73	1.02	1.04	2.19	2.72	3.26	3.73
16	open, Cl^- gel, 0.1 Al:As, 22 ˚C, 7 days	0.04	2.47	4.26	4.47	5.00	6.25	7.40	8.57	9.13
17	open, Cl^- gel, 0.1 Al:As, 22 ˚C, 1 day	0.07	3.39	4.13	4.17	4.23	5.03	5.30	5.63	5.75
18	open, Cl^- gel, 0.1 Al:As, 22 ˚C, 1 day	0.03	4.14	5.88	5.86	6.61	7.76	8.93	9.95	10.64
19	open, SO_4^{2-} gel, 0.1 Al:As, 22 ˚C, 1 day	0.06	0.06	0.07	0.30	0.13	0.24	0.15	0.01	0.02
20	open, SO_4^{2-} gel, 0.1 Al:As, 22 ˚C, 1 day	0.05	0.11	0.46	0.58	0.72	0.73	0.52	0.71	0.74

Sample ID	Sample Description \ Time (Days)	71	78	85	92	99	106	129	169
8	Batch 2 scorodite	9.85	9.51	9.13	10.64	10.35	9.94	10.39	9.70
9	Scorodite + 1 wt% Bayerite	11.30	11.41	10.87	11.69	11.65	11.28	12.25	11.06
10	Scorodite + 10 wt% Bayerite	4.00	3.99	3.35	4.03	3.93	3.55	3.84	3.29
11	Scorodite + 1 wt% amorphous	11.29	12.44	11.75	12.53	12.64	12.35	13.64	12.25
12	Scorodite + 10 wt% amorphous	6.68	7.25	6.95	7.85	8.27	8.54	9.86	10.58
13a	open, Cl^- gel, 1 Al:As, 22 ˚C, 21 days	5.08	5.56	5.31	6.05	5.99	5.96	6.09	5.81
13b	open, Cl^- gel, 1 Al:As, 22 ˚C, 21 days	5.47	6.16	5.59	6.64	6.76	6.92	7.46	7.90
14	closed, Cl^- gel, 1 Al:As, 22 ˚C, 21 days	5.07	4.48	4.11	5.08	5.21	5.33	5.86	5.91
15	open, Cl^- gel, 0.1 Al:As, 22 ˚C, 21 days	3.85	4.11	3.63	4.25	4.47	4.11	4.32	4.61
16	open, Cl^- gel, 0.1 Al:As, 22 ˚C, 7 days	9.82	10.46	10.13	10.84	11.14	11.62	13.04	14.17
17	open, Cl^- gel, 0.1 Al:As, 22 ˚C, 1 day	5.78	5.82	4.96	5.39	5.45	5.36	5.76	5.65
18	open, Cl^- gel, 0.1 Al:As, 22 ˚C, 1 day	10.89	11.66	10.87	11.65	12.34	12.14	13.50	13.88
19	open, SO_4^{2-} gel, 0.1 Al:As, 22 ˚C, 1 day	0.28	0.10	0.15	0.08	0.16	0.21	0.26	0.29
20	open, SO_4^{2-} gel, 0.1 Al:As, 22 ˚C, 1 day	0.72	1.07	0.49	1.18	1.21	1.39	1.80	2.17

- Test 13a adjusted with NaOH. Test 13b adjusted with MgO slurry.

Appendix G - Variation of pH During Stability Testing of Samples Containing Batch 2 Scorodite (Test ID 8-20)

The solution pH was regularly monitored during long term stability evaluation of Batch 2 atmospheric scorodite, physical mixtures of Batch 2 scorodite with aluminum hydroxides and aged gel/Batch 2 scorodite materials, and the observed data is given below. Adjustment was conducted with 0.5 M Magnesium oxide (MgO) slurry with the exception of test 13a, where 1 M liquid sodium hydroxide (NaOH) was used.

Sample ID	Sample Description \ Time (Days)	0	0	3	6	14	17	22	31	41
8	Batch 2 scorodite	4.02	4.02	7.98	7.83	7.79	7.69	7.61	7.55	7.56
9	Scorodite + 1 wt% Bayerite	4.01	4.01	8.05	7.9	8.18	8.04	8.01	8.02	7.98
10	Scorodite + 10 wt% Bayerite	5.5	5.5	8.25	7.8	8.1	8.06	8.06	8.03	7.95
11	Scorodite + 1 wt% amorphous	3.96	3.96	8.26	7.85	8.07	8.08	7.98	7.97	7.88
12	Scorodite + 10 wt% amorphous	3.72	3.72	7.88	7.74	8.01	8.08	8.05	8.02	7.99
13a	open, Cl^- gel, 1 Al:As, 22 ˚C, 21 days	4.15	8.09	7.91	7.71	7.84	7.84	7.66	7.59	7.61
13b	open, Cl^- gel, 1 Al:As, 22 ˚C, 21 days	4.14	4.14	7.94	8.02	8.26	8.3	8.25	8.16	8.11
14	closed, Cl^- gel, 1 Al:As, 22 ˚C, 21 days	4.36	4.36	7.95	8.1	8.37	8.46	8.45	8.35	8.33
15	open, Cl^- gel, 0.1 Al:As, 22 ˚C, 21 days	5.55	5.55	8.05	7.64	7.88	7.86	7.85	7.83	7.8
16	open, Cl^- gel, 0.1 Al:As, 22 ˚C, 7 days	5.16	5.16	7.95	7.58	8.24	8.2	8.2	8.14	8.17
17	open, Cl^- gel, 0.1 Al:As, 22 ˚C, 1 day	4.62	4.62	7.93	7.69	8.16	8.31	8.2	8.18	8.23
18	open, Cl^- gel, 0.1 Al:As, 22 ˚C, 1 day	5.23	5.23	7.95	7.62	8.35	8.28	8.3	8.31	8.33
19	open, SO_4^{2-} gel, 0.1 Al:As, 22 ˚C, 1 day	4.3	4.3	7.92	7.78	8.12	8.07	7.75	7.56	7.52
20	open, SO_4^{2-} gel, 0.1 Al:As, 22 ˚C, 1 day	4.33	4.33	7.94	7.75	8.15	8.15	7.98	7.89	7.89

Sample ID	Sample Description \ Time (Days)	55	64	71	78	85	106	129	169
8	Batch 2 scorodite	7.59	7.53	7.57	7.55	7.52	7.5	7.49	7.47
9	Scorodite + 1 wt% Bayerite	7.85	7.82	7.77	7.82	7.74	7.71	7.68	7.64
10	Scorodite + 10 wt% Bayerite	7.95	7.92	7.9	7.89	7.79	7.71	7.7	7.76
11	Scorodite + 1 wt% amorphous	7.81	7.74	7.68	7.6	7.64	7.58	7.55	7.48
12	Scorodite + 10 wt% amorphous	7.8	7.77	7.91	7.85	8.02	7.93	7.9	7.91
13a	open, Cl^- gel, 1 Al:As, 22 ˚C, 21 days	7.64	7.64	7.61	7.63	7.57	7.61	7.58	7.5
13b	open, Cl^- gel, 1 Al:As, 22 ˚C, 21 days	8.1	8.09	8.05	8.13	8.09	8.03	7.9	7.82
14	closed, Cl^- gel, 1 Al:As, 22 ˚C, 21 days	8.32	8.3	8.28	8.3	8.28	8.18	8.07	7.96
15	open, Cl^- gel, 0.1 Al:As, 22 ˚C, 21 days	7.79	7.76	7.74	7.77	7.73	7.68	7.65	7.61
16	open, Cl^- gel, 0.1 Al:As, 22 ˚C, 7 days	8.32	8.25	8.2	8.27	8.27	8.29	8.25	8.24
17	open, Cl^- gel, 0.1 Al:As, 22 ˚C, 1 day	8.16	8.15	8.11	8.17	8.04	7.97	7.96	7.91
18	open, Cl^- gel, 0.1 Al:As, 22 ˚C, 1 day	8.29	8.29	8.27	8.34	8.29	8.25	8.2	8.17
19	open, SO_4^{2-} gel, 0.1 Al:As, 22 ˚C, 1 day	7.47	7.51	7.36	7.42	7.36	7.32	7.31	7.26
20	open, SO_4^{2-} gel, 0.1 Al:As, 22 ˚C, 1 day	7.97	7.89	7.85	7.89	7.87	7.92	7.94	7.9

- Test 13a adjusted with NaOH. Test 13b adjusted with MgO slurry.